UC San Diego

UC San Diego Electronic Theses and Dissertations

Title

Biomechanics and Mechanobiology of Articular Cartilage Growth and Maturation in the Distal Femur

Permalink

https://escholarship.org/uc/item/7hm5m0j8

Author

Gacasan, Erica Gallarde

Publication Date

2023

Peer reviewed|Thesis/dissertation

eScholarship.org Powered by the California Digital Library
University of California

UNIVERSITY OF CALIFORNIA SAN DIEGO

BIOMECHANICS AND MECHANOBIOLOGY OF ARTICULAR CARTILAGE GROWTH AND MATURATION IN THE DISTAL FEMUR

A Dissertation submitted in partial satisfaction of the requirements
for the degree Doctor of Philosophy

in

Bioengineering

by

Erica G. Gacasan

Committee in charge:

Professor Robert L. Sah, Chair
Professor Shengqiang Cai
Professor Stephanie I. Fraley
Professor Esther J. Kwon
Professor Koichi Masuda

2023

Copyright

Erica G. Gacasan, 2023

All rights reserved.

The Dissertation of Erica G. Gacasan is approved, and it is acceptable in quality and form for publication on microfilm and electronically.

University of California San Diego

2023

DEDICATION

This dissertation is dedicated to my loving parents, Lola, and brother.

EPIGRAPH

"But need alone is not enough to set power free: there must be knowledge."

— Ursula K. Le Guin, *A Wizard of Earthsea*

"The fabric of the joints in the human body is a subject so much the more entertaining, as it must strike every one that considers it attentively with an idea of fine mechanical composition."

— William Hunter, *Of the Structure and Diseases of Articulating Cartilages (1753)*

TABLE OF CONTENTS

DISSERTATION APPROVAL PAGE iii

DEDICATION iv

EPIGRAPH v

TABLE OF CONTENTS vi

LIST OF FIGURES ix

LIST OF TABLES xi

LIST OF ABBREVIATIONS xii

ACKNOWLEDGEMENTS xiii

VITA xv

ABSTRACT OF THE DISSERTATION xvii

CHAPTER 1 : INTRODUCTION 1

1.1. General introduction to the dissertation 1

1.2. Early joint development and maturation 4

1.3. Structure, function, and composition of mature synovial joints, osteochondral unit, and articular cartilage 7

1.4. Cartilage structure and composition varies with maturation 10

1.5. Maturation and growth mechanisms of the articular epiphyseal cartilage 16

1.6. Models of metabolism and growth 22

1.7. Significance 26

1.8. References 27

CHAPTER 2 : OVERVIEW OF ORTHOBIOLOGICS FOR ARTICULAR CARTILAGE REPAIR 39

2.1. Introduction 39

2.2. Brief biology of cartilage 41

2.3. Overview of therapeutic options: Cells, scaffolds, and signals 53

2.4. Standard approaches to cartilage repair 64

2.5. Novel orthobiologic approaches to cartilage repair 68

2.6. Summary 72

2.7. Acknowledgements 74

2.8. References 75

CHAPTER 3 : COMPRESSIVE PROPERTIES OF NORMAL HUMAN ARTICULAR CARTILAGE ARE ENHANCED BETWEEN INFANT, CHILD, AND ADULT, AND RELATED TO DISTINCTIVE TIMING OF COLLAGEN AND GLYCOSAMINOGLYCAN CONTENT 83

3.1. Abstract 83

3.2. Introduction 85

3.3. Methods 87

3.4. Results 91

3.5. Discussion 103

3.6. Acknowledgements 106

3.7. References 107

CHAPTER 4 : NORMAL HUMAN ARTICULAR CARTILAGE EXHIBITS IMPROVED TENSILE MECHANICAL PROPERTIES WITH PREPUBESCENT MATRUATION, DEPTH, AND COLLAGEN CONTENT 111

4.1. Abstract 111

4.2. Introduction 113

4.3. Methods 115

4.4. Results 118

4.5. Discussion 129

4.6. Acknowledgements 133

4.7. References 134

CHAPTER 5 : KINEMATIC MODEL OF COLLAGEN NETWORK REORIENTATION DURING MURINE FEMORAL CONDYLE GROWTH AND MATURATION 137

5.1. Abstract 137
5.2. Introduction 139
5.3. Methods 140
5.4. Results 148
5.5. Discussion 155
5.6. Acknowledgements 158
5.7. References 159
CHAPTER 6 : ARTICULAR CARTILAGE EXPLANT GROWTH IS DEPTH-VARYING, REGULATED, AND MEDIATED BY EXTRACELLULAR MATRIX 162
6.1. Abstract 162
6.2. Introduction 163
6.3. Methods 165
6.4. Results 169
6.5. Discussion 181
6.6. Acknowledgements 184
6.7. References 185
CHAPTER 7 : CONCLUSIONS 187
7.1. Summary of Findings 187
7.2. Discussion 190
7.3. References 194

LIST OF FIGURES

Figure 1.1. Overview of longitudinal bone development by endochondral ossification. 5
Figure 1.2. Postnatal development of cartilage and bone in human and murine knees. 6
Figure 1.3. . Equine articular cartilage development during growth and maturation. 9
Figure 1.4. Schematic of maturing collagen network architecture. 14
Figure 1.5. Bovine articular cartilage at fetal, calf, and adult stages. 15
Figure 1.6. Expansive mechanism of growth within central "intrinsic" articular cartilage. 21
Figure 2.1. Human knee articular cartilage often undergoes aging and osteoarthritis-related deterioration. 40
Figure 2.2. Crosstalk between cartilage and synovium is mediated by synovial fluid. 43
Figure 2.3. Growth and mineralization of the distal femur and proximal tibia. 44
Figure 2.4. Age- and depth-varying cell and matrix organization of articular cartilage. 47
Figure 2.5. Model of synovial joint growth and morphogenesis. 49
Figure 2.6. Schematic of normal osteochondral unit and spatiotemporal aspects of repair of cartilage defect repair. 56
Figure 2.7. Organ system and whole-body model of transport to, and from, synovial joints. . 57
Figure 2.8. Engineered tissue components. 58
Figure 2.9. Chondral and Osteochondral grafting techniques. 73
Figure 3.1. 3D renders of the mineralized components of the distal femur. 93
Figure 3.2. uCT scans of articular cartilage and cartilage-bone interface. 94
Figure 3.3. Effect of developmental stage on biomechanical properties. 95
Figure 3.4. Effect of developmental stage on cartilage composition. 96
Figure 3.5. Effect of maturation and ageing on cartilage compressive modulus and composition. 97
Figure 3.6. Relationship between biomechanical properties and cartilage composition. 98
Figure 4.1. Effect of developmental stage on tensile biomechanical properties. 121
Figure 4.2. Effect of developmental stage on tensile biochemical properties. 122
Figure 4.3. Relationship between cartilage tensile properties and cartilage composition. 123
Figure 5.1. Schematic model of collagen reorientation during growth. 145
Figure 5.2. The elliptic fit of the murine medial femoral condyle. 146
Figure 5.3. Maturation of the murine MFC. 150
Figure 5.4. PTA-stained murine MFC during postnatal maturation 151
Figure 5.5. Effect of maturation on gross measures of the MFC. 152

Figure 5.6. Effect of maturation on cartilage thickness. 153
Figure 5.7. Effect of deformation on collagen network. 154
Figure 6.1. Tracking cell displacement in articular cartilage at a cut surface during in vitro growth. 173
Figure 6.2. Cellular displacements in articular cartilage at a cut surface during in vitro growth. 174
Figure 6.3. Effect of treatment and culture duration on overall explant growth. 175
Figure 6.4. Effect of treatment and culture duration on viability after 15 days in culture 176
Figure 6.5. Effect of treatment and culture duration on overall explant growth. 177
Figure 6.6. Effect of treatment and culture duration on overall variation in strain with depth. 178
Figure 6.7. Effect of treatment and culture duration on overall variation in strain with lateral position. 179
Figure 6.8. Effect of treatment and culture on explant biochemical content. 180

LIST OF TABLES

Table 2.1. Repair strategies to treat chondral and osteochondral lesions. 59

Table 2.2. Orthobiologics for cartilage repair and osteoarthritis. 60

Table 3.1. Relative change in biomechanical and biochemical properties between human donors and bovine animals, relative to the human. 99

Table 3.2. Parameters of logistic fits of effect of maturation and ageing on cartilage compressive modulus and composition. 100

Table 3.3. Parameters of simple linear regression between compressive biomechanical properties and biochemical content. 101

Table 3.4. Parameters of multiple linear regression between compressive biomechanical properties and biochemical content. 102

Table 4.1. Coefficients for logistic fits of variation of tensile biomechanical properties during maturation and ageing. 124

Table 4.2. Coefficients for offset and logistic fits of variation of biochemical properties during maturation and ageing. 125

Table 4.3. Coefficients for univariate regression of tensile biomechanical properties with biochemical content in infants and children. 126

Table 4.4. Parameters of multiple linear regression between compressive biomechanical properties and biochemical content in infants and children. 127

Table 4.5. P-values for multivariate regression with the backward elimination procedure. 128

Table 5.1. MFC shape parameters from ellipse fit. 147

LIST OF ABBREVIATIONS

AC	articular cartilage
AECC	articular epiphyseal cartilage complex
BAPN	β-aminopropionitrile
C-ABC	chondroitinase ABC
CN	collagen network
CNO	collagen network orientation
COLL	collagen content
CT	computed tomography
DZ	deep zone
EC	epiphyseal cartilage
ECM	extracellular matrix
GAG	glycosaminoglycan content
H_{A0}	confined compression modulus
k_p	hydraulic permeability
MFC	medial femoral condyle
PG	proteoglycan
RES	residual content
SOC	secondary ossification center
SZ	superficial zone

ACKNOWLEDGEMENTS

I would like to acknowledge my graduate research advisor and dissertation committee Chair, Dr. Robert Sah. Thank you for your mentorship and training, and for the countless hours of discussion during this endeavor. I have grown much throughout this journey and will cherish my time in the Cartilage Tissue Engineering Lab. I would also like to thank the other members of my dissertation committee: Dr. Shengqiang Cai, Dr. Stephanie Fraley, Dr. Esther Kwon, and Dr. Koichi Masuda for their valuable questions, feedback, and suggestions.

I am especially thankful for the members of the Cartilage Tissue Engineering Lab who have helped and supported me. I would like to thank Nasim Eshragh Nia, Alborz Jelvani, Rebecca Drake, Ismael Muñoz, Jason Caffrey, and Xueyi Wan who have helped to keep me inspired and motivated, and whose friendships I cherish. This dissertation would not have been possible without Dr. Albert Chen and Van Wong whose expertise and assistance have been essential. I am also indebted to the present and past members of the CTE lab: Danielle Pham, Sean Ewalt, Delaney Donnelly, Kaitlyn Strandberg, Jay Chen, Timothy Liu, Leening Liu, Chris Long, Marieke Nijhuis, Anna Pia Bonuomo, as well as many others.

I am forever grateful for my family and all the friends who have provided endless encouragement. I thank my parents, Ethel and Weirner Gacasan, my Lola, and my brother Camilo Anthony for their love and support. I am grateful to my aunt and uncle, Tita Pie and Tito Jun who took me in when I first arrived in San Diego. I have been blessed to have made excellent friendships and bonds throughout this endeavor and would especially like to thank my roommate Lauren, as well as Ate Charisse, Dennis, and baby Charlotte for their friendship and support.

Chapter 2, in full, was published in the first edition of *Orthobiologics: Scientific and Clinical Solutions for Orthopaedic Surgeons* by Wolters Kluwer. Thanks to co-author Robert L. Sah, and book editors Roy K. Aaron. and Scott P. Bruder.

Chapter 3 is being prepared for submission for publication in *Journal of Bone and Joint Surgery.* The dissertation author was the primary author and thanks to co-authors Yehudit H. Gerassi, Albert C. Chen, Christine L. Farnsworth, William D. Bugbee, Kevin G. Shea, Eric W. Edmonds, and Robert L. Sah. This work was supported by NSF GRFP and the Wu Tsai Human Performance Alliance.

Chapter 4 is being prepared for submission for publication in *American Journal of Sports Medicine.* The dissertation author was the primary author and thanks to co-authors Albert C. Chen, Christine L. Farnsworth, William D. Bugbee, Kevin G. Shea, Eric W. Edmonds, and Robert L. Sah. This work was supported by NSF GRFP and the Wu Tsai Human Performance Alliance.

Chapter 6 is being prepared for submission for publication in *Journal of Orthopaedic Research.* The dissertation author was the primary author and thanks to co-authors Kyle D. Jadin, Sean S. M. Ewalt, Danielle H. Pham, and Robert L. Sah. This work was supported by NSF GRFP and the Wu Tsai Human Performance Alliance.

I would also like to acknowledge support by the National Institutes of Health and the UC San Diego Frontiers of Innovation Scholarship Program.

VITA

2016 Bachelor of Science, Biomedical Engineering
Texas A&M University, College Station, Texas

2019 Master of Science, Bioengineering
University of California San Diego, La Jolla, California

2023 Doctor of Philosophy, Bioengineering
University of California San Diego, La Jolla, California

BOOK CHAPTERS

Gacasan EG, Sah RL: Orthobiologics overview for cartilage repair. In: Orthobiologics: Scientific and Clinical Solutions for Orthopaedic Surgeons 1ed, Aaron RK, Bruder SP Eds.: Wolters Kluwer 2023:85-102.

Gacasan EG, Sah RL: Articular cartilage repair: Augmentation, regeneration, replacement, and substitution. In: Orthopaedic Basic Science: Foundations of Clinical Practice 5ed, Aaron RK Ed.: Wolters Kluwer 2021:415-432.

JOURNAL ARTICLES

van Rosmalen L, Zhu J, Maier G, **Gacasan EG**, Zhemchuzhnikova E; Razu S, Deota S, Ramasamy RK, Sah RL, McCulloch AD, Hut RA, Panda S. Multi-organ Transcriptome Atlas of a Mouse Model of Relative Energy Deficiency in Sport (REDs). *Cell Metab.* submitted

Abraham AA, Means AK, Clubb Jr FJ, Fei R, Locke AK, **Gacasan EG**, Coté GL, Grunlan MA. Foreign body reaction to a subcutaneously implanted self-cleaning, thermoresponsive hydrogel membrane for glucose biosensors. *ACS Biomater Sci Eng*. 2018;4:4104-11.

Gacasan EG, Sehnert RM, Ehrhardt DA, Grunlan MA. Templated, macroporous PEG-DA hydrogels and their potential utility as tissue engineering scaffolds. *Macromol Mater Eng*. 2017;302:1600512.

SELECTED ABSTRACTS

Gacasan EG, Chen AC, Farnsworth CL, Bugbee WD, Shea KG, Edmonds EW, Sah RL. Compressive Properties of Normal Human Articular Cartilage are Enhanced Between Infant, Child, and Adult and Associated with Collagen and Glycosaminoglycan Deposition. *Proc Ped Orthop Soc North Am 2018.* 2024.

Gacasan EG, Chen AC, Farnsworth CL, Bugbee WD, Shea KG, Edmonds EW, Sah RL. Compressive properties of normal human articular cartilage are enhanced between infant, child,

and adult and related to distinctive timing of collagen and glycosaminoglycan deposition. *Trans Orthop Res Soc*. 2024:1576

Eshragh Nia N, **Gacasan EG**, Jelvani A, Wan X, Sah RL. Proliferating chondrocytes are present in situ in immature bovine articular cartilage explants mostly near the articular surface. *Trans Orthop Res Soc*. 2024:1568

Weber C, **Gacasan E**, Moore T, Sah R, Cooper K. The development and evolution of mammalian tail anatomy and vertebral proportion. *Soc Dev Biol-Pan Am Soc Evo Dev Biol.* 2023.

Gacasan EG, Pham DH, Weber CM, McCulloch AD, Cooper KL, Sah RL. Volumetric growth of distal femoral cartilage and bone during murine postnatal development follows Gompertz Law. *Int Cart Rep Soc.* 2022:853.

Weber C, **Gacasan E**, Moore T, Sah R, Cooper K. The development and evolution of mammalian tail anatomy and vertebral proportion. *Soc Dev Biol-Pan Am Soc Evo Dev Biol.* 2022:250.

Gacasan EG, Jadin KD, Schumacher BL, Chen AC, Sah RL: Growth of articular cartilage explants in depth-varying, regulated, and mediated by extracellular matrix. *Trans Orthop Res Soc.* 2020:1480.

Caffrey JP, Nia NE, Jelvani A, **Gacasan EG**, Walsh KC, Hughey VS, Caccam BT, Liao A, Alvarado-Herrera EG, Mir NA, Chakraborty M. Joint-scale mechano-pathology in post-traumatic osteoarthritis: ex vivo imposed gait-like loading of ACL-transected rabbit knees induces abnormal kinematics and cartilage degeneration. *OARSI World Congress.* 2020:549.

ABSTRACT OF THE DISSERTATION

BIOMECHANICS AND MECHANOBIOLOGY OF ARTICULAR CARTILAGE GROWTH AND MATURATION IN THE DISTAL FEMUR

by

Erica G. Gacasan

Doctor of Philosophy in Bioengineering

University of California San Diego, 2023

Professor Robert L. Sah, Chair

Adult articular cartilage can function normally over decades as the load bearing, low-friction, and wear-resistant tissue in synovial joints. The primary structural macromolecules of cartilage, collagen, and proteoglycan, contribute to mechanical function and vary during antenatal growth in animal models. Collagen and proteoglycan content and assembly also affect cartilage swelling pressure and growth in vitro. However, the extent and time-course of

variation in mechanical function and biochemical content during normal human development is unclear. In addition, the way in which cartilage attains its adult form, covering an increasing joint surface area until adulthood, is not well understood. Thus, the objectives of this thesis were to (1) describe orthobiologic approaches to cartilage repair, determine maturation-related variation in (2) compressive and (3) tensile mechanical functions, and (4) biochemical content during normal human postnatal development, and delineate how (5) depth-varying tissue growth leads to formation of mature collagen network architecture, and how (6) regulatory cytokines and growth factors, as well as alterations in tissue content, affect in vitro cartilage growth. The load-bearing compressive and tensile properties of articular cartilage improved between infants, children, and adults. In particular, the equilibrium confined compression modulus increased 3-fold between children and adults, and tensile modulus and strength peaked in children. Enhanced mechanical function was positively correlated with increased collagen and glycosaminoglycan. In a kinematic model of collagen reorientation, using the mouse medial femoral condyle as a model organ, depth-varying axial and lateral deformations *in vivo*, wherein the axial stretch increases exponentially, and the lateral stretch decreases linearly, with depth from the surface yields mature-like collagen orientations. *In vitro* cartilage explant growth was regulated and was altered by the assembly of collagen and content of proteoglycan. Immature cartilage explant growth was primarily axial, with both axial and lateral growth strains highest near the articular surface. Axial and shear growth strains were enhanced in the superficial and deep cartilage by mitigation of collagen crosslink formation and diminished by removal of proteoglycans. The above studies establish benchmarks for postnatal maturation of normal human femoral condyle. The time course of variation in cartilage compressive and tensile properties during maturation is distinctive between humans and bovines and implicates

differences in loading demands, as well as onset of puberty as mechanisms of cartilage maturation. Depth-varying growth mechanisms during maturation may allow for concurrent expansion of the tissue near the articular surface and maturation of the deeper regions. Modulation of in vitro growth during assembly or design of engineered tissues may be a useful tool in recapitulating native-like structural properties.

CHAPTER 1

INTRODUCTION

1.1.General introduction to the dissertation

The functional biomechanical properties of mature articular cartilage result from the combinatorial effects of mechanical loading, from normal behaviors as well as from growth-associated deformations that result in the mature joint shape, and cellular metabolic processes. During postnatal development, functional adaptation of cartilage and bone geometries occurs to provide increased joint congruence and stability. These changes in joint shape are presupposed by alterations in the immature cartilaginous template whose properties are in part a reflection of maturation-related variation in cartilage metabolism, including matrix synthesis and degradation and the accompanying alterations in cellular proliferation, differentiation, and apoptosis of resident chondrocytes. To study the relationships between joint growth and cartilage function, an understanding of distal femoral development and cartilage maturation is needed.

The objectives of this thesis were to (1) describe orthobiologic approaches to cartilage repair, determine maturation-related variation in (2) compressive and (3) tensile mechanical functions, and (4) biochemical content during normal human postnatal development, and delineate how (5) depth-varying *in vivo* tissue growth leads to formation of mature collagen network, and (6) how regulatory cytokines and growth factors, as well as alterations in tissue content, affect *in vitro* cartilage growth.

Chapter 1 beings with a brief synopsis of early joint development and summarizes the structure, function, and composition of the mature joint and articular cartilage. Maturation-related

variation of key components of articular cartilage: collagen, proteoglycan, and chondrocytes, are outlined. A discussion of the mechanisms of growth follows. The chapter concludes with a discussion about models used to describe tissue growth and maturation.

Chapter 2, which was published in the first edition of *Orthobiologics: Scientific and Clinical Solutions for Orthopaedic Surgeons* by Wolters Kluwer and edited by Roy K. Aaron. and Scott P. Bruder, extends the introduction by providing an overview of orthobiologics for articular cartilage repair. The chapter begins with summaries of the hierarchal structure of articular cartilage, the biology of indwelling chondrocytes and their precursors, and its ECM composition, turnover, and function. The chapter reviews the three major components of cartilage orthobiologics: scaffolds, cells, and signals. In addition, within this context, established and emerging orthobiologic approaches to cartilage repair are described.

Chapter 3, which is currently being prepared for submission to *Journal of Bone and Joint Surgery*, examines the relationship between articular cartilage composition and compressive function in human infants, children, and adults. The compressive biomechanical properties of cartilage from the distal femurs of infants, children, and adults were determined and related to age and tissue composition. The implications of the distinctive timing of collagen and glycosaminoglycan deposition between humans and bovines is discussed.

Chapter 4, which is currently being prepared for submission to *American Journal of Sports Medicine*, examines the relationship between articular cartilage composition and tensile function in human infants, children, and adults. The tensile biomechanical properties of cartilage from the distal femurs of infants, children, and adults were determined and related to age, depth, and tissue composition. The implications of the variation in tensile properties during prepubescent maturation, depth, and collagen content are discussed.

Chapter 5 describes a theoretical model which relates immature cartilage growth to kinematic reorientation of the collagen network. Joint-scale growth strains during postnatal maturation were determined, based on the growth of the murine MFC as determined from measurements of microcomputed tomography datasets of mice ages P0 to P42, and fit to logistic equations. For the cases of (1) axial growth strain, (2) lateral growth strain, and (3) combined axial and lateral growth strain, and either (A) uniform or (B) depth-varying axial and lateral strain, the resulting collagen network orientations from the immature to mature stages were computed.

Chapter 6, which is currently being prepared for submission to *Journal of Orthopaedic Research,* examines the effects of regulation and extracellular matrix on *in vitro* immature cartilage explant growth. Chondrocyte function was regulated by TNF-α, and the explant biophysical state altered by diminishing GAG content by enzymatic treatment with chondroitinase-ABC, and by inhibition of collagen crosslinking by treatment with β-aminopropionitrile (BAPN). Culture-associated variation in tissue geometry and cellular position were evaluated to assess spatial-variation in growth. The implications of spatially varying growth on cartilage maturation are discussed.

Chapter 7 summarizes the major findings of the studies presented here and discusses the implications of this work on understanding the relationship between joint growth and cartilage function and on developing strategies for cartilage repair and regeneration.

1.2. Early joint development and maturation

In early embryonic limbs, joint development begins with condensation of mesenchymal cells followed by chondrocyte differentiation and bone formation. At each future joint site, an interzone consisting of mesenchymal cells forms. During embryonic development, the interzone thickens and interzone cells give rise to the tissues at each opposing epiphyseal end, forming the articular epiphyseal cartilage complex (AECC) and the nascent tissues of the joint capsule, ligaments, and other perichondral tissues.[1-3]

At birth, the epiphyses of many mammals, including mice, rabbits, and humans, are entirely cartilaginous. In skeletally immature individuals, the AECC collectively refers to the epiphyseal cartilage within the epiphysis which will form the secondary ossification center (SOC) as well as the articular cartilage.[3] During endochondral ossification, chondrocytes within the cartilage analgen proliferate, produce matrix, and hypertrophy, then at a certain stage of development, the matrix surrounding the hypertrophic chondrocytes mineralizes (**Fig. 1**).[4] Mesenchymal stem cells enter the cartilage analgen through vascular invasion and differentiate into osteoblasts, which synthesize bone matrix on the calcified cartilage, and ultimately results in formation of the primary and secondary ossification centers.[4-6] Following development of the SOC within the epiphysis, the cartilage between the SOC and the metaphysis is known as growth plate, or physeal cartilage, and cartilage at the surface of the long bone is known as hyaline articular cartilage.

The shape and size of long bones and their articulating surfaces change rapidly during postnatal development and maturation through coordinated events within the growth plate and epiphyseal cartilage (**Fig. 2**). During maturation, the rates of proliferation, hypertrophy and mineralization vary with age and species as well as bone and joint location and region to drive bone elongation as well as produce a wide range of joint shapes.[7-16]

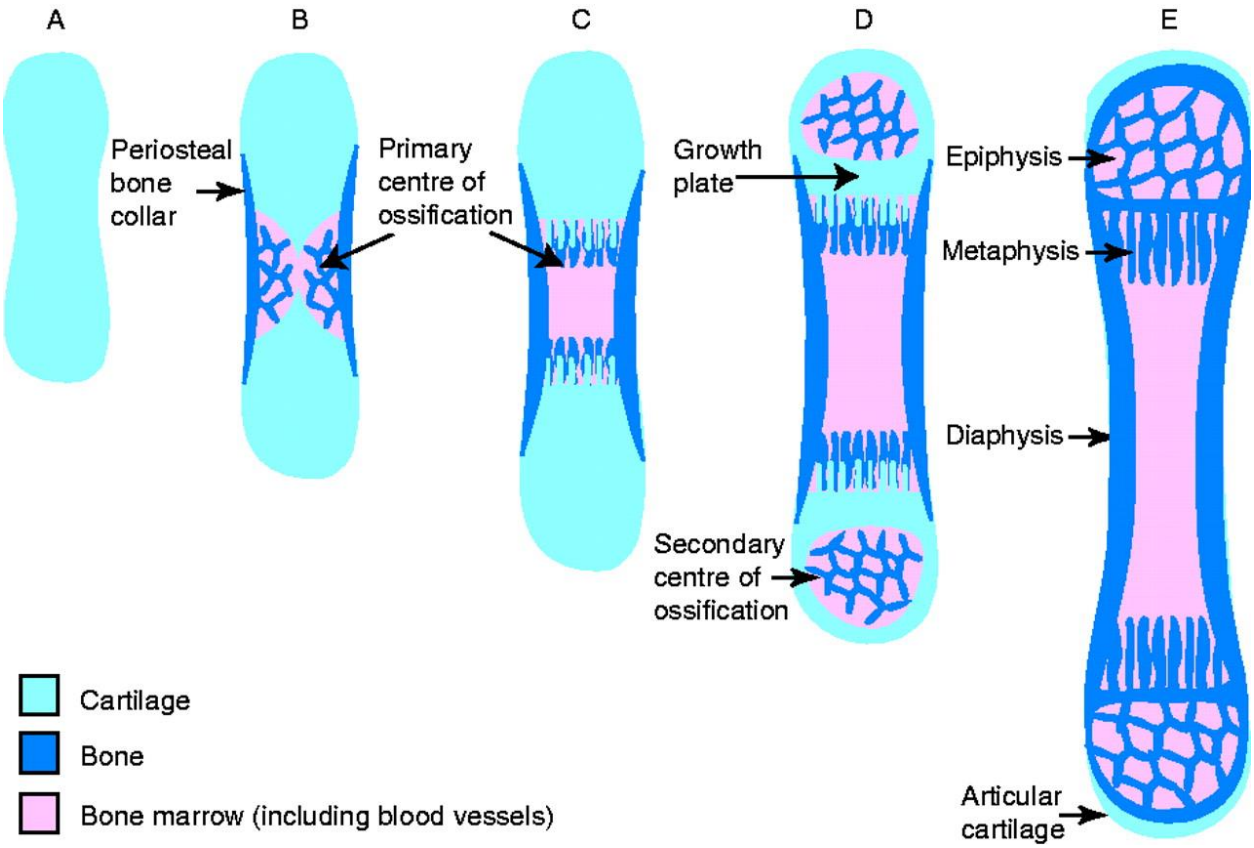


Figure 1.1. Overview of longitudinal bone development by endochondral ossification. (**A**) Nascent cartilage model. (**B**) A periosteal bone collar has formed and formation of the primary center of ossification has been initiated. (**C**) The primary center of ossification is starting to expand towards the ends of the cartilage model. (**D**) The secondary centers of ossification have formed at each end of the bone, leaving a cartilaginous growth plate between primary and secondary centers of ossification. (**E**) Skeletal maturity has been achieved, with complete replacement of the growth plate cartilage by bone. The only cartilage remaining is the articular cartilage at the ends of the bone. Figure adapted from literature.[5]

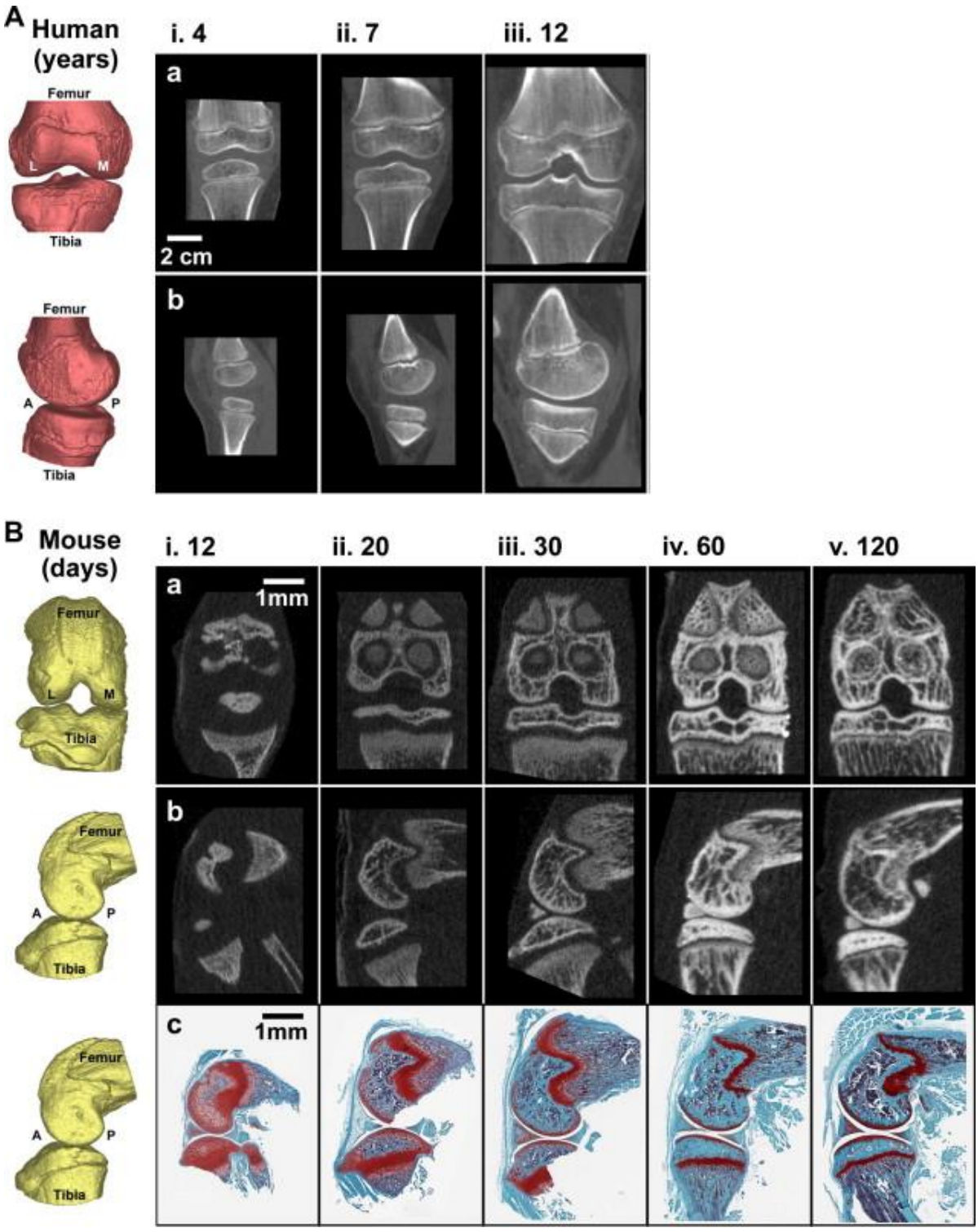


Figure 1.2. Postnatal development of cartilage and bone in human and murine knees. (**A**) Clinical CT scans of the asymptomatic human knee from (**i–iii**) ages 4 to 12 years, and (**B**) μCT scans and Safranin-O sections of C57BL/6 wild-type mouse knees from (**i–v**) postnatal days 12 to 120, in (**a**) coronal and (**b, c**) sagittal views. **A**, anterior; **L**, lateral; **M**, medial; **P**, posterior. Figure adapted from literature.[16]

1.3. Structure, function, and composition of mature synovial joints, osteochondral unit, and articular cartilage

Synovial joints are found between articulating bones and facilitate decades of stable and pain-free movement. The synovial joint unites long bones, whose articulating surfaces are covered with articular cartilage, via the joint capsule and contains synovial fluid as well as supporting ligaments. The capsule consists of a fibrous outer layer connecting the articulating bones, and an inner synovial layer, which secretes synovial fluid. The synovial fluid acts as a biomechanical lubricant, and as a conduit for distribution of metabolites, cellular waste, and soluble signaling factors within the joint. The articular cartilage is the load-bearing connective tissue which covers the bones in synovial joints and provides a low-friction, wear-resistant surface.

In skeletally mature individuals, long bone epiphyses are comprised of a thin layer of uncalcified articular cartilage that is attached to underlying trabecular bone by a subchondral plate composed of calcified cartilage and the subchondral bone plate.[17] The tidemark denotes the boundary between the articular cartilage and calcified cartilage, and the cement line denotes the boundary between the calcified cartilage and subchondral bone plate.[18,19] The combined unit of articular cartilage and subchondral bone, from the surface to the beginning of the trabecular bone is defined as the osteochondral unit. The osteochondral unit transmits joint loads between the cartilage and bone via the cartilage surface, which allows articulation, the subchondral bone, which provides a harder physical structure to withstand compressive stresses, and the calcified cartilage and subchondral bone plate, which transfers load between the cartilage and bone.

The articular cartilage provides a load bearing, low permeability, low friction, and wear-resistant surface for pain-free joint movement. Regional, site, and depth-dependent variation in tissue organization is critical to normal function under complex loading.[20,21] Healthy adult articular cartilage is composed of resident chondrocytes (~2% v/v), extracellular matrix (~20 – 40% w/w),

and water (~60 – 80% w/w).[22] The extracellular matrix is largely comprised of collagen type II (~200 mg/g wet weight) and proteoglycan (~25 mg/g wet weight).[22] The chondrocytes produce and maintain the cartilage matrix, balancing its synthesis and degradation. The collagen network contributes to overall tissue integrity and the resistance of cartilage to tension. Negatively charged proteoglycans, mainly aggrecan, are entrapped within the collagen network, and contribute to compressive resistance, providing a high osmotic pressure within the tissue. The structure and content of collagen, proteoglycan, and chondrocytes within articular cartilage vary with maturation as well as depth from the articular surface (**Fig. 3**).

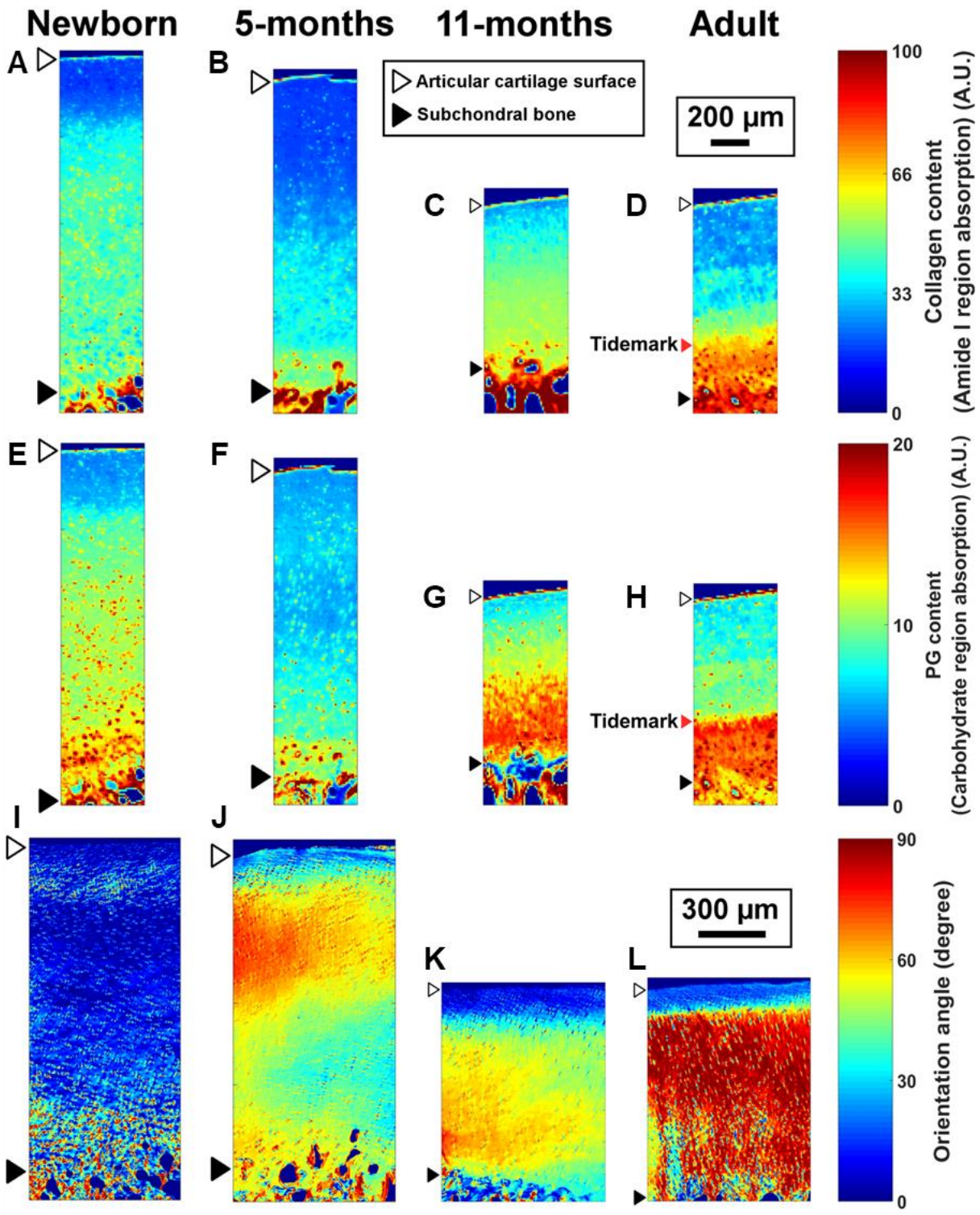


Figure 1.3. . Equine articular cartilage development during growth and maturation. (**A-D**) Collagen content (amide I absorption), (**E-H**) PG content (carbohydrate region), and (**I-L**) mean orientation angle of collagen fibril network (PLM) from (**A,E,I**) newborn, (**B,F,J**) 5-month, (**C,G,K**) 11-month, and (**D,H,L**) adult equine articular cartilage. Figure adapted from literature.[23]

1.4.Cartilage structure and composition varies with maturation

1.4.1. Maturation-related variation in collagen and collagen network architecture

Collagen network architecture, density, and crosslinking vary with maturation and growth. At birth, the perinatal collagen architecture is relatively homogenous with randomly oriented fiber network, becomes discontinuous with zones of preferred tangential orientation at the articular surface and in the deeper cartilage are separated by regions of more isotopically oriented fibers, before attaining the arcading structure characteristic of mature articular cartilage (**Fig. 4**).[23-25] At maturity, within the central load-bearing articular cartilage, the collagen network possesses an arcade-like structure, wherein the collagen orientation is a central characteristic of each zone. Collagen fibrils within the superficial zone are oriented parallel to the surface and deep zone fibrils are oriented roughly perpendicular to the articular surface and anchored in the calcified cartilage layer.[24,26,27] The tangential, also called the middle or radial, layer is the transitional zone between the superficial and deep layers where the collagen fibril orientation is less clearly defined. In addition, with cryofracture scanning electron microscopy, fibers from the periosteum, adjacent to the cartilaginous joint surface, are mechanically integrated, either interdigitated or continuous with, the superficial zone.[28] In mature articular cartilage, the superficial layer, tangential, and deep layers make up ~10-20%, ~10-20% , and ~60-80% of the cartilage thickness, respectively.[29,30]

Within the articular cartilage, collagen density increases during maturation from ~60 mg/ml to ~120 mg/ml between fetal and adult bovids and mature crosslinks form.[31,32] The enzyme lysyl oxidase mediates covalent intermolecular and intramolecular crosslinking of collagen II, IX and XI fibrils via oxidation of hydroxylysine residues to hydroxylysyl aldehydes which, through a series of reactions, lead formation of immature dehydroxylysinorleucine (DHLNL) crosslinks, then ultimately to stable pyridinoline crosslinks.[33-35] *In vivo*, there is a decrease in immature cross-links, and increase in mature pyridinoline crosslinks between immature and mature cartilage.[31,36,37]

Collagen orientation, density, and crosslinking are integral to the biomechanical function of articular cartilage. Tensile samples aligned either parallel or perpendicular to the main direction of the collagen network exhibit relatively high or low tensile integrity, respectively, when taken from mature tissues.[38-42] In addition, maturation-associated variation in tensile and compression mechanical properties are associated strongly with variation in the contents of collagen and pyridinoline crosslinks. [31,32,36] For instance, with growth from the fetus to adult, the 391-1060% increase in the equilibrium and dynamic tensile moduli and strength of bovine superficial zone cartilage correlated with an 98% increase in collagen concentration (per wet weight) and 730% increase in pyridinoline cross-link concentration.[31]

1.4.2. Proteoglycans and aggrecan variation with maturation

In the cartilage matrix, aggrecan is the major proteoglycan and forms large aggregates of ~2 MDa.[43] Sulfate and carboxylate groups on aggrecan glycosaminoglycan chains provide the tissue with a fixed negative charge that increases the tissue's propensity to swell and resist compression.[44,45]. The balance between the swelling propensity of proteoglycan molecules and the restraining function of the collagen network governs the load-bearing biomechanical function of cartilage.[46,47]

At maturity, the proteoglycan composition of articular cartilage varies with depth from the articular surface. With increasing depth, proteoglycan content increases ~2-3 fold.[23,48,49]. In contrast to collagen density, the maturation-associated changes in the GAG content of articular cartilage are small,[23,31,49] and in bovids is maintained at ~25 mg/g WW from fetal to adult stages.[32]

1.4.3.Chondrocyte density and organization vary with maturation and contribute to growth

The primary function of chondrocytes in mature articular cartilage is to synthesize and

maintain the extracellular matrix, including collagen and proteoglycan, such that it can withstand loading and facilitate articulation. Unlike other cell types, mature chondrocytes are isolated within a voluminous extracellular matrix and have depth-varying organization.[50] Cell density decreases with depth from the articular surface,[51-53]and cells are arranged into characteristic groups ranging from horizontal clusters at the surface to vertical columns in the deep region (**Fig. 5**).[15,50,51]

In immature tissues, chondrocyte organization is intricately linked to growth. Near the articular surface, horizontal clusters of tightly packed, flattened chondrocytes are observed, whereas deeper in the tissue, cells are less dense but have a more homogeneous arrangement.[50,54,55] Chondrocytes in immature tissues may contribute to overall growth, or an increase in tissue volume, by (1) proliferation and production cells, (2) increased cell volume as the cell becomes hypertrophic, and (3) matrix secretion.

Proliferating chondrocytes have been identified near the articular surface of immature tissue,[56-59] as have progenitor or stem cells.[9,60-67] It has been postulated that the superficial cell population, at birth, serves as progenitors for the entire mature articular cartilage, and that the proliferation of cells within the superficial zone leads to lateral expansion of articular surface, via planar cell division, as well as giving rise to daughter cells in a more rapidly proliferating cell population, via vertical cell division, that is responsible for vertical tissue growth.[9,64,65,67]

A separate population of chondrocyte progenitor cells are located within peri-articular tissues including the groove of Ranvier. As the epiphyses of long bones grow during postnatal maturation, the growth plate and articular cartilage must also expand to continue to span the bone diameter and fully cover the epiphyseal end. Progenitor cells within the groove of Ranvier move gradually toward the growth plate and contribute to transverse expansion and longitudinal column formation during postnatal growth.[68] It is hypothesized these progenitor cells, recruited from

periarticular sites such as the groove of Ranvier, also help to sustain postnatal epiphyseal expansion through adulthood.[1,64,69]

Chondrocytes may also contribute to cartilage maturation through substantial increases in cell size and accumulation of matrix. For instance, in the growth plate, chondrocyte hypertrophy and matrix accumulation are the primary contributors to skeletal elongation.[11,70,71] In mice, after 14 days postnatal, zone-specific increases in cell volume were major drivers of tissue thickening, while cell proliferation or death played minor roles. [64] In addition, immature cartilage has an increased biosynthetic capacity,[72-74] and elevated gene expression of cartilage matrix proteins compared to mature chondrocytes.[75] Thus, cellular proliferation and matrix production have time varying roles in cartilage maturation.

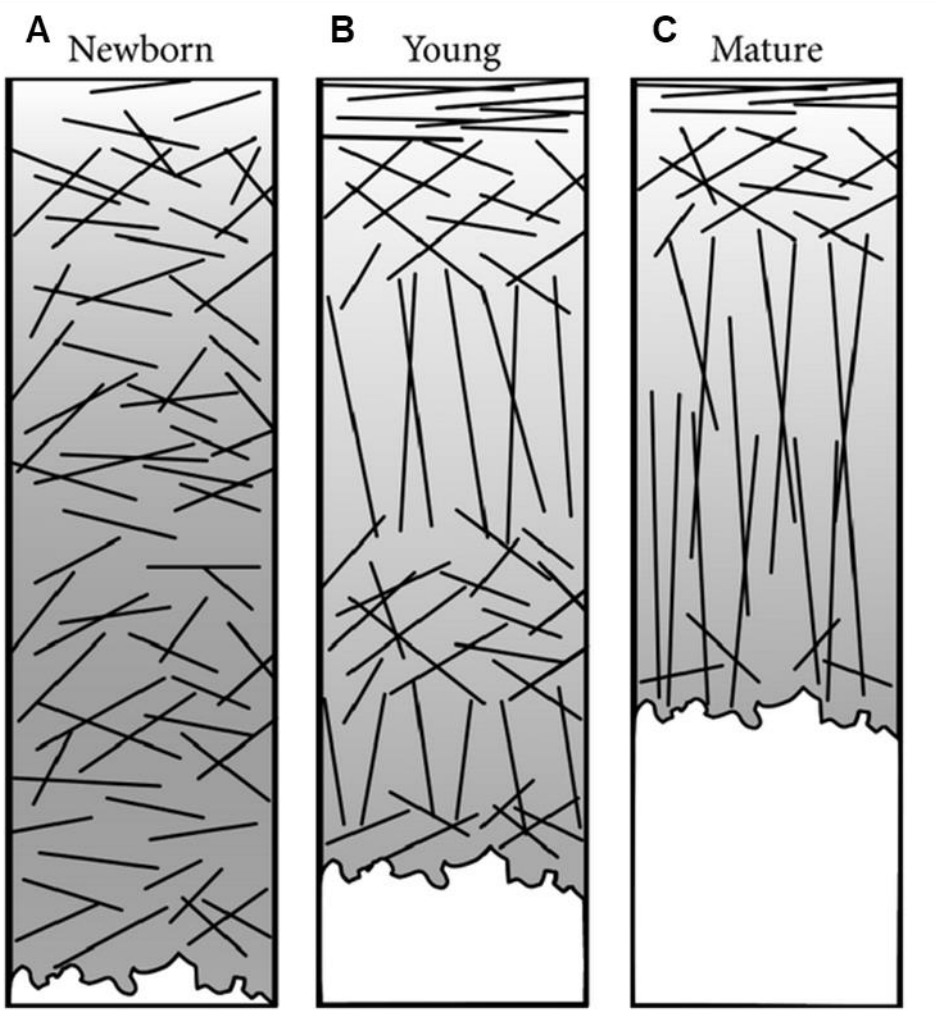


Figure 1.4. Schematic of maturing collagen network architecture. Collagen network architecture in the (**A**) newborn, (**B**) young, and (**C**) mature states. Figure adapted from literature.[76]

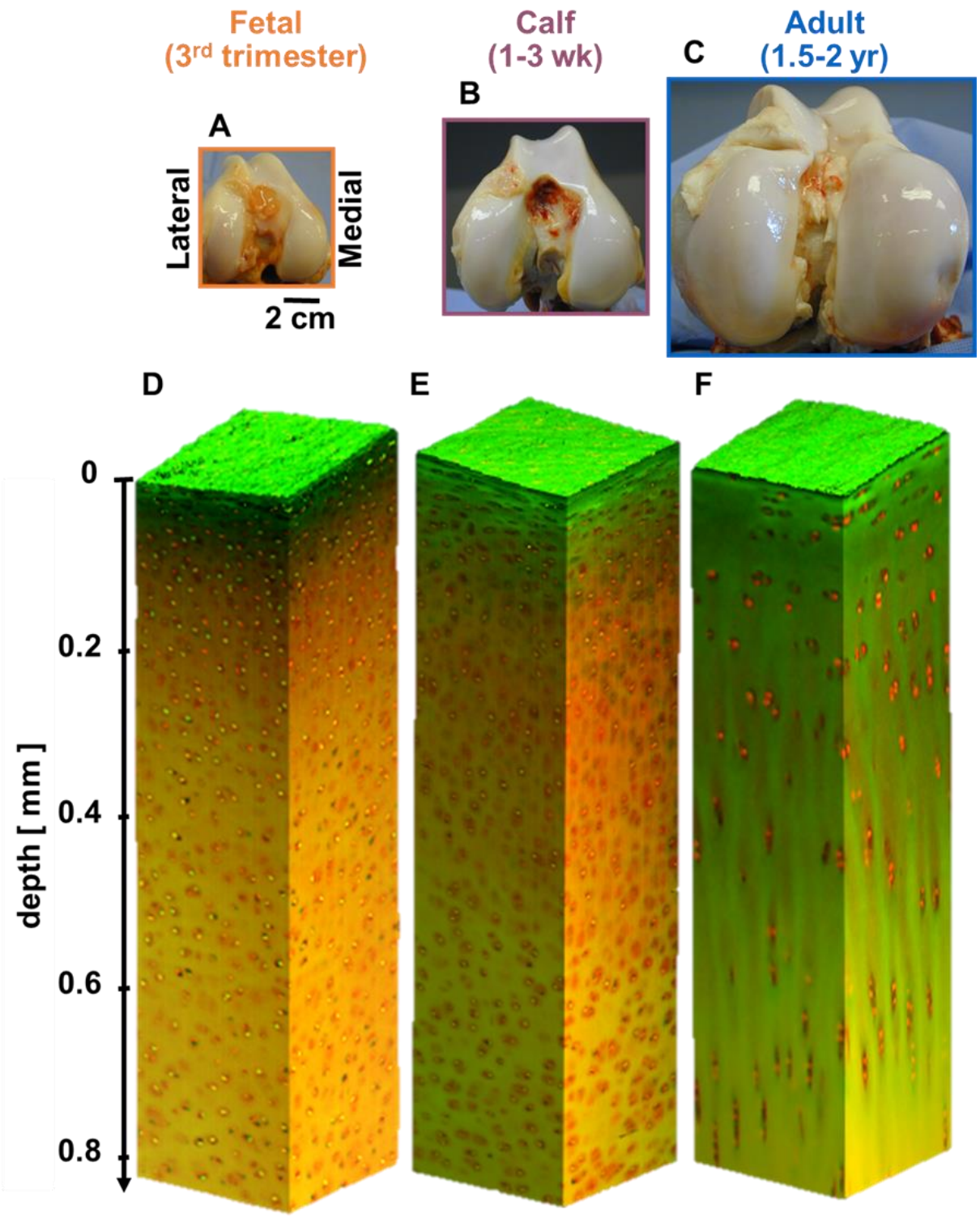


Figure 1.5. Bovine articular cartilage at fetal, calf, and adult stages. Bovine articular cartilage at fetal, calf, and adult stages. (**A-C**) Gross and (**D-F**) 3-D image renders of bovine articular cartilage at different growth stages. Images of fetal (**A,D**), calf (**B,E**), and adult (**C,F**) tissue. Figure adapted from literature.[54]

1.5. Maturation and growth mechanisms of the articular epiphyseal cartilage

1.5.1. Cartilage tissue growth relies on appositional and interstitial growth mechanisms

Articular cartilage growth occurs through biological activities of the indwelling chondrocytes that result in an increase in cell or matrix volume. Soft tissue growth is often described in terms of appositional and interstitial mechanisms, wherein the balance between these mechanisms may underlie alterations in tissue structure, composition, and function during maturation.

Appositional growth is growth which occurs at a surface by addition of new cells and tissues without altering the original tissue composition or structure by remodeling.[77] For example, appositional growth occurs during long-bone extension, where growth plate cartilage is successively calcified to elongate the bone. During articular cartilage maturation, the presence of progenitor cells within the superficial zone are evidence of appositional growth near the surface.[56] Superficial zone progenitors proliferate near the articular surface, contributing to an increase in tissue volume without altering the structure and content of deeper tissue. Appositional growth may also occur at the joint boundaries, such as the zone of Ranvier,[78] where tissue may be added from the joint periphery without altering the structure of the central region. Interstitial growth is defined as growth which results from formation of new cells and tissues within the existing tissue mass that is accompanied by remodeling or deformation of the surrounding tissue to incorporate the new material.[77] Chondrocytes throughout the cartilage contribute to tissue growth through hypertrophy and matrix accretion leading to decreased chondrocyte density.[54,55,79]

Thus, cartilage growth proceeds via a combination of appositional and interstitial growth. In the tibial plateau of adult tissues there are two central areas with, by mass-weighted average, older matrix (one in each of the lateral and medial sides) surrounded by younger later-formed cartilage towards the periphery. This data suggests that cartilage formation develops initially from

each condyle center and continuous radially outwards.[80] Within the intrinsic tissue, simultaneous appositional and interstitial growth near the articular surface as well as interstitial growth in the deeper cartilage contribute to "expansive growth" (**Fig. 6**). Expansive cartilage growth is accompanied by "circumferential growth" where tissue is continually added by apposition from the joint periphery and undergoes interstitial growth without altering the structure of the central intrinsic region. Understanding these modes of growth and the underlying biologic processes may help to elucidate maturation-dependent structure-function relationships within the articular cartilage.

1.5.2. Cartilage growth and maturation is regulated by biomechanical and biochemical signals

Cartilage responds to a variety of mechanical signals, including compression, tension, and shear, which can influence its growth, maturation, and homeostasis. Mechanical stimulation of tissues can differentially stimulate, or inhibit, matrix biosynthesis as well as affect cell behavior and phenotype based on the loading mode, pattern, duration, and intensity.

In vivo and *in vitro* alterations in mechanical loading influence the development and metabolism of articular cartilage. Deviations from normal loading during prenatal development, via oligohydramnios, embryonic paralysis, and restriction of fetal movement, lead to joint malformation and alteration in cartilage biochemical and mechanical properties.[81-83] *In vitro,* application of mechanical stimuli to cartilage explants alters chondrocyte metabolism. Static compression inhibits synthesis of PGs and proteins,[84-88] whereas dynamic compression stimulates matrix production depending on the frequency and amplitude of the stimulus.[84,89-91]

The collagen network at the articular surface has a preferred orientation which is revealed by split-lines at the surface, and which may reflect mechanisms of joint morphogenesis. During postnatal maturation of the murine distal femur, principal growth strains are directed medially

along the load-bearing region of the MFC.[16] Accordingly, cartilage split lines, which are indicative of collagen fibril orientation at the articular surface, vary characteristically across the joint surface. In the mature distal femur, split lines are oriented primarily in the medial-lateral direction at the load-bearing regions of the condyles, and in the proximal-distal direction within the patellofemoral groove.[92] Thus, as the femur increases in volume and changes in size, superficial zone collagen fibrils, which are anchored to the periosteal fibers at the periphery of the articular surface,[28] may become tensioned and align in the principal direction of growth.

A multitude of signaling proteins and molecules help to direct skeletal maturation and morphogenesis. Signals, including fibroblast growth factors (FGFs), insulin-like growth factors (IGFs), Indian hedgehog (IHH), bone morphogenetic protein (BMP), Wnt signals, and proteins of the TGF-β superfamily, regulate chondrogenesis and maintenance of chondrogenic phenotype, including the balance between synthesis and degradation of collagen and proteoglycan.[93-95] For instance, in calf articular cartilage explants, culture in medium supplemented with serum, IGF-1 or BMP-7 resulted in expansive tissue growth, stimulation of proteoglycan deposition but not of collagen, and a diminution of tensile integrity, whereas stimulation with TGF-β1 resulted in tissue homeostasis and maintenance of explant size, composition, and tensile function .[96]

Net deposition of collagen and formation of collagen crosslinks during cartilage maturation contributes to enhanced tissue tensile strength. During synthesis and assembly of procollagen into collagen fibril segments and into collagen fibrils, collagen crosslinks formation is mediated by the enzyme lysyl oxidase. Lysyl oxidase-mediated collagen crosslink formation can be inhibited with a lathyrogen such as β-aminopropionitrile (BAPN), which binds covalently and irreversibly to the active site of the enzyme.[97-100] BAPN causes a ~50% inhibition of lysyl oxidase at a concentration of 3–5 μM, [99] with negligible effect on matrix synthesis by chondrocytes.[98,101] In calf articular

cartilage explants, culture in medium supplemented with BAPN resulted in an increase in tissue size and decrease in tensile integrity, compared to serum-supplemented culture, without affecting collagen and proteoglycan content.[102] Thus, BAPN is a useful tool to study the effect of dysfunctional collagen network formation on collagen network integrity during cartilage growth.

In contrast, the collagen content and collagen crosslink density which increase throughout maturation, there is little or no change in the GAG content during postnatal growth.[103-105] *In vivo,* aggrecan molecules are susceptible to degradation by a variety of proteinases including MMPs and aggrecanases.[106-109] In addition, chondroitinase ABC (C-ABC) depolymerizes chondroitin sulfate (CS) and dermatan sulfate (DS) and, to some degree, hyaluronic acid (HA), thus affecting CS and DS-containing molecules, including aggrecan and proteoglycan aggregates.[110] Since collagen and collagen network arrangement are generally unaffected by C-ABC treatment,[111-113] Calf cartilage explants pre-treated with C-ABC and subsequently cultured in serum-supplemented media had a marked reduction in GAG content and enhancement of tensile integrity with minimal changes in tissue volume compared to explants not treated with C-ABC.[114] Thus, C-ABC is a useful tool to study the effect of impeded proteoglycan deposition on tissue integrity during cartilage growth.

1.5.3. In vivo and In vitro models of cartilage growth and maturation

In vivo and *in vitro* models are commonly used to study cartilage growth and maturation as well as repair and regeneration. Many animal models have been used to study cartilage *in vivo,* including mice, rats, rabbits, pigs, sheep, and bovine animals; tissues and cells are often extracted from these animals and cultured *in vitro* as tissue explants or in cell monolayers to study the effects of specific stimuli.[115,116] These models allow for the study of musculoskeletal development, maturation, and growth at a variety of timescales and dimensions which can be related to human anatomy and physiology. Experimental models help to provide a more comprehensive

understanding of the interactions between tissue composition, structure, and function throughout maturation and how these relationships are regulated by biomechanical and biochemical signals.

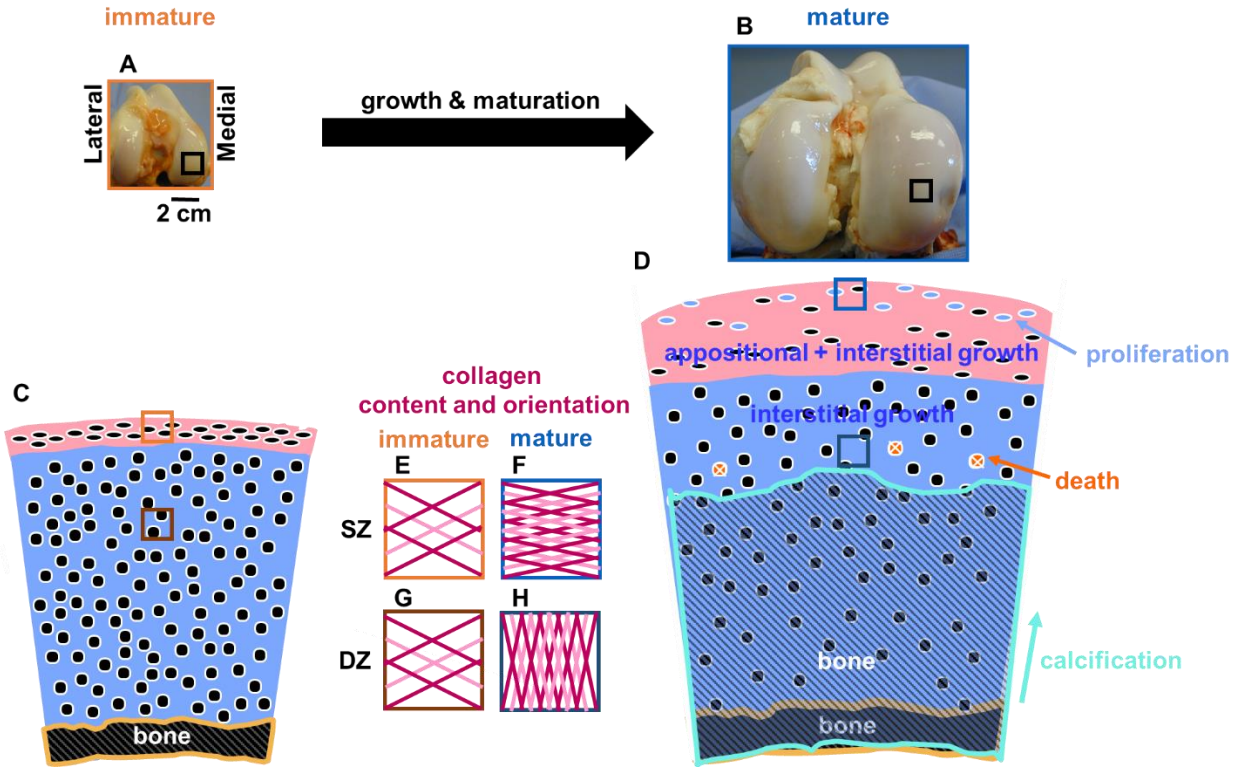


Figure 1.6. Expansive mechanism of growth within central "intrinsic" articular cartilage. (**A,B**) Gross images of bovine distal femur. Schematic of tissue (**C,D**) structure and content and (**E-H**) collagen orientation in the (**A,C,E,G**) immature and (**B,D,F,H**) mature states. (SZ) superficial and (DZ) deep zone of articular cartilage.

1.6. Models of metabolism and growth

1.6.1. Models of cartilage growth and remodeling

Models of tissue growth and remodeling incorporate metabolic processes, including matrix synthesis and degradation, to describe changing tissue volume and composition. For cartilage, growth and remodeling models are primarily based on the contributions of collagen and proteoglycan.

Continuum mixture models of growth and remodeling may be useful for predicting the geometry, composition, and biomechanical properties of cartilage. In these models, an arbitrary number of components contribute to mass deposition and mechanical deformation within the tissue. The contributions of proteoglycans, collagen, collagen crosslinks, and cells, within an inviscid fluid, to cartilage growth have been investigated.[117-121] In these models, growth is decomposed into two separate tensors which describe growth deformations from mass deposition and mechanical deformations which provide compatibility of the constituents in an equilibrium stress state. Mechanical theories of cartilage growth may be used to describe the complex relationship between the evolving compositional and mechanical properties during articular cartilage development and are informed by experiments which identify cellular metabolic cell fate dynamics within the tissue.

Compartmental metabolic models account for the spatially averaged concentration of metabolites within a discrete compartment and are useful in determining the kinetics of biochemical reactions for specific metabolic pathways. For instance, single compartment models have been widely utilized in the analysis of radiolabel experiments to determine the molecular rates of synthesis and degradation and to quantify the effects of chemical and mechanical stimuli on the metabolism of cartilage proteoglycans and collagens.[84,97,122,123] Compartmental models typically involve systems of ordinary differential equations which describe the rates of change of

the concentration of metabolites within a specified compartment over time.

Conversely, continuum models utilize partial differential equations to describe the transport and transformation of metabolites in space and time. In addition to principles of mass balance, continuum models are also based on thermodynamic principles of molecular diffusion and convection. Continuum metabolic models have been developed, considering matrix synthesis, transport, binding, and degradation, to understand proteoglycan distribution within articular cartilage and to analyze the effect of fluid flow and membrane permeability on the development of depth varying composition of engineered cartilage cultured in a perfusion bioreactor.[124,125]

Cellular kinetic models are a useful tool to study the dynamics of a population of cells over time. Kinetic models are based on a set of mathematical equations that describe the rates at which cells undergo various cell fate processes including cell division, differentiation, and loss, through apoptosis or necrosis, and are used to predict how cells will behave under specific conditions. Cellular kinetic models have been used in a variety of musculoskeletal applications, including in cancer, tissue engineering, and drug development, as well as in the contribution of growth plate cartilage to bone elongation.[10,11,126-133] However, there are few studies which have utilized kinetic models to evaluate cellular population dynamics within the AECC during postnatal maturation of cartilaginous epiphyses.

1.6.2. Growth generates tissue strains and stresses

Biological events, including cellular proliferation, hypertrophy, and matrix accretion impose local stresses and deformation on cells and extracellular matrix.[134] Growth-generated strains and growth-generated stresses refer to the local deformations and corresponding internal force intensities that are created by growth in developing tissues. Growth can be regarded as the integrated result of the growth of infinitesimal elements which constitute the tissue. Thus, growth

can be mathematically described by a time-dependent displacement field identifying the material point paths (in space-time) of the mass points which make up the animal or plant.[77,135,136]

Growth-generated stresses and strains can directly influence changes in tissue structure or organization without the need for an active cellular process. For instance, collagen fiber directions in the perichondrium and periosteum align with the preferential directions of long bone growth,[137] and in *in vitro* experiments, collagen fibrils in articular cartilage reorganize when exposed to tensile loading, correlating with an increase in tensile modulus particularly in superficial zone tissue.[29]

1.6.3. Quantification of tissue deformation and morphogenesis

There are several methods for tracking tissue deformation. In cartilage, tissue displacement fields have been analyzed by tracking motion of intrinsic or extrinsic surface markers. The spatially varying tissue strain induced during osmotic swelling of cartilage was assessed by tracking enamel markers applied on the tissue surface,[138] and the displacement of cartilage due to mechanical loading was quantified by mapping the relative motion of labeled cell nuclei.[139,140] Tissue deformations may also be quantified from analysis of matrix structure and organization. For instance, deformation tracking of fluorescently stained tissues with microscopy have been utilized to establish tissue injury criteria for the medial collateral ligament,[141] and strain of collagenous tissues have been quantified by tracking collagen fiber alignment.[142] Similarly, 3D imaging techniques, including MRI and CT,[143,144] paired with computational image correlation techniques to measure strain in soft tissues, may provide insight into tissue structural micromechanics and bridge micromechanical measurements to the micromechanical environment experienced by cells.

Morphogenesis at tissue and organ scales have been studied using advanced imaging and genetic labeling techniques to track the movement and deformation of tissues and specific cells of

interest during morphogenesis. Spatiotemporal patterns in morphogenetic processes have been assessed in *Drosophilia*, as well as avian and murine embryonic limb buds, and related to quantifiable cell behaviors including proliferation and apoptosis, cell division, rearrangement, and hypertrophy, as well as matrix production.[145-149]

1.7. Significance

Although physiologically and clinically significant, there is limited information on the mechanisms that lead to joint morphogenesis.[150] A greater understanding of joint formation and tissue maturation can provide insight for development of strategies to restore and repair joint function following injury and disease.

1.8. References

1. Decker RS, Koyama E, Pacifici M: Articular cartilage: Structural and developmental intricacies and questions. *Curr Osteoporos Rep.* 2015;13:407-14.

2. Pacifici M, Koyama E, Iwamoto M: Mechanisms of synovial joint and articular cartilage formation: recent advances, but many lingering mysteries. *Birth Defects Res C Embryo Today.* 2005;75:237-48.

3. Carlson CS, Hilley HD, Henrikson CK: Ultrastructure of normal epiphyseal cartilage of the articular-epiphyseal cartilage complex in growing swine. *Am J Vet Res.* 1985;46:306-13.

4. Mackie EJ, Ahmed YA, Tatarczuch L, Chen KS, Mirams M: Endochondral ossification: how cartilage is converted into bone in the developing skeleton. *Int J Biochem Cell Biol.* 2008;40:46-62.

5. Mackie EJ, Tatarczuch L, Mirams M: The skeleton: a multi-functional complex organ: the growth plate chondrocyte and endochondral ossification. *J Endocrinol.* 2011;211:109-21.

6. Long F, Ornitz DM: Development of the endochondral skeleton. *Cold Spring Harb Perspect Biol.* 2013;5:a008334.

7. Farnum CE, Wilsman NJ: Determination of proliferative characteristics of growth plate chondrocytes by labeling with bromodeoxyuridine. *Calcif Tissue Int.* 1993;52:110-19.

8. Hunziker EB: Mechanism of longitudinal bone growth and its regulation by growth plate chondrocytes. *Microsc Res Tech.* 1994;28:505-19.

9. Hunziker EB, Kapfinger E, Geiss J: The structural architecture of adult mammalian articular cartilage evolves by a synchronized process of tissue resorption and neoformation during postnatal development. *Osteoarthritis Cartilage.* 2007;15:403-13.

10. Wilsman NJ, Farnum CE, Green EM, Lieferman EM, Clayton MK: Cell cycle analysis of proliferative zone chondrocytes in growth plates elongating at different rates. *J Orthop Res.* 1996;14:562-72.

11. Wilsman NJ, Farnum CE, Leiferman EM, Fry M, Barreto C: Differential growth by growth plates as a function of multiple parameters of chondrocytic kinetics. *J Orthop Res.* 1996;14:927-36.

12. Yoshioka Y, Siu D, Cooke TD: The anatomy and functional axes of the femur. *J Bone Joint Surg Am.* 1987;69:873-80.

13. Biscevic M, Hebibovic M, Smrke D: Variations of femoral condyle shape. *Coll Antropol.* 2005;29:409-14.

14. Eger W, Schumacher BL, Mollenhauer J, Kuettner KE, Cole AA: Human knee and ankle cartilage explants: catabolic differences. *J Orthop Res.* 2002;20:526-34.

15. Schumacher BL, Su JL, Lindley KM, Kuettner KE, Cole AA: Horizontally oriented clusters of multiple chondrons in the superficial zone of ankle, but not knee articular cartilage. *Anat Rec.* 2002;266:241-48.

16. Chan EF, Harjanto R, Asahara H, Inoue N, Masuda K, Bugbee WD, Firestein GS, Hosalkar HS, Lotz MK, Sah RL: Structural and functional maturation of distal femoral cartilage and bone during postnatal development and growth in humans and mice. *Orthop Clin North Am.* 2012;43:173-85.

17. Oegema TR, Jr., Carpenter RJ, Hofmeister F, Thompson RC, Jr.: The interaction of the zone of calcified cartilage and subchondral bone in osteoarthritis. *Microsc Res Tech.* 1997;37:324-32.

18. Redler I, Mow VC, Zimny ML, Mansell J: The ultrastructure and biomechanical significance of the tidemark of articular cartilage. *Clin Orthop Relat Res.* 1975;112:357-62.

19. Clark JM, Huber JD: The structure of the human subchondral plate. *J Bone Joint Surg Br.* 1990;72:866-73.

20. Hunziker E, Quinn T, Shimaoka E, Hauselmann H: Quantitative structural organization of the normal adult human articular cartilage. *Trans Orthop Res Soc.* 2002;27:357.

21. Poole AR, Kojima T, Yasuda T, Mwale F, Kobayashi M, Laverty S: Composition and structure of articular cartilage: a template for tissue repair. *Clin Orthop Relat Res.* 2001:S26-33.

22. Temple MM, Bae WC, Chen MQ, Lotz M, Amiel D, Coutts RD, Sah RL: Age- and site-associated biomechanical weakening of human articular cartilage of the femoral condyle. *Osteoarthritis Cartilage.* 2007;15:1042-52.

23. Oinas J, Ronkainen AP, Rieppo L, Finnilä MAJ, Iivarinen JT, van Weeren PR, Helminen HJ, Brama PAJ, Korhonen RK, Saarakkala S: Composition, structure and tensile biomechanical properties of equine articular cartilage during growth and maturation. *Sci Rep.* 2018:11357.

24. Julkunen P, Iivarinen J, Brama PA, Arokoski J, Jurvelin JS, Helminen HJ: Maturation of collagen fibril network structure in tibial and femoral cartilage of rabbits. *Osteoarthritis Cartilage.* 2010;18:406-15.

25. Gründer W: MRI assessment of cartilage ultrastructure. *NMR Biomed.* 2006;19:855-76.

26. Rieppo J, Hyttinen MM, Halmesmaki E, Ruotsalainen H, Vasara A, Kiviranta I, Jurvelin JS, Helminen HJ: Changes in spatial collagen content and collagen network architecture in porcine articular cartilage during growth and maturation. *Osteoarthritis Cartilage.* 2009;17:448-55.

27. van Turnhout MC, Schipper H, Engel B, Buist W, Kranenbarg S, van Leeuwen JL: Postnatal development of collagen structure in ovine articular cartilage. *BMC Dev Biol.* 2010;10:62.

28. Clark JM: The organisation of collagen fibrils in the superficial zones of articular cartilage. *J Anat.* 1990;171:117-30.

29. Mansfield JC, Mandalia V, Toms A, Winlove CP, Brasselet S: Collagen reorganization in cartilage under strain probed by polarization sensitive second harmonic generation microscopy. *J R Soc Interface.* 2019;16:20180611.

30. Mansfield JC, Winlove CP, Moger JJ, Matcher SJ: Collagen fiber arrangement in normal and diseased cartilage studied by polarization sensitive nonlinear microscopy. *J Biomed Opt.* 2008;13:044020.

31. Williamson AK, Chen AC, Masuda K, Thonar EJ-MA, Sah RL: Tensile mechanical properties of bovine articular cartilage: variations with growth and relationships to collagen network components. *J Orthop Res.* 2003;21:872-80.

32. Williamson AK, Chen AC, Sah RL: Compressive properties and function-composition relationships of developing bovine articular cartilage. *J Orthop Res.* 2001;19:1113-21.

33. Eyre DR: Collagens and cartilage matrix homeostasis. *Clin Orthop Relat Res.* 2004:S118-22.

34. Eyre DR, Pietka T, Weis MA, Wu JJ: Covalent cross-linking of the NC1 domain of collagen type IX to collagen type II in cartilage. *J Biol Chem.* 2004;279:2568-74.

35. Reiser K, McCormick RJ, Rucker RB: Enzymatic and nonenzymatic cross-linking of collagen and elastin. *FASEB J.* 1992;6:2439-49.

36. Julkunen P, Harjula T, Iivarinen J, Marjanen J, Seppanen K, Narhi T, Arokoski J, Lammi MJ, Brama PA, Jurvelin JS, Helminen HJ: Biomechanical, biochemical and structural correlations in immature and mature rabbit articular cartilage. *Osteoarthritis Cartilage.* 2009;17:1628-38.

37. Gannon AR, Nagel T, Bell AP, Avery NC, Kelly DJ: Postnatal changes to the mechanical properties of articular cartilage are driven by the evolution of its collagen network. *Eur Cell Mater.* 2015;29:105-23.

38. Bae WC, Wong VW, Hwang J, Antonacci JM, Nugent-Derfus GE, Blewis ME, Temple-Wong MM, Sah RL: Wear-lines and split-lines of human patellar cartilage: relation to tensile biomechanical properties. *Osteoarthritis Cartilage.* 2008;16:841-5.

39. Sasazaki Y, Shore R, Seedhom BB: Deformation and failure of cartilage in the tensile mode. *J Anat.* 2006;208:681-94.

40. Woo SL, Akeson WH, Jemmott GF: Measurements of nonhomogeneous, directional mechanical properties of articular cartilage in tension. *J Biomech.* 1976;9:785-91.

41. Roth V, Mow VC: The intrinsic tensile behavior of the matrix of bovine articular cartilage and its variation with age. *J Bone Joint Surg Am.* 1980;62-A:1102-17.

42. Kempson GE, Muir H, Pollard C, Tuke M: The tensile properties of the cartilage of human femoral condyles related to the content of collagen and glycosaminoglycans. *Biochim Biophys Acta.* 1973;297:456-72.

43. Hardingham TE, Fosang AJ: Proteoglycans: many forms and many functions. *FASEB J.* 1992;6:861-70.

44. Basser PJ, Schneiderman R, Bank RA, Wachtel E, Maroudas A: Mechanical properties of the collagen network in human articular cartilage as measured by osmotic stress technique. *Arch Biochem Biophys.* 1998;351:207-19.

45. Lai WM, Hou JS, Mow VC: A triphasic theory for the swelling and deformation behaviors of articular cartilage. *J Biomech Eng.* 1991;113:245-58.

46. Maroudas AI: Balance between swelling pressure and collagen tension in normal and degenerate cartilage. *Nature.* 1976;260:808-9.

47. Han E, Chen SS, Klisch SM, Sah RL: Contribution of proteoglycan osmotic swelling pressure to the compressive properties of articular cartilage. *Biophys J.* 2011;101:916-24.

48. Bayliss MT, Venn M, Maroudas A, Ali SY: Structure of proteoglycans from different layers of human articular cartilage. *Biochem J.* 1983;209:387-400.

49. Hyttinen MM, Holopainen J, van Weeren PR, Firth EC, Helminen HJ, Brama PA: Changes in collagen fibril network organization and proteoglycan distribution in equine articular cartilage during maturation and growth. *J Anat.* 2009;215:584-91.

50. Hunziker EB: Articular cartilage structure in humans and experimental animals. In: *Articular Cartilage and Osteoarthritis,* ed by KE Kuettner, R Schleyerbach, JG Peyron, and VC Hascall, Raven Press, New York, 1992, pp 183-99.

51. Hunziker EB, Quinn TM, Hauselmann HJ: Quantitative structural organization of normal adult human articular cartilage. *Osteoarthritis Cartilage.* 2002;10:564-72.

52. Mitrovic D, Quintero M, Stankovic A, Ryckewaert A: Cell density of adult human femoral condylar articular cartilage. *Lab Invest.* 1983;49:309-16.

53. Stockwell RA: The interrelationship of cell density and cartilage thickness in mammalian cartilage. *J Anat.* 1971;109:411-21.

54. Jadin KD, Bae WC, Schumacher BL, Sah RL: Three-dimensional (3-D) imaging of chondrocytes in articular cartilage: growth-associated changes in cell organization. *Biomaterials.* 2007;28:230-9.

55. Jadin KD, Wong BL, Bae WC, Li KW, Williamson AK, Schumacher BL, Price JH, Sah RL: Depth-varying density and organization of chondrocyte in immature and mature bovine articular cartilage assessed by 3-D imaging and analysis. *J Histochem Cytochem.* 2005;53:1109-19.

56. Hayes AJ, MacPherson S, Morrison H, Dowthwaite G, Archer CW: The development of articular cartilage: evidence for an appositional growth mechanism. *Anat Embryol (Berl).* 2001;203:469-79.

57. Kavanagh E: Division and death of cells in developing synovial joints and long bones. *Cell Biol Int.* 2002;26:679-88.

58. Mankin HJ: Localization of tritiated thymidine in articular cartilage of rabbits. I. growth in immature cartilage. *J Bone Joint Surg Am.* 1962;44-A:682-98.

59. Mankin HJ: Localization of tritiated thymidine in articular cartilage of rabbits. II. repair in immature cartilage. *J Bone Joint Surg Am.* 1962;44-A:688-98.

60. Alsalameh S, Amin R, Gemba T, Lotz M: Identification of mesenchymal progenitor cells in normal and osteoarthritic human articular cartilage. *Arthritis Rheum.* 2004;50:1522-32.

61. Dowthwaite GP, Bishop JC, Redman SN, Khan IM, Rooney P, Evans DJ, Haughton L, Bayram Z, Boyer S, Thomson B, Wolfe MS, Archer CW: The surface of articular cartilage contains a progenitor cell population. *J Cell Sci.* 2004;117:889-97.

62. Fickert S, Fiedler J, Brenner RE: Identification of subpopulations with characteristics of mesenchymal progenitor cells from human osteoarthritic cartilage using triple staining for cell surface markers. *Arthritis Res Ther.* 2004;6:R422-32.

63. Thornemo MT, T. Sjogren Jansson, E. Larsson, A. Lovstedt, K. Nannmark, U. Brittberg, M. Lindahl, A.: Clonal Populations of Chondrocytes with Progenitor Properties Identified within Human Articular Cartilage. *Cells Tissues Organs.* 2005;180:141-50.

64. Decker RS, Um HB, Dyment NA, Cottingham N, Usami Y, Enomoto-Iwamoto M, Kronenberg MS, Maye P, Rowe DW, Koyama E, Pacifici M: Cell origin, volume and

arrangement are drivers of articular cartilage formation, morphogenesis and response to injury in mouse limbs. *Dev Biol.* 2017;426:56-68.

65. Kozhemyakina E, Zhang M, Ionescu A, Ayturk UM, Ono N, Kobayashi A, Kronenberg H, Warman ML, Lassar AB: Identification of a Prg4-positive articular cartilage progenitor cell population. *Arthritis Rheumatol.* 2015.

66. Koyama E, Shibukawa Y, Nagayama M, Sugito H, Young B, Yuasa T, Okabe T, Ochiai T, Kamiya N, Rountree RB, Kingsley DM, Iwamoto M, Enomoto-Iwamoto M, Pacifici M: A distinct cohort of progenitor cells participates in synovial joint and articular cartilage formation during mouse limb skeletogenesis. *Dev Biol.* 2008;316:62-73.

67. Li L, Newton PT, Bouderlique T, Sejnohova M, Zikmund T, Kozhemyakina E, Xie M, Krivanek J, Kaiser J, Qian H, Dyachuk V, Lassar A, Warman ML, Barenius B, Adameyko I, Chagin A: Superficial cells are self-renewing chondrocyte progenitors, which form the articular cartilage in juvenile mice. *FASEB J.* 2016;31:1067-84.

68. Lui JC: Home for a rest: stem cell niche of the postnatal growth plate. *J Endocrinol.* 2020;246:R1-R11.

69. Decker RS, Koyama E, Pacifici M: Genesis and morphogenesis of limb synovial joints and articular cartilage. *Matrix Biol.* 2014;39:5-10.

70. Breur GJ, VanEnkevort BA, Farnum CE, Wilsman NJ: Linear relationship between the volume of hypertrophic chondrocytes and the rate of longitudinal bone growth in growth plates. *J Orthop Res.* 1991;9:348-59.

71. Cooper KL, Oh S, Sung Y, Dasari RR, Kirschner MW, Tabin CJ: Multiple phases of chondrocyte enlargement underlie differences in skeletal proportions. *Nature.* 2013;495:375-8.

72. Sah RL, Chen AC, Grodzinsky AJ, Trippel SB: Differential effects of bFGF and IGF-I on matrix metabolism in calf and adult bovine cartilage explants. *Arch Biochem Biophys.* 1994;308:137-47.

73. Plaas AH, Sandy JD, Kimura JH: Biosynthesis of cartilage proteoglycan and link protein by articular chondrocytes from immature and mature rabbits. *J Biol Chem.* 1988;263:7560-66.

74. Tew S, Redman S, Kwan A, Walker E, Khan I, Dowthwaite G, Thomson B, Archer CW: Differences in repair responses between immature and mature cartilage. *Clin Orthop Relat Res.* 2001:S142-52.

75. Hidaka C, Cheng C, Alexandre D, Bhargava M, Torzilli PA: Maturational differences in superficial and deep zone articular chondrocytes. *Cell Tissue Res.* 2006;323:127-35.

76. Julkunen P, Wilson W, Isaksson H, Jurvelin JS, Walter Herzog W, Korhonen RK: A review of the combination of experimental measurements and fibril-reinforced modeling for investigation of articular cartilage and chondrocyte response to loading. *Comput Math Methods Med.* 2013;2013:326150.

77. Skalak R, Gasgupta G, Moss M, Otten E, Dullemeijer P, Vilmann H: Analytical description of growth. *J Theor Biol.* 1982;94:555-77.

78. Karlsson C, Thornemo M, Henriksson HB, Lindahl A: Identification of a stem cell niche in the zone of Ranvier within the knee joint. *J Anat.* 2009;215:355-63.

79. Aydelotte MB, Kuettner KE: Differences between sub-populations of cultured bovine articular chondrocytes. I. morphology and cartilage matrix production. *Connect Tissue Res.* 1988;18:205-22.

80. Jørgensen AEM, Schjerling P, Krogsgaard MR, Petersen MM, Olsen J, Kjær M, Heinemeier KM: Collagen growth pattern in human articular cartilage of the knee. *Cartilage.* 2021;13 (2_suppl):408s-18s.

81. Chan A, McCaul KA, Cundy PJ, Haan EA, Byron-Scott R: Perinatal risk factors for developmental dysplasia of the hip. *Arch Dis Child Fetal Neonatal Ed.* 1997;76:F94-100.

82. Hashimoto R, Kihara I, Otani H: Perinatal development of the rat hip joint with restrained fetal movement. *Congenit Anom (Kyoto).* 2002;42:135-42.

83. Mikic B, Johnson TL, Chhabra AB, Schalet BJ, Wong M, Hunziker EB: Differential effects of embryonic immobilization on the development of fibrocartilaginous skeletal elements. *J Rehabil Res Dev.* 2000;37:127-33.

84. Sah RL, Kim YJ, Doong JH, Grodzinsky AJ, Plaas AHK, Sandy JD: Biosynthetic response of cartilage explants to dynamic compression. *J Orthop Res.* 1989;7:619-36.

85. Jones IL, Klamfeldt DDS, Sandstrom T: The effect of continuous mechanical pressure upon the turnover of articular cartilage proteoglycans in vitro. *Clin Orthop Relat Res.* 1982;165:283-89.

86. Schneiderman R, Keret D, Maroudas A: Effects of mechanical and osmotic pressure on the rate of glycosaminoglycan synthesis in the human adult femoral head cartilage: an in vitro study. *J Orthop Res.* 1986;4:393-408.

87. Gray ML, Pizzanelli AM, Grodzinsky AJ, Lee RC: Mechanical and physicochemical determinants of the chondrocyte biosynthetic response. *J Orthop Res.* 1988;6:777-92.

88. Guilak F, Meyer BC, Ratcliffe A, Mow VC: The effects of matrix compression on proteoglycan metabolism in articular cartilage explants. *Osteoarthritis Cartilage.* 1994;2:91-101.

89. Kim YJ, Sah RL, Grodzinsky AJ, Plaas AH, Sandy JD: Mechanical regulation of cartilage biosynthetic behavior: physical stimuli. *Arch Biochem Biophys.* 1994;311:1-12.

90. Li KW, Williamson AK, Wang AS, Sah RL: Growth responses of cartilage to static and dynamic compression. *Clin Orthop Relat Res.* 2001;391S:34-48.

91. Larsson T, Aspden RM, Heinegard D: Effects of mechanical load on cartilage matrix biosynthesis in vitro. *Matrix.* 1991;11:388-94.

92. Below S, Arnoczky SP, Dodds J, Kooima C, Walter N: The split-line pattern of the distal femur: A consideration in the orientation of autologous cartilage grafts. *Arthroscopy.* 2002;18:613-7.

93. Las Heras F, Gahunia HK, Pritzker KP: Articular cartilage development: a molecular perspective. *Orthop Clin North Am.* 2012;43:155-71, v.

94. Kozhemyakina E, Lassar AB, Zelzer E: A pathway to bone: signaling molecules and transcription factors involved in chondrocyte development and maturation. *Development.* 2015;142:817-31.

95. DeLise AM, Fischer L, Tuan RS: Cellular interactions and signaling in cartilage development. *Osteoarthritis Cartilage.* 2000;8:309-34.

96. Asanbaeva A, Masuda K, Thonar EJ-MA, Klisch SM, Sah RL: Regulation of immature cartilage growth by IGF-I, TGF-beta1, BMP-7, and PDGF-AB: role of metabolic balance between fixed charge and collagen network. *Biomech Model Mechanobiol.* 2008;7:263-76.

97. Ahsan T, Harwood F, McGowan KB, Amiel D, Sah RL: Kinetics of collagen crosslinking in adult bovine articular cartilage. *Osteoarthritis Cartilage.* 2005;13:709-15.

98. Ahsan T, Lottman LM, Harwood FL, Amiel D, Sah RL: Integrative cartilage repair: inhibition by beta-aminoproprionitrile. *J Orthop Res.* 1999;17:850-7.

99. Kagan HM: Characterization and regulation of lysyl oxidase. In: *Regulation of Matrix Accumulation,* ed by RP Mecham, Academic Press, Inc., Orlando, 1986, pp 321-98.

100. Kagan HM, Sullivan KA: Lysyl oxidase: preparation and role in elastin biosynthesis. *Methods Enzymol.* 1982;82:637-49.

101. DiMicco MA, Waters SN, Akeson WH, Sah RL: Integrative articular cartilage repair: dependence on developmental stage and collagen metabolism. *Osteoarthritis Cartilage.* 2002;10:218-25.

102. Asanbaeva A, Masuda K, Thonar EJ-MA, Klisch SM, Sah RL: Cartilage growth and remodeling: modulation of balance between proteoglycan and collagen in vitro with beta-aminopropionitrile. *Osteoarthritis Cartilage.* 2008;16:1-11.

103. Pal S, Tang LH, Choi H, Habermann E, Rosenberg L, Roughley P, Poole AR: Structural changes during development in bovine fetal epiphyseal cartilage. *Coll Relat Res.* 1981;1:151-76.

104. Strider W, Pal S, Rosenberg L: Comparison of proteoglycans from bovine articular cartilage. *Biochim Biophys Acta.* 1975;379:271-81.

105. Thonar EJ-M, Sweet MBE: Maturation-related changes in proteoglycans of fetal articular cartilage. *Arch Biochem Biophys.* 1981;208:535-47.

106. Bartholomew JS, Lowther DA, Handley CJ: Changes in proteoglycan biosynthesis following leukocyte elastase treatment of bovine articular cartilage in culture. *Arthritis Rheum.* 1984;27:905-12.

107. Hardingham TE, Fosang AJ: The structure of aggrecan and its turnover in cartilage. *J Rheumatol.* 1995;22S:86-90.

108. Mort JS, Magny MC, Lee ER: Cathepsin B: an alternative protease for the generation of aggrecan 'metalloproteinase' cleavage neoepitope. *Biochem J.* 1998;335:491-4.

109. Stanton H, Rogerson FM, East CJ, Golub SB, Lawlor KE, Meeker CT, Little CB, Last K, Farmer PJ, Campbell IK, Fourie AM, Fosang AJ: ADAMTS5 is the major aggrecanase in mouse cartilage in vivo and in vitro. *Nature.* 2005;434:648-52.

110. Yamagata T, Saito H, Habuchi O, Suzuki S: Purification and properties of bacterial chondroitinases and chondrosulfatases. *J Biol Chem.* 1968;243:1523-35.

111. Chun LE, Koob TJ, Eyre DR: Sequential enzymic dissection of the proteoglycan complex from articular cartilage. *Trans Orthop Res Soc.* 1986;11:96.

112. Lyyra T, Arokoski JP, Oksala N, Vihko A, Hyttinen M, Jurvelin JS, Kiviranta I: Experimental validation of arthroscopic cartilage stiffness measurement using enzymatically degraded cartilage samples. *Phys Med Biol.* 1999;44:525-35.

113. Nahir AM, Shomrat D, Awad M: Chondroitinase ABC affects the activity of intracellular enzymes in rabbit articular cartilage chondrocytes. *J Rheumatol.* 1995;22:702-7.

114. Asanbaeva A, Masuda K, Thonar EJ, Klisch SM, Sah RL: Mechanisms of cartilage growth: modulation of balance between proteoglycan and collagen in vitro using chondroitinase ABC. *Arthritis Rheum.* 2007;56:188-98.

115. Chu CR, Szczodry M, Bruno S: Animal models for cartilage regeneration and repair. *Tissue Eng Part B Rev.* 2010;16:105-15.

116. Reinholz GG, Lu L, Saris DB, Yaszemski MJ, O'Driscoll SW: Animal models for cartilage reconstruction. *Biomaterials.* 2004;25:1511-21.

117. Klisch SM, Asanbaeva A, Oungoulian SR, Masuda K, Thonar EJ, Davol A, Sah RL: A cartilage growth mixture model with collagen remodeling: validation protocols. *J Biomech Eng.* 2008;130:031006.

118. Klisch SM, Chen SS, Hoger A, Sah RL: A growth and remodeling mixture model and the biomechanics of developing bovine articular cartilage. *Ann Biomed Eng.* 2002;S:2.2.3.5.

119. Klisch SM, Chen SS, Sah RL, Hoger A: A growth mixture theory for cartilage with applications to growth-related experiments on cartilage explants. *J Biomech Eng.* 2003;125:169-79.

120. Klisch SM, Sah RL, Hoger A: A growth mixture theory for cartilage. In: *Mechanics in Biology,* ed by J Casey and G Bao, ASME, 2000, pp 229-42.

121. Klisch SM, Sah RL, Hoger A: A cartilage growth mixture model for infinitesimal strains: solutions of boundary-value problems related to in vitro growth experiments. *Biomech Model Mechanobiol.* 2005;3:209-23.

122. Luyten FP, Hascall VC, Nissley SP, Morales TI, Reddi AH: Insulin-like growth factors maintain steady-state metabolism of proteoglycans in bovine articular cartilage explants. *Arch Biochem Biophys.* 1988;267:416-25.

123. Hascall VC, Luyten FP, Plaas AHK, Sandy JD: Steady-state metabolism of proteoglycans in bovine articular cartilage. In: *Methods in Cartilage Research,* ed by A Maroudas and K Kuettner, Academic Press, San Diego, 1990, pp 108-12.

124. DiMicco MA, Sah RL: Dependence of cartilage matrix composition on biosynthesis, diffusion, and reaction. *Transport Porous Media.* 2003;50:57-73.

125. Klein TJ, Sah RL: Modulation of depth-dependent properties in tissue-engineered cartilage with a semi-permeable membrane and perfusion: a continuum model of matrix metabolism and transport. *Biomech Model Mechanobiol.* 2007;6:21-32.

126. Banfi A, Muraglia A, Dozin B, Mastrogiacomo M, Cancedda R, Quarto R: Proliferation kinetics and differentiation potential of ex vivo expanded human bone marrow stromal cells: Implications for their use in cell therapy. *Exp Hematol.* 2000;28:707-15.

127. Freed LE, Marquis JC, Langer R, Vunjak-Novakovic G: Kinetics of chondrocyte growth in cell-polymer implants. *Biotechnol Bioeng.* 1994;43:597-604.

128. Galban CJ, Locke BR: Analysis of cell growth kinetics and substrate diffusion in a polymer scaffold. *Biotechnol Bioeng.* 1999;65:121-32.

129. Jaffray P, Ronot X, Adolphe M, Fontagne J, Lechat P: Effects of D-penicillamine on growth and cell cycle kinetics of cultured rabbit articular chondrocytes. *Ann Rheum Dis.* 1984;43:333-8.

130. Muschler GF, Midura RJ, Nakamoto C: Practical modeling concepts for connective tissue stem cell and progenitor compartment kinetics. *J Biomed Biotechnol.* 2003;2003:170-93.

131. Rao BM, Lauffenburger DA, Wittrup KD: Integrating cell-level kinetic modeling into the deisgn of engineered protein therapeutics. *Nat Biotech.* 2005;23:191.

132. Ronot X, Adolphe M: Modulating effects of drugs on cell cycle kinetics. *Biol Cell.* 1986;58:139-46.

133. Hall BK, *Cartilage Vol 1: Structure, Function, and Biochemistry*. 1983, Academic Press. pp.

134. Henderson JH, Carter DR: Mechanical induction in limb morphogenesis: the role of growth-generated strains and pressures. *Bone.* 2002;31:645-53.

135. Skalak R: Growth as a finite displacement field. In *Proceedings of the IUTAM Symposium on Finite Elasticity, 1981*. Martinus Nijhoff, The Hague.

136. Skalak R, Farrow DA, Hoger A: Kinematics of surface growth. *J Math Biol.* 1997;35:869-907.

137. Foolen J, van Donkelaar C, Nowlan N, Murphy P, Huiskes R, Ito K: Collagen orientation in periosteum and perichondrium is aligned with preferential directions of tissue growth. *J Orthop Res.* 2008;26:1263-8.

138. Narmoneva DA, Wang JY, Setton LA: Nonuniform swelling-induced residual strains in articular cartilage. *J Biomech.* 1999;32:401-08.

139. Klein TJ, Chaudhry M, Bae WC, Sah RL: Depth-dependent biomechanical and biochemical properties of fetal, newborn, and tissue-engineered articular cartilage. *J Biomech.* 2007;40:182-90.

140. Schinagl RM, Ting MK, Price JH, Sah RL: Video microscopy to quantitate the inhomogeneous equilibrium strain within articular cartilage during confined compression. *Ann Biomed Eng.* 1996;24:500-12.

141. Luetkemeyer CM, Neu CP, Calve S: A method for defining tissue injury criteria reveals ligament deformation thresholds are multimodal. *bioRxiv.* 2023:2023.01.31.526318.

142. Quinn KP, Winkelstein BA: Full field strain measurements of collagenous tissue by tracking fiber alignment through vector correlation. *J Biomech.* 2010*;*43:2637-40.

143. Disney CM, Lee PD, Hoyland JA, Sherratt MJ, Bay BK: A review of techniques for visualising soft tissue microstructure deformation and quantifying strain Ex Vivo. *J Microsc.* 2018*;*272:165-79.

144. Disney CM, Mo J, Eckersley A, Bodey AJ, Hoyland JA, Sherratt MJ, Pitsillides AA, Lee PD, Bay BK: Regional variations in discrete collagen fibre mechanics within intact intervertebral disc resolved using synchrotron computed tomography and digital volume correlation. *Acta Biomater.* 2021*;*138:361-74.

145. Blanchard GB, Kabla AJ, Schultz NL, Butler LC, Sanson B, Gorfinkiel N, Mahadevan L, Adams RJ: Tissue tectonics: morphogenetic strain rates, cell shape change and intercalation. *Nat Methods.* 2009*;*6:458-64.

146. Li Y, Trivedi V, Truong TV, Koos DS, Lansford R, Chuong CM, Warburton D, Moats RA, Fraser SE: Dynamic imaging of the growth plate cartilage reveals multiple contributors to skeletal morphogenesis. *Nat Commun.* 2015*;*6:6798.

147. Green JBA: Resolving morphogenesis into quantifiable cell behaviours. *Development.* 2022*;*149:dev199794.

148. Boehm B, Westerberg H, Lesnicar-Pucko G, Raja S, Rautschka M, Cotterell J, Swoger J, Sharpe J: The role of spatially controlled cell proliferation in limb bud morphogenesis. *Plos Biol.* 2010*;*8:e1000420.

149. Acuna A, Sofronici SH, Goergen CJ, Calve S: In situ measurement of native extracellular matrix strain. *Exp Mech.* 2019*;*59:1307-21.

150. Longobardi L, Li T, Tagliafierro L, Temple JD, Willcockson HH, Ye P, Esposito A, Xu F, Spagnoli A: Synovial joints: from development to homeostasis. *Curr Osteoporos Rep.* 2015*;*13:41-51.

CHAPTER 2

OVERVIEW OF ORTHOBIOLOGICS FOR ARTICULAR CARTILAGE REPAIR

2.1. Introduction

The predilection of articular cartilage (AC) to be damaged, along with its biology and extracellular matrix (ECM) structure, renders it a target for orthobiologics. Throughout an adult's life, AC normally functions as a key component of diarthrodial joints, withstanding years of repetitive loading and facilitating pain-free motion. However, with injury and aging, AC is often damaged. Unfortunately, damaged adult AC exhibits a limited intrinsic repair response and often deteriorates (**Fig. 1**), making it an attractive candidate for orthobiologics.[1] Orthobiologics address tissue repair, protection, healing, and regeneration based on individual or combination products comprised of cells, biomaterials and/or bioactive factors. Orthobiologics can be classified based on having one or more of three classical components: cells, scaffolds, and signals. These components can be derived from naturally occurring substances, such as tissues or blood, or consist of synthesized or modified materials or cells, such as engineered proteins, gene therapies, and culture-expanded cells. Effective orthobiologic treatments may induce repairs that range from the ideally regenerated normal adult AC to tissues which variably restore function. An overview of orthobiologics for AC repair is provided. It begins with summaries of the hierarchal structure of AC, the biology of indwelling chondrocytes and their precursors, and its extracellular matrix composition, turnover, and function. It then reviews the three major components of cartilage orthobiologics: scaffolds, cells, and signals. In addition, within this context, established and emerging orthobiologic approaches to cartilage repair are described.

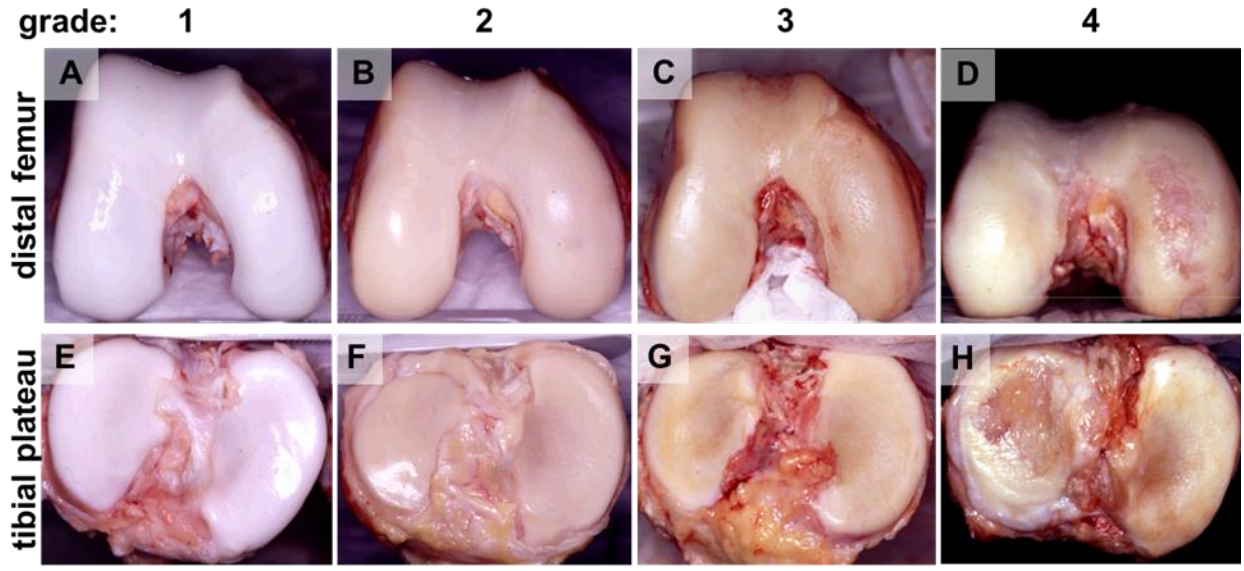


Figure 2.1. Human knee articular cartilage often undergoes aging and osteoarthritis-related deterioration. Human (**A-D**) distal femur and (**E-H**) tibial plateau. Diffuse cartilage degeneration due to chronic wear or osteoarthritis at ICRS (**A,E**) grade I, (**B,F**) grade II, (**C,G**) grade III, and (**D,H**) grade IV.

2.2. Brief biology of cartilage

The biology of AC is fundamentally coupled through its ECM to its biomechanical and biotransport properties, which vary during growth, homeostasis, and disease. AC is a component of joints that function as an organ, with interactions and crosstalk between tissues, including AC, synovium, and underlying bone, mediated by synovial fluid (**Fig. 2**). Chondrocytes, the indwelling cells of cartilage, elaborate and remodel the cartilage ECM, affecting their microenvironment. Conversely, chondrocytes are regulated by the milieu of insoluble (ECM), soluble (cytokines, growth factors, extracellular vesicles), and mechanical factors (due to joint loading). Thus, chondrocytes interact reciprocally with their surrounding matrix and fluid to form and maintain the structure and function of cartilage tissue.

The articular surface is bathed in synovial fluid that affects cartilage biology and physiology. Synovial fluid is a dialysate of plasma that contains substances originating from the local joint tissues. Synovial fluid helps lubricate the articulating joint surfaces, due to its high concentration of hyaluronic acid and lubricin/proteoglycan-4 (PRG4) lubricant molecules. Synovial fluid also mediates regulation and degradation of AC through synovium-secreted cytokines and proteases. In general, synovial fluid acts as a transport medium to provide cartilage with basic nutrients, including carbohydrates such as glucose, lipids, proteins, vitamins, minerals, and water.[2]

Cartilage growth, remodeling, maturation, and morphogenesis typically occur concurrently during joint development. During postnatal growth, the overall size and volume of joints increase (**Fig. 3**). In skeletally immature individuals, the covering of bone ends includes a layer of epiphyseal growth cartilage and AC which are collectively known as the articular–epiphyseal cartilage complex.[3,4] This complex grows before being either replaced by mineralized tissue via endochondral ossification, or retained as AC. The overall growth of the joint involves expansion

of the joint surface with concomitant thinning of the AC. The normal homeostatic balance between matrix synthesis and loss may become disrupted not only by direct damage or infiltrating enzymes, but by dysregulated chondrocytes, displaying an aberrant or development-like phenotype.[5] Common regulatory pathways of matrix turnover in normal joint development and joint pathology can provide avenues for orthobiologic interventions.

Cartilage homeostasis is sensitive to mechanical stimuli, depending on magnitude, duration, and nature, in part through receptors which are responsive to mechanical stimulation. In vivo, AC is subjected to time-averaged static and time-varying dynamic cyclic compression, articulation inducing shear stress, and resultant hydrostatic pressure, and compressive, shear, and tensile strain.[6] Mechanosensitive receptors can transmit mechanical information from the ECM to the chondrocyte and may activate or repress a variety of mechanotransduction pathways which alter the balance between catabolic and anabolic activity.[7] Catabolic activation may occur through both reduced loading and overloading as well as chronic pathological joint-loading. Net cartilage degradation and thinning are induced by elevated levels of peak stress, high strain rates, and long-term pathologic mechanical loading (e.g., joint malalignment) as well as prolonged immobilization.[6]

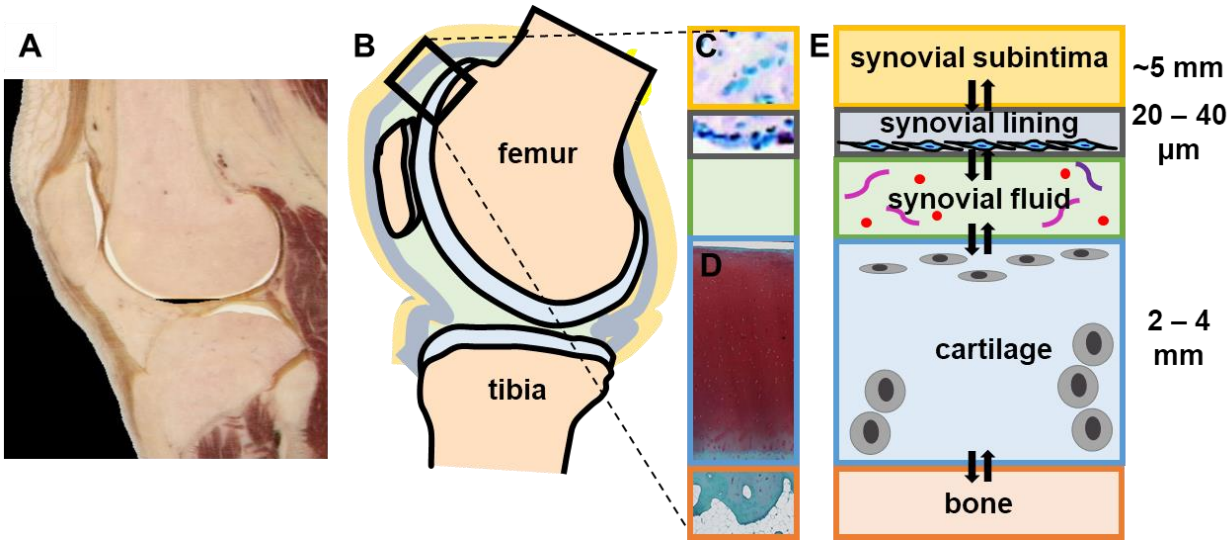


Figure 2.2. Crosstalk between cartilage and synovium is mediated by synovial fluid. . (**A**) Gross photograph of knee in the sagittal view. (**B**) Schematic representation of knee joint. Photomicrographs of human (**C**) synovial lining and (**D**) articular cartilage and bone. (**E**) Compartmental model of crosstalk between joint tissues. Panel (**A**) courtesy of Dr. Walter Carpenter, PhD, MD. Panels (**B**) and (**E**) adapted with permission.[87]

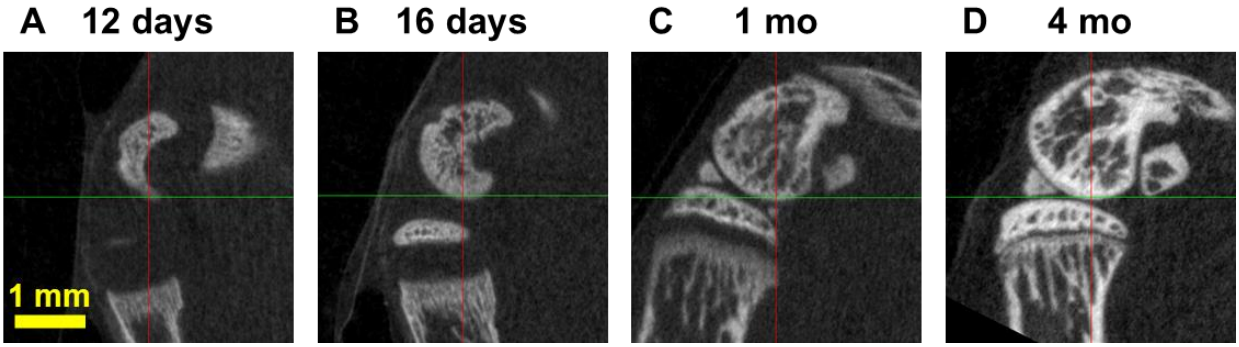


Figure 2.3. Growth and mineralization of the distal femur and proximal tibia. Micro-computed tomography scans of C57BL/6 wild-type mouse knees from (**A**) 12 days, (**B**) 16 days, (**C**) 1 month, and (**D**) 4 months postnatal.

2.2.1. Hierarchy of cartilage structure

The major load-bearing structure of synovial joints is the osteochondral unit, consisting of AC, calcified cartilage, and underlying subchondral bone. The calcified cartilage is a thin tissue layer between the AC and subchondral bone and is bounded histologically by the tidemark, between the uncalcified hyaline cartilage and calcified cartilage, and the cement line, between the calcified cartilage and subchondral bone. The calcified cartilage provides load transfer, structural integration, and a barrier to solute transport between the uncalcified cartilage and the subchondral bone.[8]

The cartilage matrix has zonal, regional, and site variation that facilitates tissue function under complex loading and which changes with growth (**Fig. 4**). The main extracellular matrix components of AC include large aggregates of the proteoglycan aggrecan and fibrils of predominantly type II collagen, which contribute to cartilage's unique biomechanical properties. Aggrecan associates with hyaluronan and link protein to form large multimolecular aggregates (~109 Da) that are effectively retained within cartilage. Due to the large number of polyanionic glycosaminoglycan chains on aggrecan, and the restraining and space-filling nature of the dense collagen network, the aggregates provide a high negative fixed charge density and osmotic swelling pressure within the tissue, with a high water content and compressive resistance.[9,10] In contrast to its dense matrix and compared to other tissues, normal adult AC has a relatively low density of cells, and is also avascular, alymphatic, and aneural.

AC exhibits depth-wise variation, with (1) superficial, (2) middle, and (3) deep zones, as well as (4) calcified cartilage. Within the superficial zone, chondrocytes are flattened and aligned parallel to the surface, collagen fibrils run parallel to the articular surface, and aggrecan content is relatively low. With depth, cell density decreases, chondrocytes exhibit a larger and more rounded hypertrophic appearance, collagen orientation is increasingly perpendicular to the articular surface,

and the matrix becomes progressively aggrecan rich.

The cartilage matrix surrounding chondrocytes also exhibits distinctive arrangements at increasing distances from the cell surface. The pericellular matrix lies immediately around the cell and is the zone where molecules that interact with cell surface receptors are located. Slightly further from the cell is the territorial matrix, and even further is the interterritorial matrix. The types of collagens and the collagen-binding proteins that form the matrices are different in each zone.[11] Further, the compositional, structural, and functional properties of AC vary across joint surfaces, consistent with modulation by the extent and pattern of joint loading.[12]

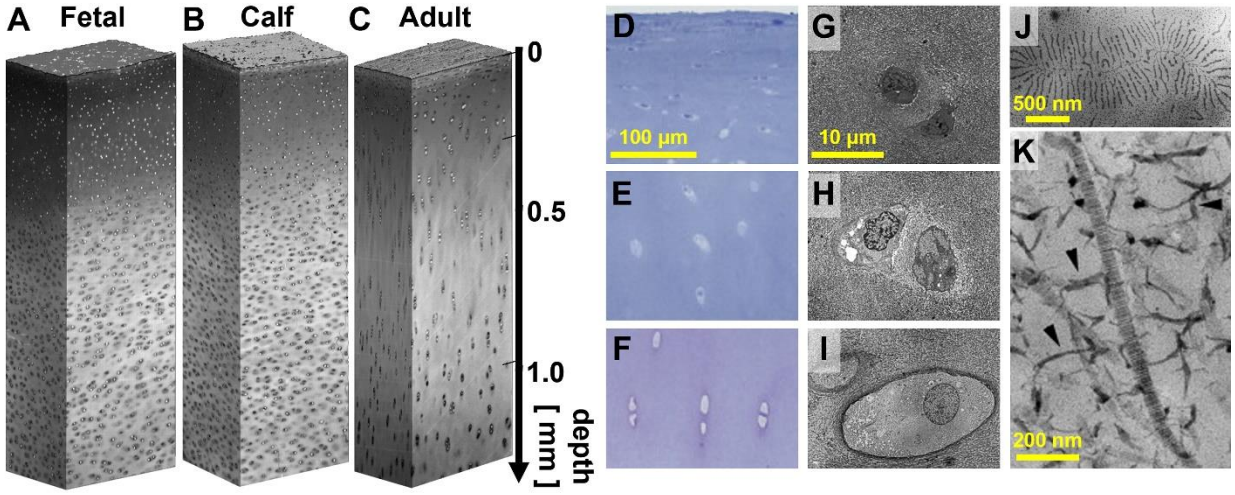


Figure 2.4. Age- and depth-varying cell and matrix organization of articular cartilage. Three-dimensional rendering of bovine (**A**) fetal, (**B**) calf, and (**C**) adult tissue. (**D-F**) Light and (**G-I**) transmission electron micrographs of chondrocytes within the (**D,G**) superficial, (**E,H**) transitional middle, and (**F,I**) deep zones. (**J**) Electron micrograph of proteoglycan aggregate isolated from bovine cartilage. (**K**) Micrograph of hyaline cartilage with type II collagen fibril lying parallel to the section plane and proteoglycans (arrowheads). Magnification is the same among panels (**D-F**), and among panels (**G-I**). Panels (**A-C**) adapted with permission.[89] Panels (**D-I**) adapted with permission.[90] Panel (**J**) adapted with permission.[91] Panel (**K**) adapted with permission.[92]

2.2.2. Chondrocyte biology and lineage

Articular chondrocyte biology varies with depth from the articular surface, in health and disease. For example, superficial zone chondrocytes are a major source of the synovial fluid lubricant, PRG4. Further, gene expression profiles may help to elucidate stages of disease by reflecting the evolving expression of anabolic and catabolic genes during different phases of maturation and disease.[13] In normal adult AC, the greatest differences in gene expression occurs between the superficial and deep zones, which reflects the differing functional roles of the superficial zone, in maintaining the low-friction articulating surface, and the deep zone, where an enhanced biosynthetic capacity is necessary to form and maintain the dense matrix.[14,15]

The natural transitional growth of immature epiphyseal cartilage to adult AC provides a paradigm for regenerative strategies of orthobiologics. Mature articular chondrocytes arise from multiple pools of progenitor cells from the superficial zone and perichondral tissues. Synovial joint formation involves descendants of mesenchymal cells (MSCs) from the interzone area of embryonic limbs which give rise to joint tissues. AC maturation is driven mainly by increase in cell volume, cellular rearrangement, matrix deposition, with limited cellular proliferation in the neonatal stages (**Fig. 5**).[16,17] In mice, superficial zone PRG4+ cells expressing stem cells markers facilitate appositional and interstitial growth of AC and entirely reconstitute adult cartilage during growth and maturation.[18] PRG4+ cells found in the synovial lining proliferate in response to injury and may contribute to healing.[17] A population of cells positive for progenitor markers in the perichondral groove of Ranvier have also been identified and contribute appositionally to the AC from the joint periphery.[19] In mature tissue, MSCs from bone marrow and adipose tissue are capable of differentiating into chondrocytes and may contribute to cartilage repair. Thus, lineage-tracing studies have substantial implications for how orthobiologics may target endogenous and exogenous cell populations to repair or regenerate cartilage.

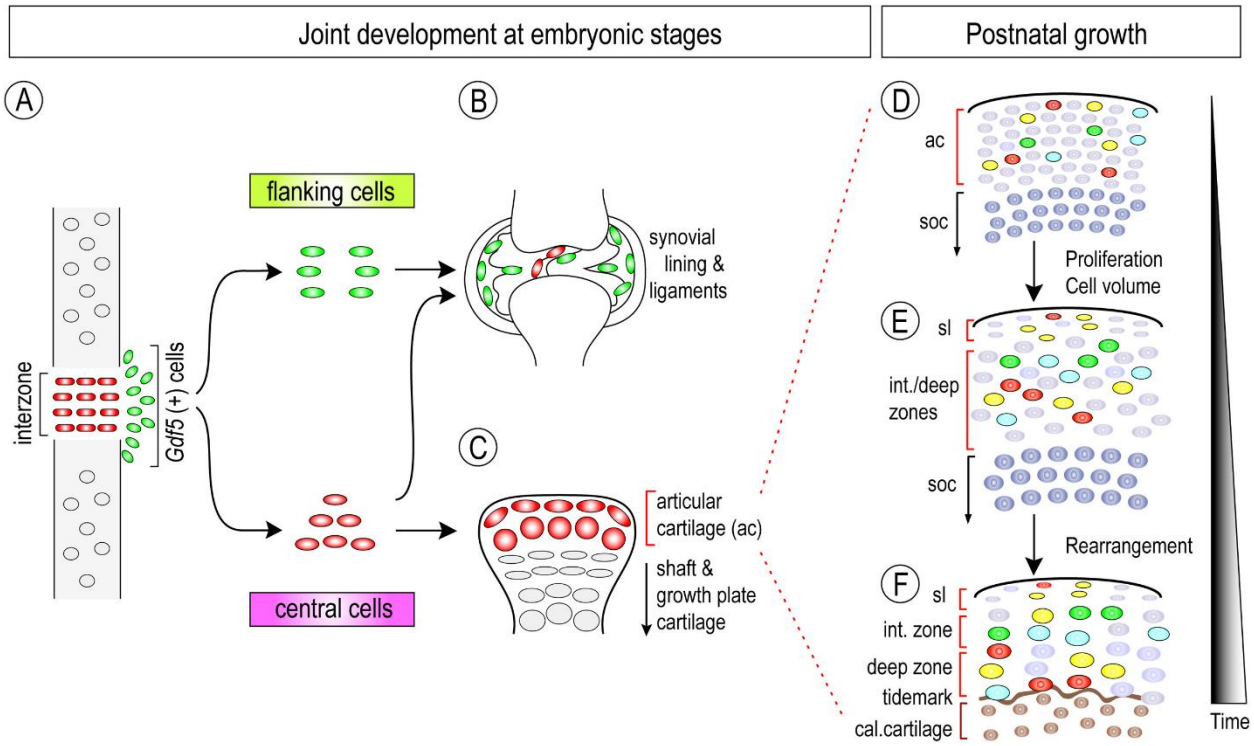


Figure 2.5. Model of synovial joint growth and morphogenesis. (**A**) Mesenchymal Gdf5+ cells constituting the interzone area at incipient joint sites in early embryonic limbs comprise centrally located descendants of chondrocytes (red color) and flanking cells recruited from surrounding tissues into the Gdf5 lineage (green color). (**B-C**) Both populations increase in number, but do not migrate significantly over time and give rise to distinct local tissues, with the flanking cells largely producing synovial lining, capsule and peripheral ligaments and central cells generating articular cartilage and intrajoint ligaments. (**D-F**) Starting at neonatal stages and proceeding into adulthood, knee articular cartilage (ac) progressively acquires its functional organization and structure that include: superficial layers (sl); intermediate (int.) and deep zones; and a tidemark overlaying the calcified (cal.) cartilage and secondary ossification center (soc). Growth in thickness is driven by limited proliferation at neonatal stages (**D**) and by cell volume increases at subsequent stages (**E-F**). The characteristic cell stacks perpendicular to the articular surface entail repositioning and intercalation of neighboring chondrocytes, producing stacks of non-daughter cells. Reproduced with permission.[17]

2.2.3. ECM composition and homeostasis

The ECM of cartilage is maintained at levels that depend on synthesis and accumulation of structural molecules, as balanced by their degradation and loss. The composition and functional properties of cartilage change during maturation and with pathology and reflect several biologic and physical processes.

Collagen biosynthesis and assembly follows the normal pathway for a secreted protein. Many distinct types of collagen molecules are expressed in AC but the backbone polymeric template during development is a copolymer of collagens II, IX and XI. After skeletal growth has ceased, the rate of type II collagen synthesis by articular chondrocytes drops dramatically, with an estimated turnover time of 400 years for human femoral head cartilage.[20] The classical concept of collagen fibril degradation is through an initial cleavage of the collagen molecule (type I, II or III) by collagenase into three-quarter and one quarter length fragments.[21]

Secreted aggrecan replaces those that are damaged by mechanical loading, removed by aggrecanases and/or proteases, or transported through the cartilage tissue via its migration down its concentration gradient, eventually exiting through the cartilage surface.[22-24] Other proteogylcans, including syndecans, glypican, small leucine rich proteoglycans, decorin, biglycan, and perlecan, among others are expressed during chondrogenesis and aid in assembly and maintenance of the cartilage ECM.[25]

The ECM contains a variety of matrix-degrading enzymes that are present in precursor and active forms. The activation of stress- and inflammation-induced signaling and transcriptional and posttranscriptional events results in release of the chondrocytes from growth arrest, imbalanced homeostasis, and chondrocyte activation with aberrant expression of inflammation-related genes.[7] The ECM acts as a depot, storing growth factors and other signaling molecules. Changes in physiologic conditions can trigger protease activity that enables the release of such depots and

activation of catabolism and inflammation, which can be modulated by targeted delivery of drugs and other signaling factors.[26]

2.2.4. Tissue composition affects efficacy of orthobiologic interventions

The therapeutic effect of orthobiologic interventions is dependent on the residence time of the intervention within the joint space, if implemented by intraarticular injection, as well as penetration and residence time within the cartilage tissue itself. Soluble therapeutics, (e.g. growth factors, cytokines, etc.) are subject to convective and diffusive effects within the joint tissues.

Retention of solutes within cartilage is affected by loading, extracellular matrix content and integrity, as well as electrostatic interactions between the tissue and solute. Transport occurs relatively rapidly in areas of low matrix density, such as near the articular surface, but is also affected by mechanical loading, and residence time within the synovial fluid, and cartilage.[27]

Synovial fluid is an ultrafiltrate of plasma with additional molecules secreted by local cell populations. The composition of synovial fluid is normally in dynamic equilibrium and reflects a balance between cellular secretion and loss due to transport through the synovial capillaries, synovial interstitium, and the lymphatic drainage system.[28,29] The residence time of molecules within the synovial fluid depends on molecular mass and shape as well as joint state, including inflammation, vascular permeability, and synovial thickening.[29,30] The half-life of drugs in the synovial fluid after injection is as short as ~1 hr (e.g. paracetamol).[31] However, residence time can be higher with increased molecular size, increased viscous and aggregating properties, and enhanced interaction with joint tissues, including the synovium and cartilage.[32]

Turnover of synovial fluid constituents is driven, in part, by size-dependent clearance through the lymphatic and capillary systems. Clearance of particles from the joint may occur through the lymphatics for larger species, and through venous capillaries for smaller species.[33] In

the rabbit model, after anterior cruciate ligament transection, the molecular weight distribution of injected hyaluronan within the knee shifted towards a predominance of lower molecular weight species (<1000 kDa) and a lower hyaluronan residence time.[34] Synovial permeability also depends on disease state. Increased synovial inflammation in patients with various form of arthritis is associated with increases in vascular and lymphatic permeability, synovial hyperplasia, and cellular infiltration.[29,34,35] Thus, strategies to increase retention time of therapeutic solutes within an inflammatory joint environment may be important for effective orthobiologic interventions.

Within the cartilage, fluid flows produced by mechanical loading induce convection of solutes.[27] Further, as cartilage degrades, the collagen network is disrupted, proteoglycans are lost from the tissue, and tissue permeability increases. Increased permeability of diseased cartilage enables enhanced transport of therapeutic agents within the cartilage, and allows for transport of large molecules, but can reduce retention times within the tissue.

The dense polyanionic ECM of AC not only provides the tissue with its essential load-bearing properties, but also governs the regulation of chondrocytes by soluble factors. Because of the net negative fixed charge density within cartilage, solute partitioning within the tissue is hindered, or enhanced, by the molecular size and charge of the solute.[36] According to effects of steric exclusion and Donnan equilibrium, the distribution as well as the diffusion coefficients of a particular solute decreases with increasing molecular weight and size, and are sensitive to variations in fixed charge density.[37] These physicochemical principles affect the access of solutes to chondrocytes and may be the basis of biological therapies. For instance, cationic carrier molecules may enhance the transport of biologically active molecules into cartilage.[32] However, cationic molecules have the potential to neutralize tissue fixed charge, which could counteract the natural load-bearing mechanism of cartilage and affect chondrocyte behavior.[38]

2.3.Overview of therapeutic options: Cells, scaffolds, and signals

Therapeutic approaches and developments target particular forms and stages of AC damage. Focal chondral and osteochondral defects are injuries or areas of degeneration which are limited to a defined area. Focal defects may occur due to acute traumatic injury or may be idiopathic. Defects can present as (1) partial-thickness chondral defects where damage is restricted to the chondral layer, (2) full-thickness chondral defects extending to the calcified cartilage or subchondral bone and (3) osteochondral defects which affect both the cartilage and underlying bone (**Fig. 6**). Defects may present as softened or partially eroded tissue and are classified according to size, and geometry.[39] Conversely, osteoarthritis is characterized by widespread joint degeneration due to progressive loss of AC and pathophysiologic bone and cartilage remodeling including fibrocartilage formation, sclerosis of subchondral bone, and osteophyte formation.[40,41] Repair of cartilage and osteochondral injuries involve not only replacement or regeneration of the bulk cartilage tissue, but also integration with appropriate interfaces for the various types of defect repair.

Cartilage repair strategies can be classified according to the type of therapeutic modality, either mechanical or biologic, as well as the method in which the therapy is delivered (**Table 1**). Mechanically directed treatment strategies aim to correct abnormal joint loading and joint malalignment, or provide tissues or tissue substitutes which promptly restore mechanical (i.e. load bearing) function. Conversely, regenerative therapies enable a biological response which aim to regenerate the tissue or establish a reparative microenvironment that restores normal structure and function, and which have a longer time-horizon to achieve functional repair.

Therapeutic interventions, and their evaluation, can be delivered, or assessed, at the tissue, organ, and whole-body levels (**Fig. 7**). Although most orthobiologic interventions, discussed in the next paragraphs, are delivered directly to the joint, by intra-articular injection or surgical

procedures, soluble signals may be administered orally or intravenously. In addition, therapeutic efficacy may be assessed from a holistic perspective (i.e. surveys and questionnaires regarding patient-reported measures of pain, function, etc.),[42] as well as locally at multiple scales by clinical imaging of the joint and biopsy of the joint tissues.[43] Biochemical analysis of fluids, including urine, blood, and synovial fluid, may also be used to identify byproducts of joint degeneration and assess the metabolic state of the body or joint.

Orthobiologic substances can be categorized into three substances: (1) scaffolds, (2) signals, and (3) cells which can be utilized individually, or in combination, to elicit a biological response which aids in repair, regeneration, or restoration of injured tissue (**Fig. 8**). Scaffolds, either natural or synthetic in nature, provide a supportive material to guide matrix synthesis and organization and can be manufactured with complex geometries and topography.[44] Signals, which regulate behavior of either endogenous or delivered cells, can either be biochemical or mechanical in nature. Biochemical signals include growth factors (TGF-β , PDGFs, BMP, etc.), drugs, gene and exosome therapies, as well as other agents which inhibit or activate specific enzymes and metabolic pathways.[45-48] Additionally, blood products such as such as platelet rich plasma and bone marrow aspirate concentrate contain a milieu of reparative factors which may influence cellular behavior.[49,50] Both autologous and allogeneic cells have been utilized in developing orthobiologic therapies and are often expanded in vitro, imbued within scaffolds, and preconditioned with mechanical and biomechanical stimulation. Allogeneic cell sources, often cartilage stem or progenitor cells, have been derived from bone marrow, adipose, muscle, bone, synovium, periosteum, umbilical cord and amniotic tissues.[51] Cells, in particular MSCs, can also be utilized as a paracrine signaling source that establishes a regenerative microenvironment by secreting factors that regulate the local immune response.[52] Biomechanical conditioning of cells

and cellular scaffolds with regimens of compression, shear, and/or hydrostatic pressure modulate cellular phenotype and can enhance chondrogenesis and matrix biosynthesis.[46] Thus, many orthobiologic therapies for cartilage repair involve a combination of scaffolds, signals, and cells which ideally form and maintain repair tissue (**Table 2**).

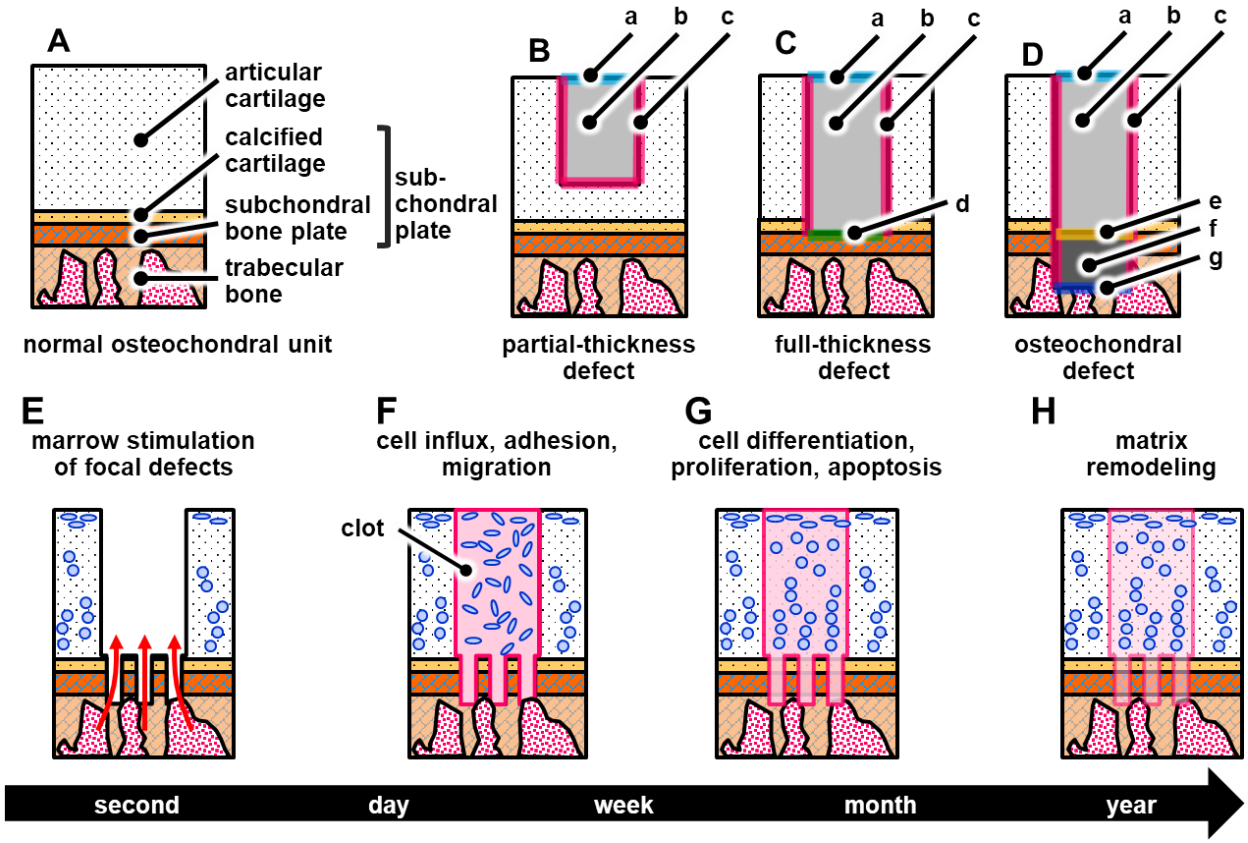


Figure 2.6. Schematic of normal osteochondral unit and spatiotemporal aspects of repair of cartilage defect repair. (**A**) Normal osteochondral unit. Defects that are (**B**) partial-thickness, (**C**) full-thickness, and (**D**) osteochondral and spatial aspects of repair strategies. Specialized surfaces, tissues and interfaces include the (a) articular surface, (b) bulk cartilage, (c) interface of repair with host cartilage, (d) interface of repair cartilage with subchondral plate, (e) formation of a bone-cartilage interface, (f) repair of trabecular bone, and (g) interface of repair with host bone. In microfracture, (**E**) penetration of the subchondral bone plate leads to (**F**) formation of a clot containing cells, growth factors, and matrix molecules. Over time, (**G**) cells remain at the defect site, differentiate, and (**H**) form and maintain the repair tissue. Adapted with permission.[93]

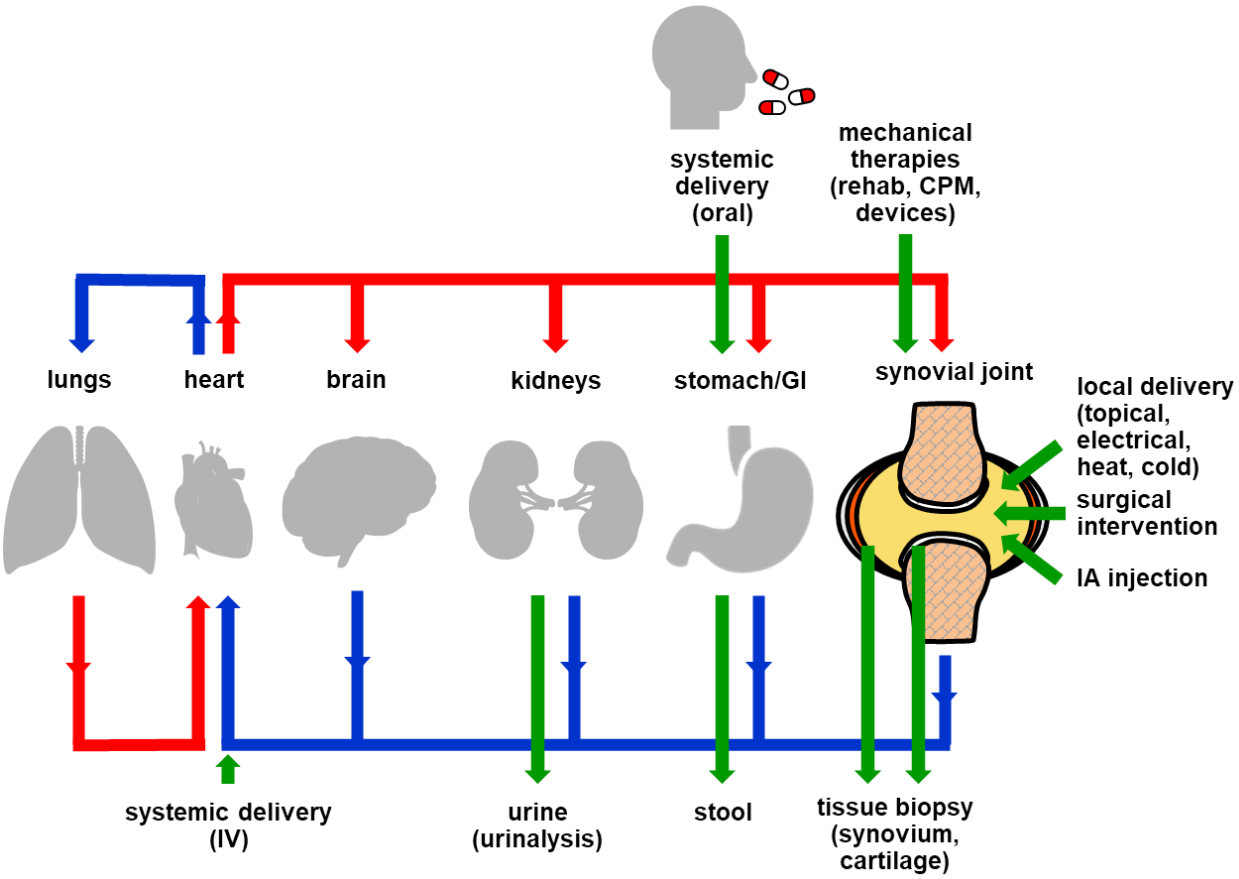


Figure 2.7. Organ system and whole-body model of transport to, and from, synovial joints. Different metrics and methodologies can be used to assess cartilage and overall joint health, before and after therapeutic interventions. Monitoring and sampling can facilitate evaluation of the general state of the body as well as the condition of specific sites within the joint or repair tissue. Red: flow of oxygenated blood. Blue: flow of deoxygenated blood. Green: system or tissue where intervention or assessment is undertaken. Adapted with permission.[93]

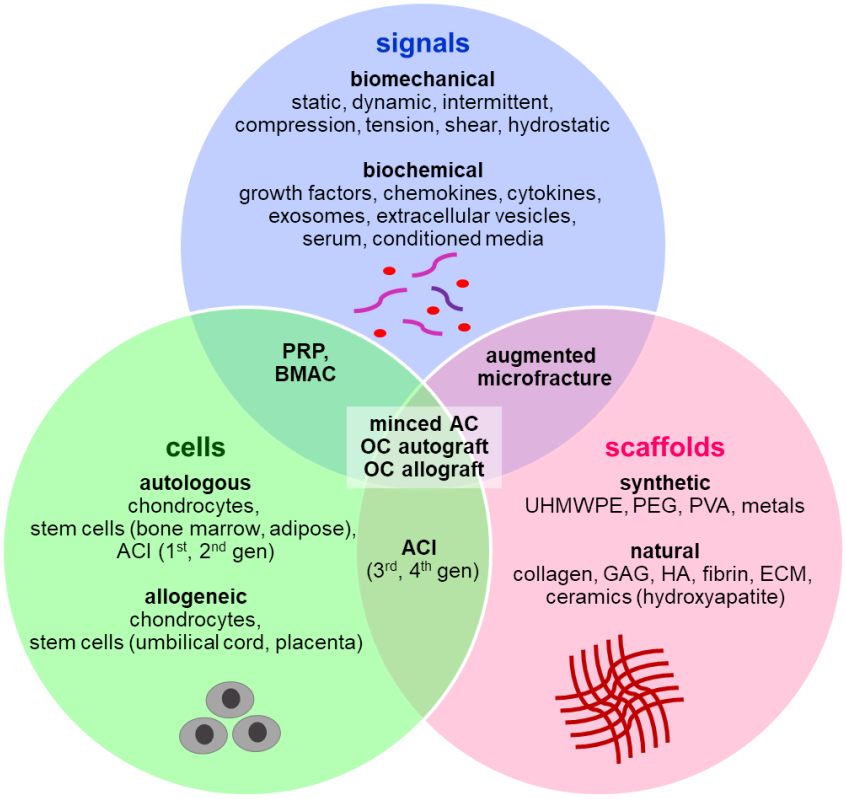


Figure 2.8. Engineered tissue components. Signals, cells, and scaffolds are the major elements of pharmacologic and tissue engineering approaches to cartilage repair. These elements may be used separately, or in combination, to treat symptomology or affect regeneration or restoration of tissue function. Adapted with permission.[93]

Table 2.1. Repair strategies to treat chondral and osteochondral lesions. Repair strategies can be classified according to their primary therapeutic mode of action, biomechanical or biological, and also by mode of delivery (systemic, local, or surgical). Table adapted with permission.[93]

		Therapy	
		Mechanical	**Biologic**
Mode of Delivery	**Systemic** (oral, intravenous)	Exercise/Physical Therapy, weight loss, orthotics	NSAIDs, analgesics, nutritional supplements
	Local (intra-articular, topical)	Viscosupplements, CPM, braces	Corticosteroids, stem cells, PRP, BMAC, GFs, EVs, drugs
	Surgical	Osteotomy, allografts, autografts, total/partial joint replacement	Bone marrow stimulation, ACI, engineered grafts, joint distraction

Table 2.2. Orthobiologics for cartilage repair and osteoarthritis. The national clinical trials number (NCT) of recently registered studies are indicated as well as if the product is marketed in the United States for use in cartilage repair as a minimally manipulated human cells, tissues, and cellular and tissue-based products (HCT/Ps), or under a biologics license application (BLA).

# (NCT)	Product/ Trade Name	Company	Cell Type	Scaffold Material	Signal	Delivery	Market Status (USA)
1	Cartiform	Osiris Therapeutics (Columbia, MD)	Allogeneic chondrocytes	Osteochondral allograft		Surgical	✓ (HCT/P)
2	CartiMax	MTF Biologics (Edison, NJ)	Allogeneic chondrocytes	Lyophilized extracellular matrix		Surgical	✓ (HCT/P)
3 (01733186)	CartiStem	Medipost (Seoul, South Korea)	Allogeneic umbilical cord-derived MSCs	Hyaluronic acid-based		Surgical	
4 (01329445)	DeNovo NT	Zimmer Biomet (Warsaw, IN)	Allogeneic chondrocytes	Minced juvenile cartilage allograft		Surgical	✓ (HCT/P)
5 (03588975)	MACI	Vericel Corporation (Cambridge, MA)	Autologous chondrocytes	Collagen membrane		Surgical	✓ (BLA)
6 (01957722)	Novocart 3D	Aesculap Biologics (Center Valley, PA)	Autologous chondrocytes	Biphasic collagen scaffold with chondroitin sulfate		Surgical	
7 (03319797)	Novocart Inject Plus	Tetec AG (Reutlingen, Germany)	Autologous chondrocytes	In situ polymerizable hydrogel (albumin, hyaluronic acid)		Surgical	
8 (03873545)	ProChondrix CR	Allosource (Centennial, CO)	Allogeneic chondrocytes	Laser-etched, cryopreserved fresh osteochondral allograft		Surgical	✓ (HCT/P)
9 (02844751)	StroMed	VivaTech International, Inc. (Harrisville, PA)	Autologous adipose-derived MSCs	Adipose ECM		Intra-articular	

Table 2.2. Orthobiologics for cartilage repair and osteoarthritis. (Continued)

# (NCT)	Product/ Trade Name	Company	Cell Type	Scaffold Material	Signal	Delivery	Market Status (USA)
10 (03383081)	19#iSC Life-OA	Sclnow Biotechnology Co., Ltd. (Beijing, China)	Allogeneic umbilical cord-derived MSCs			Intra-articular	
11 (04208646)	AlloJoin	Cellular Biomedicine Group Ltd (Shanghai, China)	Allogeneic adipose-derived MSCs			Intra-articular	
12 (04744402)	CartiLife	Biosolution Co., Ltd. (Seoul, South Korea)	Autologous chondrocytes (cell spheroids)			Surgical	
13 (04863183)	Cellistem OA	Cells for Cells (Santiago, Chile)	Allogeneic umbilical cord-derived MSCs			Intra-articular	
14 (04520945)	Chondrogen	Meluha Life Sciences SDN BHD (Putrajaya, Malaysia)	Allogeneic umbilical cord-derived MSCs			Intra-articular	
15 (01222559)	Chondro-Sphere	Co.Don AG (Teltow, Germany)	Autologous chondrocytes (cell spheroids)			Surgical	
16 (03203330)	TissueGene-C	Kolon TissueGene (Rockville, MD)	Allogeneic non-transduced chondrocytes, irradiated transduced human GP2-293 cells expressing TGF-β1			Intra-articular	
17 (03696394)	BioCartilage	Arthrex (Naples, FL)		Allogeneic micronized cartilage matrix		Surgical	✓ (HCT/P)
18 (01246895)	BST CarGel	Smith & Nephew (London, United Kingdom)		Chitosan		Surgical	

Table 2.2. Orthobiologics for cartilage repair and osteoarthritis. (Continued)

# (NCT)	Product/ Trade Name	Company	Cell Type	Scaffold Material	Signal	Delivery	Market Status (USA)
19 (01410136)	Chondrofix	Zimmer Biomet (Warsaw, IN)		Allogeneic decellularized osteochondral graft		Surgical	✓ (HCT/P)
20 (04537013)	Chondro-Gide	Geistlich Pharma (Wolhusen, Switzerland)		Bilayer collagen I/III membrane		Surgical	
21 (02659215)	Hyalofast	Anika Therapeutics (Bedford, MA)		Hyaluronic acid-based		Surgical	
22 (03968913)	Kineret	Sobi (Stockholm, Sweden)			Anakinra (IL1-β receptor antagonis)	Intra-articular	
23 (03727022)		Biosplice Therapeutics, Inc. (San Diego, CA)			SM04690 (Wnt inhibitor)	Intra-articular	
24 (03072147)		Eli Lilly and Company (Indianapolis, IN)			Teriparatide (promotes bone formation)	Intra-muscular	
25 (04875754)		ICM Biotech (Seoul, Korea)			ICM-203 (gene therapy)	Intra-articular	
26 (01919164)		Merck (Darmstadt, Germany)			Sprifermin (rhFGF-18)	Intra-articular	
27 (03275064)		Novartis (Basel, Switzerland)			LNA043 (ANGPTL3 agonist)	Intra-articular	
28 (04097379)		Novartis (Basel, Switzerland)			LRX712 (pro-regenerative)	Intra-articular	
29 (02837900)		OrthoTrophix, Inc (Oakland, CA)			TPX-100 (regulates hard tissue, phosphate metabolism)	Intra-articular	
30 (04318041)	Artrodar	TRB Chemedica (Geneva, Switzerland)			Diacerein (IL-1β inhibitor)	Oral	
31 (03595618)		Galapagos NV (Mechelen, Belgium)			GLPG1972 (ADAMTS-5 inhibitor)	Oral	

Table 2.2. Orthobiologics for cartilage repair and osteoarthritis. (Continued)

# (NCT)	Product/ Trade Name	Company	Cell Type	Scaffold Material	Signal	Delivery	Market Status (USA)
32 (02705625)		Medivir (Huddinge, Sweden)			MIV-711 (Cathepsin K inhibitor)	Oral	

2.4. Standard approaches to cartilage repair

2.4.1. Functional tissue replacement: osteochondral grafting

Osteochondral grafting involves transfer of intact osteochondral units from autologous or allogeneic sources to replace damaged tissue and restore normal load-bearing function. Osteochondral grafts consist of full-thickness viable AC and a layer of attached devitalized subchondral bone to provide a (1) mechanically functional (a) hyaline cartilage tissue and (b) osteoinductive, osteoconductive, and osteogenic scaffold, and (2) viable chondrocytes in normal organization. In addition, implanted tissue may function as a depot of pro-regenerative factors which are retained in, and slowly released from, the graft.

Autologous grafts, either by single or multiple (mosaicplasty) plugs, are generally used to resurface focal defects 1 – 4 cm^2, and can be accomplished arthroscopically, or as an open procedure. Conversely, allogeneic grafting involves the transfer of size-matched osteochondral allograft (OCA) tissue from a cadaveric donor, into chondral and osteochondral defects (> 2 cm^2).[53] To ensure fit, the lesion location, size and the overall shape and contour of the joint are assessed such that a size-matched graft can be harvested from the donor. Depending on defect size and severity, allograft morphology may range from a single osteochondral plug to massive osteoarticular allografts.

Good 5- and 10-year survival rates (>80%) and high rates of patient satisfaction are dependent on selection of suitable patient populations, often with full-thickness non-kissing defects and who do not have lesions with degenerative etiology, uncorrectable joint malalignment, nor high body mass index (>35 kg/m^2).[54-57] Graft survival rate also depends on chondrocyte viability and appropriate matching of cartilage surface topography.[58,59] The utility of mosaicplasty may also be constrained by donor-site availability and morbidity; and availability of appropriately matched OCA donor tissue may be limited.

2.4.2. Autologous chondrocyte implantation

Autologous chondrocyte implantation (ACI), or autologous chondrocyte transplantation, was the first commercially marketed cell-based therapy for cartilage regeneration. ACI is a two-stage procedure involving arthroscopic biopsy of cartilage from a non-loadbearing area, isolation and in vitro expansion of chondrocytes, and implantation of the chondrocyte suspension into the defect site. Cartilage (200 – 300 mg) is harvested from healthy tissue and the sample is sent to a commercial GMP facility to isolate and expand chondrocytes in vitro. The final product is a liquid suspension of cells,[60] or cell-laden scaffold,[61] which is extensively tested for chondrocyte morphology, sterility, viability, and endotoxins before it is shipped for implantation in the second-stage. Indications for ACI are mixed and may be used for treatment of full-thickness injuries (> 2 cm^2) as a primary intervention or in patients who have failed another primary intervention.[62]

First developed in the 1990s by Brittberg et al.,[60] ACI evolved from successful pre-clinical studies in a rabbit model.[63] ACI has undergone several generations of development wherein the method of in vitro expansion and anchorage to the defect site during the secondary procedure has varied.[62] First-generation ACI involved suturing of autologous periosteum over the defect and implantation of expanded chondrocytes by syringe through the periosteal flap. However, to reduce complexity and potential complications, second generation ACI procedures employed purpose-designed collagen membranes such as Chondro-Gide (Geistlich Biomaterials; Wolhusen, Switzerland) instead of periosteum. Third-generation ACI techniques involve implantation of a chondrocyte-laden biomaterial scaffold. Matrix assisted chondrocyte transplantation (MACT) allows for culture of chondrocytes in a more physiologically relevant environment, and facilitates a simpler, more rapid, and less morbid operation by removing the need for periosteal harvest or membrane suturing. Third generation ACI procedures include MACI (Vericel; Cambridge, MA) and Novocart 3D (Tetec; Reutlingen, Germany) among others which differ in their preparation

and culture of autologous chondrocytes and choice of biomaterial scaffold.

Additional advances in bioreactor design and cell-culture methodologies have resulted in the development of fourth-generation ACI techniques where culture conditions facilitate extracellular matrix production and preservation of chondrogenic phenotype. For instance, cell-spheroid based ACI techniques, including ChondroSphere (Co.Don; Teltow, Germany) and CartiLife (Biosolution; Seoul, South Korea), utilize autologous chondrocytes that are cultivated into spheroids containing cell aggregates and autologous cartilage-like extracellular matrix.[61] Although third and fourth generation products have shown promising results, limitations of all ACI methodologies include high cost due to in vitro cell expansion in a commercial GMP facility and fragility of the initial repair tissue.

2.4.3. Augmentation of intrinsic repair: Bone marrow stimulation

For symptomatic defects of small size (< 2 cm^2), bone marrow stimulation by breach of the subchondral bone through various means including microfracture, microdrilling, and other methods, is typically a first-line treatment due to the relatively low cost and straightforward technique compared to other surgical interventions (**Fig. 6E-H**). Marrow stimulation leverages the intrinsic cartilage repair response after subchondral bone penetration by releasing a milieu of marrow elements, including MSCs, growth factors, and other signals, into the injured site to promote formation of fibrocartilaginous repair tissue.[64,65] At the defect, the marrow clots and provides a structural framework, or scaffold, upon which repair can occur. However, lack of control on the differentiation process often leads to variable formation of suboptimal fibrocartilage repair tissue with inferior biochemical and biomechanical properties having a higher proportion of type I collagen than hyaline cartilage.[65,66]

Recent advances in microfracture involve augmentation with biomaterial scaffolds to

stabilize clot formation and promote chondrogenesis and formation of hyaline cartilage, in a method often referred to as autologous matrix induced chondrogenesis (AMIC). AMIC may be achieved using micronized or particulated allogeneic cartilage (BioCartilage, Arthrex; Naples, FL), as well as biomaterial scaffolds such as chitosan (BST-CarGel, Smith & Nephew; London, United Kingdom) and hyaluronan (Hyalofast, Anika Therapeutics; Bedford, MA). In addition to biomaterials scaffolds, marrow stimulation techniques are often paired with bone marrow aspirate concentrate or platelet rich plasma to enhance cartilage repair

2.5. Novel orthobiologic approaches to cartilage repair

Approaches to orthobiologic repair aim to modulate or activate the response of endogenous or exogenous cells, as a stand-alone procedure or to augment cartilage restoration surgery, to promote formation of hyaline-like cartilaginous repair tissue. Many orthobiologic interventions aim to enhance matrix formation by promoting anabolic or suppressing catabolic pathways.

2.5.1.Platelet rich plasma and bone marrow aspirate concentrate

Platelet rich plasma (PRP) and bone marrow aspirate concentrate (BMAC) have demonstrated promising results in the clinical application for repair of chondral defects as an adjuvant procedure (e.g. to bone marrow stimulation), or as an independent management technique via intraarticular injection.[49,50] PRP and BMAC are cellular preparations of autologous blood and bone marrow aspirate, respectively, that have been concentrated, usually by centrifugation, and are often activated with thrombin. These autologous point-of-care cell therapies contain a high concentration of platelets, growth factors, chemokines, and cytokines as well as MSCs and a variety of hematopoietic cells which provide potentially beneficial anabolic and anti-inflammatory mediators.[67] Although translational studies have demonstrated good clinical efficacy of PRP and BMAC, methods of preparation are variable and there is inherent patient-to-patient variability in composition.[49] Standardized, and high-quality studies are needed to demonstrate efficacy.

2.5.2. Extracellular vesicles

Treatments utilizing extracellular vesicles (EVs) represent a novel class of therapeutics that act to modulate the inflammatory response and stimulate matrix production to restore and maintain cartilage homeostasis.[68] EVs, including exosomes and microvesicles, are secreted membrane-enclosed vesicles. EVs are isolated from extracellular fluids (conditioned cell culture media, body

fluids) and may contain proteins, including growth factors and cytokines, functional nucleic acids (mRNA, miRNA, etc.), and lipids which function as intercellular communication vehicles.[69,70] Pre-clinical in vitro and in vivo studies have demonstrated that the immunomodulatory, chondroprotective, and regenerative effects of MSC-derived EVs (MSC-EVs) are equivalent or superior to MSCs alone.[68] Compared to cell-based therapies, EV-based treatments minimize difficulties associated with living-cell therapeutics (viability, potency, differentiation).

2.5.3. Gene therapy strategies

Gene therapy strategies for cartilage repair often aim to reduce inflammation, inhibit matrix degradation, and increase matrix synthesis through the delivery of nucleic acids to target tissues or cells using viral (adenovirus, lentivirus, retroviruses, etc.) or non-viral (siRNAs, miRNAs) vectors. Gene therapies targeting the IL-1, TNF-α, IFN-β, and Hif-2α pathways, which mediate chondrocyte catabolism, as well as IGF-1, TGF-β, SOX9, and PRG4, which mediate anabolism and chondrogenesis, have been investigated pre-clinically with some being evaluated in clinical trials.[71] Recently, TissueGene-C (Kolon TissueGene; Rockville, MD), a biologic drug product consisting of allogeneic human chondrocytes virally transduced to express TGF-β1, promoted cartilage regeneration in rabbit preclinical studies, and is considered safe and effective for improving pain and motor scores in patients with moderate to severe disease. [71] TissueGene-C was approved in Korea for treatment of moderate knee OA for which standard of care has failed, and is currently in phase 3 clinical trials in the United States (NCT03203330).

2.5.4. Additional targets for small molecule therapies

Other biologic therapies target inflammatory or biosynthetic pathways by interacting with cell receptors or providing growth factors. Anti-inflammatory agents such as bradykinin-B2

receptor agonists, which reduce OA knee pain compared to placebo, anakinra, an IL-1β receptor antagonist that reduces pain and improves knee function 2 weeks after acute injury compared to placebo, as well as TNF inhibitors (infliximab, etanercept), have been proposed to manage knee OA.[72,73] In addition, growth factor treatments with recombinant human bone morphogenetic protein 7 (rhBMP7) and recombinant human fibroblast growth factor 18 (rhFGF18, sprifermin) have demonstrated positive outcomes (reduction in Western Ontario and McMaster Universities Osteoarthritis Index pain scores) compared to placebo, but have not been evaluated in long-term clinical studies.[48] Therapeutic utility of these agents, typically delivered by intra-articular injection, is diminished by short retention times within the joint space as well as limited transport within the cartilage tissue. Such limitations may be ameliorated by coupling the therapeutic agent to positively charged carriers of optimal size and charge so that the cartilage can function as a reservoir for sustained intra-tissue delivery.[32]

2.5.5. Alternative cell sources

Investigations into the feasibility and clinical utility of alternative cell sources for cartilage repair are ongoing. Unfortunately, the use of autologous chondrocytes is limited by donor site morbidity and complicated by the relatively low cellularity in adult AC, requiring in vitro expansion. Furthermore, repair tissue involving autologous chondrocytes is often fibrocartilaginous in nature and not characteristic of native hyaline cartilage.[51]

Mesenchymal stem cells (MSCs) have been studied extensively in vitro and in vivo within the context of cartilage repair.[51,74] MSCs are capable of differentiating into bone and cartilage and have been derived from bone marrow, bone, synovium, periosteum, muscle, dermis, adipose, umbilical cord, and placental tissues. In particular, bone marrow-derived MSCs secrete a variety of synthetic, proliferative, and regenerative factors that, when introduced to the joint, interact with

endogenous cells to modulate the repair response.[75] However, since the number of bone marrow-derived MSCs decreases significantly with age,[76] MSCs isolated from umbilical cord and adipose tissues, which are readily available and highly cellular, have been developed and are in clinical trials.[51,77] Additional cell sources which have been investigated include induced pluripotent stem cells, as well as stem cells from peripheral blood and amniotic tissue.[46,51,78]

Utilization of cell-based therapies is limited by the undefined dose, regimen, and mode of delivery of cells to the injured site. Cells may be pre-conditioned in vitro with biomechanical and biochemical stimuli to modulate phenotype and behavior, and subsequently used as a stand-alone drug or biologic, delivered by intra-articular injection, or as a component of a more complex intervention. Future studies are necessary to establish the long-term clinical benefit of cell-based therapeutics for cartilage repair and identify indications and criteria for their use.

Bioreactors are used in the development and production of orthobiologics to apply a combination of mechanical and biochemical signals. During development of engineered AC or osteochondral tissues, mechanical stimulation during culture regulates and improves the mechanical properties of the engineered tissue.[79,80] In addition, bioreactors are used to screen for drug candidates and evaluate cartilage repair strategies. Emerging microfluidic chip-based platforms enable high-throughput screening of drug-candidates. Cartilage- and joint- on-a-chip models mimic aspects of the joint and recapitulate physiologic responses in response to drug candidates.[81,82] 3D culture of chondrocytes within engineered constructs or in explanted tissues are also used to evaluate drug candidates and cartilage repair strategies at multiple scales.[83,84] Bioreactor systems are also used in bioprocessing to produce of therapeutic tissues, cells, and cellular derivatives, such as gene and EV therapies. Production of these biologics may require cellular expansion, cultivation on 3D material scaffolds, and additional purification.[46,85,86]

2.6. Summary

Repair of cartilage injuries, due to traumatic focal defects or chronic disease, aim to restore cartilage function and prevent slow, or reverse cartilage degeneration. Conventional treatments for cartilage repair, including osteochondral grafting and autologous chondrocyte implantation, are limited by donor availability, donor-site morbidity, and are difficult to scale and produce as off-the-shelf products. Ultimately, orthobiologic therapies may help to reduce the use of allogeneic or autologous tissue grafts for treatment of focal and widespread joint deterioration (**Fig. 9**).

Emerging orthobiologic interventions provide a combination of cells, scaffolds, and signals which aim to establish a regenerative environment to facilitate repair. Local delivery of PRP, BMAC, and extracellular vesicles, which are enriched with growth factors and cytokines, as well as gene therapies and other small molecule therapeutics modulate matrix formation and cellular behavior by targeting anabolic and catabolic pathways. In addition, PRP and BMAC contain MSCs which aid in repair. Furthermore, cellular therapies utilizing autologous and allogeneic MSC sources are being developed as an alternative to autologous chondrocytes. Therapeutic components should be engineered to maximize retention within the joint space and synovial fluid, if introduced via intra-articular injection, and within the cartilage itself by utilizing the native physicochemical properties of the tissue.

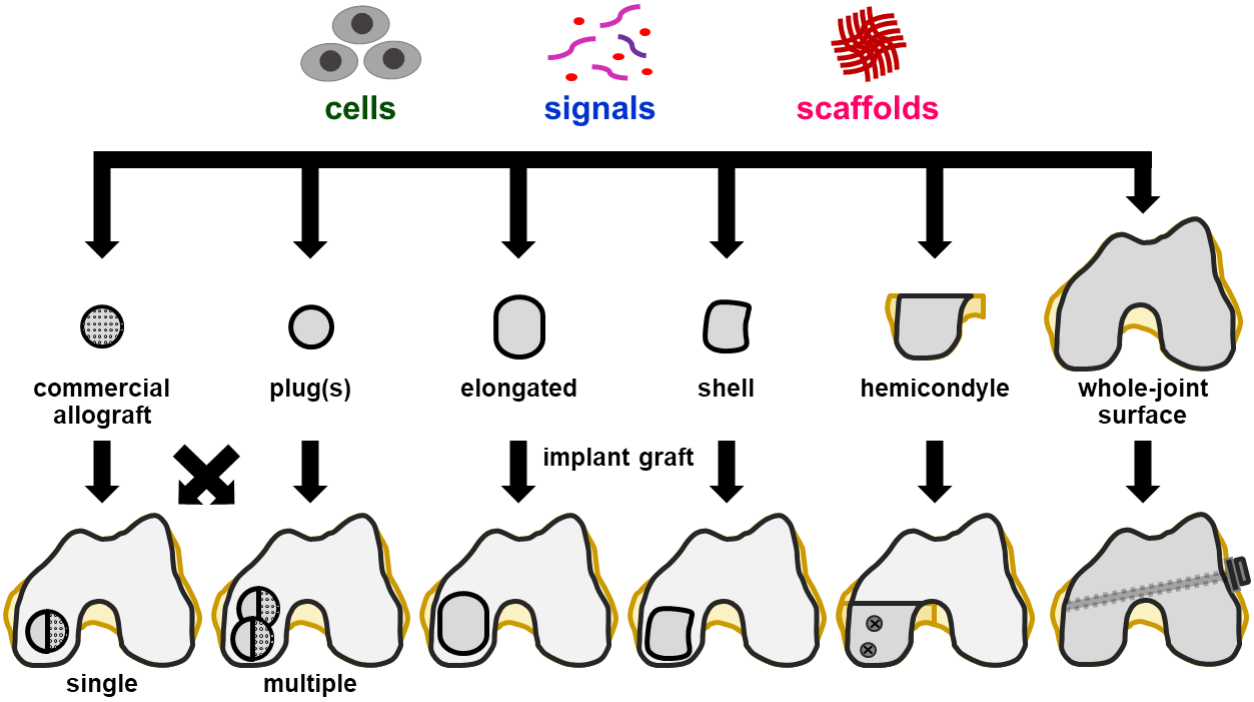


Figure 2.9. Chondral and Osteochondral grafting techniques. Depending on the size of the defect, cartilage and osteochondral lesions may be treated with allogeneic or autologous as well as tissue engineered (osteo)chondral grafts. Adapted with permission.[93]

2.7. Acknowledgements

This chapter, in full, was published in the first edition of *Orthobiologics: Scientific and Clinical Solutions for Orthopaedic Surgeons* published by Wolters Kluwer. Thanks to book editors Roy K. Aaron, MD., and Scott P. Bruder, MD. PhD.

2.8. References

1. Hunter W: Of the structure and disease of articulating cartilages. *Philos Trans R Soc London*. 1743;42:514-21.

2. Brannan SR, Jerrard DA: Synovial fluid analysis. *J Emerg Med*. 2006;30:331-9.

3. Carlson CS, Cullins LD, Meuten DJ: Osteochondrosis of the articular-epiphyseal cartilage complex in young horses: evidence for a defect in cartilage canal blood supply. *Vet Pathol*. 1995;32:641-7.

4. Carlson CS, Hilley HD, Henrikson CK: Ultrastructure of normal epiphyseal cartilage of the articular-epiphyseal cartilage complex in growing swine. *Am J Vet Res*. 1985;46:306-13.

5. Aspden RM: Osteoarthritis: a problem of growth not decay? *Rheumatology (Oxford)*. 2008;47:1452-60.

6. Sun HB: Mechanical loading, cartilage degeneration, and arthritis. *Ann N Y Acad Sci*. 2010;1211:37-50.

7. Goldring MB: Articular cartilage degradation in osteoarthritis. *HSS J*. 2012;8:7-9.

8. Poole AR, Kojima T, Yasuda T, Mwale F, Kobayashi M, Laverty S: Composition and structure of articular cartilage: a template for tissue repair. *Clin Orthop Relat Res*. 2001:S26-33.

9. Han E, Chen SS, Klisch SM, Sah RL: Contribution of proteoglycan osmotic swelling pressure to the compressive properties of articular cartilage. *Biophys J*. 2011;101:916-24.

10. Dudhia J: Aggrecan, aging and assembly in articular cartilage. *Cell Mol Life Sci*. 2005;62:2241-56.

11. Heinegard D, Saxne T: The role of the cartilage matrix in osteoarthritis. *Nat Rev Rheumatol*. 2011;7:50-6.

12. Temple MM, Bae WC, Chen MQ, Lotz M, Amiel D, Coutts RD, Sah RL: Age- and site-associated biomechanical weakening of human articular cartilage of the femoral condyle. *Osteoarthritis Cartilage*. 2007;15:1042-52.

13. Aigner T, Zien A, Gehrsitz A, Gebhard PM, McKenna L: Anabolic and catabolic gene expression pattern analysis in normal versus osteoarthritic cartilage using complementary DNA-array technology. *Arthritis Rheum*. 2001;44:2777-89.

14. Grogan SP, Duffy SF, Pauli C, Koziol JA, Su AI, D'Lima DD, Lotz MK: Zone-specific gene expression patterns in articular cartilage. *Arthritis Rheum*. 2013;65:418-28.

15. Darling EM, Hu JC, Athanasiou KA: Zonal and topographical differences in articular cartilage gene expression. *J Orthop Res*. 2004;22:1182-7.

16. Kozhemyakina E, Zhang M, Ionescu A, Ayturk UM, Ono N, Kobayashi A, Kronenberg H, Warman ML, Lassar AB: Identification of a Prg4-positive articular cartilage progenitor cell population. *Arthritis Rheumatol*. 2015.

17. Decker RS, Um HB, Dyment NA, Cottingham N, Usami Y, Enomoto-Iwamoto M, Kronenberg MS, Maye P, Rowe DW, Koyama E, Pacifici M: Cell origin, volume and arrangement are drivers of articular cartilage formation, morphogenesis and response to injury in mouse limbs. *Dev Biol*. 2017;426:56-68.

18. Li L, Newton PT, Bouderlique T, Sejnohova M, Zikmund T, Kozhemyakina E, Xie M, Krivanek J, Kaiser J, Qian H, Dyachuk V, Lassar A, Warman ML, Barenius B, Adameyko I, Chagin A: Superficial cells are self-renewing chondrocyte progenitors, which form the articular cartilage in juvenile mice. *FASEB J*. 2016;31:1067-84.

19. Karlsson C, Thornemo M, Henriksson HB, Lindahl A: Identification of a stem cell niche in the zone of Ranvier within the knee joint. *J Anat*. 2009;215:355-63.

20. Maroudas A: Physicochemical Properties of Articular Cartilage. In: *Adult Articular Cartilage*, ed by MAR Freeman, Pitman Medical, Tunbridge Wells, England, 1979, pp 215-90.

21. Eyre DR, Weis MA, Wu J-J: Articular cartilage collagen: an irreplaceable framework? *Eur Cell Mater*. 2006;12:57-63.

22. Belcher C, Yaqub R, Fawthrop F, Bayliss M, Doherty M: Synovial fluid chondroitin and keratan sulphate epitopes, glycosaminoglycans, and hyaluronan in arthritic and normal knees. *Ann Rheum Dis*. 1997;56:299-307.

23. Bayliss MT, Howat S, Davidson C, Dudhia J: The organization of aggrecan in human articular cartilage. Evidence for age-related changes in the rate of aggregation of newly synthesized molecules. *J Biol Chem*. 2000;275:6321-7.

24. Smith DW, Gardiner BS, Zhang L, Grodzinsky AJ: Cartilage Tissue Homeostasis. In: *Articular Cartilage Dynamics*, ed, Springer, Singapore, 2019, pp 65-243.

25. Knudson CB, Knudson W: Cartilage proteoglycans. *Semin Cell Dev Biol*. 2001;12:69-78.

26. Gao Y, Shuyun L, Huang J, Guo W, Chen J, Zhang L, Zhao B, Peng J, Wang A, Wang Y, Xu W, Lu S, Yuan M, Guo Q: The ECM-cell interaction of cartilage extracellular matrix on chondrocytes. *Biomed Res Int*. 2014;2014:648459.

27. DiDomenico CD, Lintz M, Bonassar LJ: Molecular transport in articular cartilage - what have we learned from the past 50 years? *Nat Rev Rheumatol*. 2018;14:393-403.

28. Levick JR, McDonald JN: Fluid movement across synovium in healthy joints: role of synovial fluid macromolecules. *Ann Rheum Dis*. 1995;54:417-23.

29. Hui AY, McCarty WJ, Masuda K, Firestein GS, Sah RL: A systems bIology approach to synovial joint lubrication in health, injury, and disease. *Wiley Interdiscip Rev Syst Biol Med*. 2012;4:15-37.

30. Levick JR: A method for estimating macromolecular reflection by human synovium, using measurements of intra-articular half-lives. *Ann Rheum Dis*. 1998;57:339-44.

31. Owen SG, Francis HW, Roberts MS: Disappearance kinetics of solutes from synovial fluid after intra-articular injection. *Br J Clin Pharmacol*. 1994;38:349-55.

32. Bajpayee AG, Grodzinsky AJ: Cartilage-targeting drug delivery: can electrostatic interactions help? *Nat Rev Rheumatol*. 2017;13:183-93.

33. Doan TN, Bernard FC, McKinney JM, Dixon JB, Willett NJ: Endothelin-1 inhibits size dependent lymphatic clearance of PEG-based conjugates after intra-articular injection into the rat knee. *Acta Biomater*. 2019;93:270-81.

34. McCarty WJ, Cheng JC, Hansen BC, Yamaguchi T, Masuda K, Sah RL: The biophysical mechanisms of altered hyaluronan concentration in synovial fluid after anterior cruciate ligament transection. *Arthritis Rheum.* 2012;64:3993-4003.

35. Bouta EM, Bell RD, Rahimi H, Xing L, Wood RW, Bingham CO, 3rd, Ritchlin CT, Schwarz EM: Targeting lymphatic function as a novel therapeutic intervention for rheumatoid arthritis. *Nat Rev Rheumatol*. 2018;14:94.

36. Lesperance LM, Gray ML, Burstein D: Determination of fixed charge density in cartilage using nuclear magnetic resonance. *J Orthop Res*. 1992;10:1-13.

37. Maroudas A: Distribution and diffusion of solutes in articular cartilage. *Biophys J.* 1970;10:365-79.

38. Eisenberg SR, Grodzinsky AJ: Swelling of articular cartilage and other connective tissues: electromechanochemical forces. *J Orthop Res*. 1985;3:148-59.

39. Hjelle K, Solheim E, Strand T, Muri R, Brittberg M: Articular cartilage defects in 1,000 knee arthroscopies. *Arthroscopy*. 2002;18:730-4.

40. Buckwalter JA, Saltzman C, Brown T: The impact of osteoarthritis: implications for research. *Clin Orthop Relat Res*. 2004:S6-15.

41. Bijlsma JW, Berenbaum F, Lafeber FP: Osteoarthritis: an update with relevance for clinical practice. *Lancet*. 2011;377:2115-26.

42. Lotz M, Loeser RF: Effects of aging on articular cartilage homeostasis. *Bone*. 2012;51:241-8.

43. Marlovits S, Singer P, Zeller P, Mandl I, Haller J, Trattnig S: Magnetic resonance observation of cartilage repair tissue (MOCART) for the evaluation of autologous chondrocyte transplantation: determination of interobserver variability and correlation to clinical outcome after 2 years. *Eur J Radiol*. 2006;57:16-23.

44. Smith BD, Grande DA: The current state of scaffolds for musculoskeletal regenerative applications. *Nat Rev Rheumatol*. 2015;11:213-22.

45. Mastbergen SC, Saris DB, Lafeber FP: Functional articular cartilage repair: here, near, or is the best approach not yet clear? *Nat Rev Rheumatol*. 2013;9:277-90.

46. Kwon H, Brown WE, Lee CA, Wang D, Paschos N, Hu JC, Athanasiou KA: Surgical and tissue engineering strategies for articular cartilage and meniscus repair. N*at Rev Rheumatol*. 2019;15:550-70.

47. Steinert AF, Noth U, Tuan RS: Concepts in gene therapy for cartilage repair. *Injury*. 2008;39 Suppl 1:S97-113.

48. Jones IA, Togashi R, Wilson ML, Heckmann N, Vangsness CT, Jr.: Intra-articular treatment options for knee osteoarthritis. *Nat Rev Rheumatol*. 2019;15:77-90.

49. Chahla J, Cinque ME, Piuzzi NS, Mannava S, Geeslin AG, Murray IR, Dornan GJ, Muschler GF, LaPrade RF: A call for standardization in platelet-rich plasma preparation protocols and composition reporting: a systematic review of the clinical orthopaedic literature. *J Bone Joint Surg Am*. 2017;99:1769-79.

50. Piuzzi NS, Hussain ZB, Chahla J, Cinque ME, Moatshe G, Mantripragada VP, Muschler GF, LaPrade RF: Variability in the preparation, reporting, and use of bone marrow aspirate concentrate in musculoskeletal disorders: A systematic review of the clinical orthopaedic literature. *J Bone Joint Surg Am*. 2018;100:517-25.

51. Makris EA, Gomoll AH, Malizos KN, Hu JC, Athanasiou KA: Repair and tissue engineering techniques for articular cartilage. *Nat Rev Rheumatol*. 2015;11:21-34.

52. Caplan AI, Correa D: The MSC: an injury drugstore. *Cell Stem Cell*. 2011;9:11-5.

53. Chahal J, Gross AE, Gross C, Mall N, Dwyer T, Chahal A, Whelan DB, Cole BJ: Outcomes of osteochondral allograft transplantation in the knee. *Arthroscopy*. 2013;29:575-88.

54. Frank RM, Lee S, Levy D, Poland S, Smith M, Scalise N, Cvetanovich GL, Cole BJ: Osteochondral allograft transplantation of the knee. Analysis of failures at 5 years. *Am J Sports Med*. 2017;45:864-74.

55. Cavendish PA, Everhart JS, Peters NJ, Sommerfeldt MF, Flanigan DC: Osteochondral allograft transplantation for knee cartilage and osteochondral defects: A review of indications, technique, rehabilitation, and outcomes. *JBJS Rev*. 2019;7:e7.

56. Wang D, Chang B, Coxe FR, Pais MD, Wickiewicz TL, Warren RF, Rodeo SA, Williams RJ, 3rd: Clinically meaningful improvement after treatment of cartilage defects of the knee with osteochondral grafts. *Am J Sports Med*. 2019;47:71-81.

57. Hangody L, Fules P: Autologous osteochondral mosaicplasty for the treatment of full-thickness defects of weight-bearing joints. Ten years of experimental and clinical experience. *J Bone Joint Surg Am*. 2003;85-A, Supplement 2:25-32.

58. Sherman SL, Garrity J, Bauer K, Cook J, Stannard J, Bugbee W: Fresh osteochondral allograft transplantation for the knee: current concepts. *J Am Acad Orthop Surg*. 2014;22:121-33.

59. Chahla J, Hinckel BB, Yanke AB, Farr J, Bugbee WD, Carey JL, Cole BJ, Crawford DC, Fleischli JE, Getgood A, Gomoll AH, Gortz S, Gross AE, Jones DG, Krych AJ, Lattermann C, Mandelbaum BR, Mandt PR, Minas T, Mirzayan R, Mologne TS, Polousky JD, Provencher MT, Rodeo SA, Safir O, Sherman SL, Strauss ED, Strickland SM, Wahl CJ, Williams RJ, 3rd: An expert consensus statement on the management of large chondral and osteochondral defects in the patellofemoral joint. *Orthop J Sports Med*. 2020;8:2325967120907343.

60. Brittberg M, Lindahl A, Nilsson A, Ohlsson C, Isaksson O, Peterson L: Treatment of deep cartilage defects in the knee with autologous chondrocyte transplantation. *N Engl J Med*. 1994;331:889-95.

61. Huang BJ, Hu JC, Athanasiou KA: Cell-based tissue engineering strategies used in the clinical repair of articular cartilage. *Biomaterials.* 2016;98:1-22.

62. Krill M, Early N, Everhart JS, Flanigan DC: Autologous Chondrocyte Implantation (ACI) for knee cartilage defects: A review of indications, technique, and outcomes. *JBJS Rev*. 2018;6:e5.

63. Grande DA, Pitman MI, Peterson L, Menche D, Klein M: The repair of experimentally produced defects in rabbit articular cartilage by autologous chondrocyte transplantation. *J Orthop Res*. 1989;7:208-18.

64. Rutgers M, van Pelt MJ, Dhert WJ, Creemers LB, Saris DB: Evaluation of histological scoring systems for tissue-engineered, repaired and osteoarthritic cartilage. *Osteoarthritis Cartilage*. 2010;18:12-23.

65. Mithoefer K, McAdams T, Williams RJ, Kreuz PC, Mandelbaum BR: Clinical efficacy of the microfracture technique for articular cartilage repair in the knee: an evidence-based systematic analysis. *Am J Sports Med*. 2009;37:2053-63.

66. Steadman JR, Briggs KK, Rodrigo JJ, Kocher MS, Gill TJ, Rodkey WG: Outcomes of microfracture for traumatic chondral defects of the knee: average 11-year follow-up. *Arthroscopy*. 2003;19:477-84.

67. Kennedy MI, Whitney K, Evans T, LaPrade RF: Platelet-rich plasma and cartilage repair. *Curr Rev Musculoskelet Med*. 2018;11:573-82.

68. Velot É, Madry H, Venkatesan JK, Bianchi A, Cucchiarini M: Is extracellular vesicle-based therapy the next answer for cartilage regeneration? *Front Bioeng Biotechnol*. 2021;9:645039.

69. Lötvall J, Hill AF, Hochberg F, Buzás EI, Di Vizio D, Gardiner C, Gho YS, Kurochkin IV, Mathivanan S, Quesenberry P, Sahoo S, Tahara H, Wauben MH, Witwer KW, Théry C: Minimal experimental requirements for definition of extracellular vesicles and their functions: a position statement from the International Society for Extracellular Vesicles. *J Extracell Vesicles.* 2014;3:26913.

70. Toh WS, Lai RC, Hui JHP, Lim SK: MSC exosome as a cell-free MSC therapy for cartilage regeneration: Implications for osteoarthritis treatment. *Semin Cell Dev Biol*. 2017;67:56-64.

71. Grol MW, Lee BH: Gene therapy for repair and regeneration of bone and cartilage. *Curr Opin Pharmacol*. 2018;40:59-66.

72. Kraus VB, Birmingham J, Stabler TV, Feng S, Taylor DC, Moorman CT, 3rd, Garrett WE, Toth AP: Effects of intraarticular IL1-Ra for acute anterior cruciate ligament knee injury: a randomized controlled pilot trial (NCT00332254). *Osteoarthritis Cartilage*. 2012;20:271-8.

73. Hunter DJ: Are there promising biologic therapies for osteoarthritis? *Curr Rheumatol Rep*. 2008;10:19-25.

74. Noth U, Steinert AF, Tuan RS: Technology insight: adult mesenchymal stem cells for osteoarthritis therapy. *Nat Clin Pract Rheumatol*. 2008;4:371-80.

75. Pittenger MF, Discher DE, Péault BM, Phinney DG, Hare JM, Caplan AI: Mesenchymal stem cell perspective: cell biology to clinical progress. *NPJ Regen Med.* 2019;4:22.

76. Rao MS, Mattson MP: Stem cells and aging: expanding the possibilities. *Mech Ageing Dev*. 2001;122:713-34.

77. Wang L, Tran I, Seshareddy K, Weiss ML, Detamore MS: A comparison of human bone marrow-derived mesenchymal stem cells and human umbilical cord-derived mesenchymal stromal cells for cartilage tissue engineering. *Tissue Eng Part A*. 2009;15:2259-66.

78. Gomoll AH, Farr J, Cole BJ, Flanigan DC, Lattermann C, Mandelbaum BR, Strickland SM, Zaslav KR, Kimmerling KA, Mowry KC: Safety and efficacy of an amniotic suspension allograft injection over 12 Months in a single-blinded, randomized controlled trial for symptomatic osteoarthritis of the knee. *Arthroscopy*. 2021;37:2246-57.

79. Salinas EY, Hu JC, Athanasiou K: A guide for using mechanical stimulation to enhance tissue-engineered articular cartilage properties. *Tissue Eng Part B Rev*. 2018;24:345-58.

80. Martin I, Smith T, Wendt D: Bioreactor-based roadmap for the translation of tissue engineering strategies into clinical products. *Trends Biotechnol*. 2009;27:495-502.

81. Occhetta P, Mainardi A, Votta E, Vallmajo-Martin Q, Ehrbar M, Martin I, Barbero A, Rasponi M: Hyperphysiological compression of articular cartilage induces an osteoarthritic phenotype in a cartilage-on-a-chip model. *Nat Biomed Eng*. 2019;3:545-57.

82. Paggi CA, Teixeira LM, Le Gac S, Karperien M: Joint-on-chip platforms: entering a new era of in vitro models for arthritis. *Nat Rev Rheumatol.* 2022;18:217-31.

83. Makarczyk MJ, Gao Q, He Y, Li Z, Gold MS, Hochberg MC, Bunnell BA, Tuan RS, Goodman SB, Lin H: Current models for development of disease-modifying osteoarthritis drugs. *Tissue Eng Part C Methods*. 2021;27:124-38.

84. Nugent-Derfus GE, Takara T, O'Neill JK, Cahill SB, Gortz S, Pong T, Inoue H, Aneloski NM, Wang WW, Vega KI, Klein TJ, Hsieh-Bonassera ND, Bae WC, Burke JD, Bugbee WD, Sah RL: Continuous passive motion applied to whole joints stimulates chondrocyte biosynthesis of PRG4. *Osteoarthritis Cartilage*. 2007;15:566-74.

85. Moutsatsou P, Ochs J, Schmitt RH, Hewitt CJ, Hanga MP: Automation in cell and gene therapy manufacturing: from past to future. *Biotechnol Lett*. 2019;41:1245-53.

86. Grangier A, Branchu J, Volatron J, Piffoux M, Gazeau F, Wilhelm C, Silva AKA: Technological advances towards extracellular vesicles mass production. *Adv Drug Deliv Rev*. 2021;176:113843.

87. Raleigh AR, McCarty WJ, Chen AC, Meinert C, Klein TJ, Sah RL: Synovial joints: Mechanobiology and tissue engineering of articular cartilage and synovial fluid. In: *Comprehensive Biomaterials*, ed by P Ducheyne, KE Healey, DE Hutmacher, DE Grainger, and CJ Kirkpatrick, Elsevier, 2017, pp 107-34.

88. Freemont AJ: 5 - Histopathology of the Rheumatoid Joint. In: *Mechanisms and Models in Rheumatoid Arthritis*, ed by B Henderson, JCW Edwards, and ER Pettipher, Academic Press, 1995, pp 83-113.

89. Jadin KD, Bae WC, Schumacher BL, Sah RL: Three-dimensional (3-D) imaging of chondrocytes in articular cartilage: growth-associated changes in cell organization. *Biomaterials*. 2007;28:230-9.

90. Quinn TM, Häuselmann HJ, Shintani N, Hunziker EB: Cell and matrix morphology in articular cartilage from adult human knee and ankle joints suggests depth-associated adaptations to biomechanical and anatomical roles. *Osteoarthritis Cartilage*. 2013;21:1904-12.

91. Buckwalter JA, Roughley PJ, Rosenberg LC: Age-related changes in cartilage proteoglycans: quantitative electron microscopic studies. *Microsc Res Tech*. 1994;28:398-408.

92. Keene DR, Tufa SF: Transmission electron microscopy of cartilage and bone. *Methods Cell Biol*. 2010;96:443-73.

93. Gacasan EG, Sah RL: Articular Cartilage Repair: Augmentation, Regeneration, Replacement, and Substitution. In: *Orthopaedic Basic Science: Foundations of Clinical Practice*, ed by RK Aaron, American Academy of Orthopaedic Surgeons, Rosemont, IL, 2021, pp 415-32.

CHAPTER 3

COMPRESSIVE PROPERTIES OF NORMAL HUMAN ARTICULAR CARTILAGE ARE ENHANCED BETWEEN INFANT, CHILD, AND ADULT, AND RELATED TO DISTINCTIVE TIMING OF COLLAGEN AND GLYCOSAMINOGLYCAN CONTENT

3.1. Abstract

Adult articular cartilage (AC) function and composition results from growth and maturation of epiphyseal cartilage. Immature AC compressive properties, and the basis for age-related variations in humans, are unknown. Infants, children, and adults exhibit distinctive growth stages, with rapid, decelerating, and no (completed) height velocities, respectively. The hypothesis of this study was that AC compressive properties improve between infants, children, and adults and are related to increases in collagen and GAG. Distal femoral AC from infants (0-2 yr), children (2-10 yr), and adult (18+ yr) donors were assessed for confined compression modulus, H_{A0}, and hydraulic permeability, k_p. Tissue composition, including sulfated GAG, collagen, and DNA, was measured. Dependencies of mechanical properties on composition were assessed by multivariate linear regression. H_{A0} increased between children (0.11 MPa) and adults (0.33 MPa). k_p decreased with compression and between infants and children. Water content diminished incrementally from infants (88%) to adults (75%). Collagen increased between infants (48 mg/g WW) to children and adults (~115 mg/g WW). GAG was elevated from infants and children (~18 mg/g WW) to adults (35 mg/g WW). Cellularity decreased from infants (36×10^6 cells/g WW) to children and adults ($\sim12\times10^6$ cells/g WW). H_{A0} increased coordinately with collagen and GAG, and k_p varied with collagen, cellularity, and residual contents. The softness of immature AC, relative to adult, may

reflect its conforming and remodeling functions during growth. The early ~2-fold increase in collagen between infants and children and later ~2-fold increase in GAG between children and adults is likely responsible for the corresponding elevation in H_{A0}. The time course of matrix changes in human AC appear different than in bovine knees, and may be related to differences in mechanical demands during early postnatal growth. These mechanical and biochemical properties serve as benchmarks for postnatal maturation of normal human femoral condyle AC. The growth sequence of increasing collagen, then GAG, may be targeted as biomimetic cartilage regeneration strategies.

3.2. Introduction

Infants, children, and adults exhibit distinctive stages of growth. Based on typical growth velocity curves for height in females and males, there are four distinct phases of growth during maturation: rapid initial growth during infancy (0-2 yrs), growth deceleration during childhood (2-10 yrs), a period of growth rate acceleration ("growth spurt") coinciding with onset of puberty (~10 yrs) followed by height maintenance as the individual proceeds into adulthood (~18 yrs).[1,2] During early postnatal development, the distal femur, and the constituent articular cartilage (AC) undergo rapid alterations in structure.[3,4]

The compressive load bearing properties of AC improve with maturation between fetal and adult bovines. Confined compression tests are commonly used to evaluate the tissue equilibrium confined compression modulus H_{A0}, and hydraulic permeability, k_p, the ease at which fluid flows through tissue.[5-8] Bovine H_{A0} achieves its adult levels by increasing 3-fold from late fetus to early calf, but not changing substantially between calf and adult.[9] Similarly, k_p, decreases, becomes less permeable, by 70% from fetus to adult, but does not change substantially between calf and adult.[9] Similarly, in equine animals, compressive modulus tended to increase with age.[10] Analogous maturation-related variations in compressive properties of human AC are unknown.

AC is primarily comprised of water and structural macromolecules including collagen (COL), proteoglycan (PG), and other noncollagenous proteins and glycoproteins.[11-13] COL fibrils form a network which entraps large aggregating PG, rich in negatively charged hydrophilic glycosaminoglycans (GAGs).[12,13] The COL and GAG content of mature human AC is ~200 mg/g WW and 30 mg/g WW, respectively.[14] During maturation of bovine and equine animals, there is ~2-3-fold elevation in COL content of AC between fetal (~50 mg/g WW) or newborns and adult (~100 mg/g WW), while GAG is maintained at ~25 mg/g WW throughout postnatal growth.[9,15] Similar maturation-related variations in biochemical properties of human AC are unknown.

The interaction between tissue fluid and ECM constituents impacts the compressive load bearing properties of AC. The GAG-associated fixed charge density imparts a swelling pressure that is restrained by the collagen network, and allows AC to resist compression.[16-20] In bovines, the compressive modulus and permeability of AC during postnatal maturation is correlated with GAG, COL, and the residual matrix not attributed to GAG, COL, or cells.[9] However similar composition-function relationships during maturation of human AC are unknown.

During human development there is little known about AC compressive properties, and the basis for age-related variations. The hypothesis of this study was that AC compressive properties improve between infants, children, and adults, and that functional AC changes are related to increases in COL and GAG contents. The specific aims of this study are to assess AC compressive properties and biochemical composition and determine if enhanced biomechanics is correlated with matrix constituents.

3.3. Methods

3.3.1.Study Design

Osteochondral cores from grossly normal distal femurs were assessed for qualitative morphological features by microcomputed tomography and for compressive biomechanics and biochemistry. Osteochondral cores (6 mm diameter) were isolated from previously frozen cadaveric knees of anonymized donors (n=22), including from the distal femurs of infants (0-2 yr, 4M+4F, 0.5±0.1 yr), and the medial femoral condyles of children (2-10 yr, 6M+2F, 6.1±1.0 yr), and adults (18+ yr, 5M+1F, 22.3±1.4 yr). Clinical imaging (CT) was available for a subset of donors. Cadaveric knee specimens from 8 infant and 8 child donors who were 1 mo to 10 yrs of age, provided by AlloSource, were presumed to be normal and without evidence of joint disease. Specimens were received and kept frozen prior to sample preparation. Adult cadaveric knee specimens from 6 donors were obtained from tissue banks with donation areas in the Western and Southern areas of the United States.

3.3.2.Imaging

For the subset of donors where clinical imaging data (CT) was available, a volume including the left distal femur was resliced (Mimics, Materialise) to $(150\ \mu m)^3$ isotropic voxel size, oversampling the original data resolution. 2D orthogonal images were viewed (Dataviewer, Bruker). The mineralized components were segmented from the soft tissues by global thresholding (CTAn, Bruker) and rendered in 3D (CTvox, Bruker). To visualize cartilage thickness and underlying morphology of the bone-cartilage interface, osteochondral cores were scanned by microcomputed tomography at $(9\ \mu m)^3$ isotropic voxel resolution (SkyScan 1076; SkyScan. Kontich, Belgium; 70 kVp, 140 μA, 0.025 mm titanium filter, 1850 ms exposure, 180° scan, Δ=0.8°). Images were reconstructed using NRecon (Bruker, Belgium) with a smoothing factor of

1, ring artifact reduction factor of 6, beam hardening correction factor of 40%, and with a dynamic range from -0.0055 to 0.045 attenuation units.

3.3.3.Sample Preparation

AC discs, including the articular surface, were obtained using a 3.2 mm punch. The discs were maintained in phosphate buffered saline without magnesium and calcium and supplemented with proteinase inhibitors (PBS+PIs; 2 mM Na_2-EDTA, 1 mM phenylmethylsulfonyl fluoride, 5 mM benzamidine-HCl, 10 mM N-Ethylmaleimide). Prior to mechanical testing, the thickness of each cartilage disk was measured using a contact-sensing micrometer at 3 predetermined locations (2 towards the edge, and 1 at the center of the disc).

3.3.4.Mechanical Testing

Static and dynamic confined compression tests were performed as previously described to determine the confined compression modulus at the free-swelling thickness, H_{A0}, and hydraulic permeability, k_p.[6,9,21] Briefly, each cartilage disk was transferred into a confining chamber between two porous titanium platens, attached to a mechanical spectrometer (Dynastat, IMASS, Accord, MA), and bathed with PBS+PIs. A test sequence of 0-15% ramp compression over 400 s was applied to the sample and allowed to relax to equilibrium. This was followed by a series of oscillatory displacements decreasing in amplitude from 1% to 0.3% strain, at frequencies of 0.01, 0.02, 0.05, 0.1, 0.2 and 0.5 Hz. The sample was then subjected to additional ramp compressions to 30% and then 45%, with oscillatory tests at each static offset compression level. H_{A0} was estimated by using a least-squares method to fit the equilibrium stress-strain.[22,23] k_p at each compressive strain level, ε, was estimated by fitting the measured dynamic stiffnesses to the theoretical solution using the computed value of modulus, $H_A(\varepsilon)$ (from H_{A0} and the offset compression).[6] From these

estimates of $k_p(\varepsilon)$, the parameters (k_{p0}) of a strain dependent permeability function were fit.[22]

Confined compression modulus additional adult donors (ages 20-80 years) were assessed in a confining chamber using an automated computer-controlled micromechanical test system previously described.[23-25]

3.3.5.Biochemical Analysis

Water, sulfated GAG, collagen, and DNA content of cartilage discs were assessed from tissue digests after conclusion of the compression test. Each disc was weighted wet, lyophilized, weighed dry, and solubilized with Proteinase K. Each sample was digested with 100 µl Proteinase K (0.5 mg/ml in 100 mM phosphate and 10 mM EDTA, pH 7.1) at 60°C for 18 hours and diluted to 500 µl with water before storage at -20°C. Portions of solubilized tissues were used to determine total sulfated GAG,[26] hydroxyproline,[27] and DNA content.[28] The hydroxyproline content was converted to collagen (COL) content assuming a mass ratio of collagen to hydroxyproline of 7.1.[29] The DNA content was converted to cell content assuming a conversion constant of 7.3 pg DNA/chondrocyte (CELL).[30] The total dry mass attributed to the cells was then calculated using a conversion of 0.1 ng dry weight/cell.[31] The residual dry weight (RES) was computed as the remaining dry weight not accounted for by GAG, collagen, or the mass of the cells. The mass of various constituents was expressed normalized to the tissue wet weight.

3.3.6.Statistical Analysis

The effect of developmental stage (infant, child, adult) and species (human, bovine) on biomechanical (H_{A0}, k_p) and biochemical (water, COL, GAG, CELL, RES) were analyzed by multiway analysis of variance (ANOVA) with GraphPad Prism 10.0.2. Where significant ($p<0.05$) effects were detected, comparisons between groups were performed using the Tukey post-hoc test.

To assess dependence of mechanical function and biochemical content on age, measures were fit by least-squares regression to either a single logistic function, or a sum of two logistic functions, of the form $\boldsymbol{Y(t)} = \left(\boldsymbol{B_1} + \frac{\boldsymbol{A_1 - B_1}}{\boldsymbol{1 + \left(\frac{t}{C_1}\right)^{D_1}}} \right) + \left(\boldsymbol{B_2} + \frac{\boldsymbol{A_2 - B_2}}{\boldsymbol{1 + \left(\frac{t}{C_2}\right)^{D_2}}} \right)$ where $Y(t)$ is the property value with respect to age, $t\,[yr]$ is the age of the donor, A is the left (immature) horizontal asymptote, B is the right (mature) horizontal asymptote, C is the age at which the property value is halfway between the minimum and maximum value, and D is a measure of the slope of the curve. The sum of two logistic functions form was utilized if the data featured a peak or trough during intermediate age groups.

The dependencies of mechanical properties on biochemical constituents were analyzed by univariate regression and multivariate regression utilizing the backward elimination procedure.[32] All data are expressed as mean ± SEM.

3.4. Results

During maturation, secondary ossification center (SOC) bone volume increases and changes shape (**Fig. 1**), and the AC thins (**Fig. 2**). Qualitatively, the SOC progresses from a small sphere (~1 mo), before taking on asymmetric shape.

AC biomechanical properties varied with developmental stage. The compressive modulus, H_{A0}, varied with stage (**Fig. 3A**, $p<0.001$). H_{A0} increased ($p<0.001$) between children (0.11 MPa) and adults (0.33 MPa), but not between infants ($p=0.40$, 0.05 MPa) and children. The hydraulic permeability, k_p, varied with degree of offset compression (**Fig. 3B**, $p<0.0001$) and tended to be less permeable ($p=0.08$) with age. k_p decreased ($p<0.05$) between infants and children at 45% offset compression.

AC biochemical composition varied with developmental stage ($p<0.05$). Water content decreased (**Fig. 4A**, $p<0.001$) between infants (88%), children (81%), and adults (75%). COL (**Fig. 4C**) increased between infants and children ($p<0.01$, 48 to 103 mg/g WW), and trended higher between children and adults ($p=0.06$, 132 mg/g WW). GAG (**Fig. 4E**) increased between children and adults ($p<0.05$, 19 to 35 mg/g WW), but not between infants ($p=0.91$, 17 mg/g WW) and children. CELL (**Fig. 4G**) decreased between infants and children ($p<0.01$, 36 to 11×10^6 cells/g WW), but not between children and adults ($p=0.94$, 14×10^6 cells/g WW). RES (**Fig. 4I**) increased between infants and adults ($p<0.05$, 52 to 84 mg/g WW).

Compared to previously published bovine AC properties,[9] the progression of immature human AC biomechanical and biochemical properties to mature levels is more gradual (**Table 1**). H_{A0} (**Fig. 3AC**), water (**Fig. 4AB**) CELL (**Fig. 4GH**) and RES (**Fig. 4IJ**) varied with species ($p<0.05$) and developmental stage ($p<0.01$). COL (**Fig. 4CD**) and GAG (**Fig. 4EF**) varied with developmental stage ($p<0.05$). H_{A0} and was not different ($p>0.90$) among fetal bovines and human infants and children. Water and COL was not different ($p>0.8$) between infants and fetal bovines,

nor between children and bovine calves and adults. GAG was similar among human infants and children and all bovine developmental stages. Generally, CELL was greater, and RES reduced in bovines than in humans.

Considering additional adult donors, ages 30-80 yrs, compressive modulus and composition in humans varied logistically with age (**Fig. 5, Table 2**). The age at which water (**Fig. 5B**), COL (**Fig. 5C**), and RES (**Fig. 5E**) were halfway between the minimum and maximum value occurred during childhood development, at 4.8, 4.2, and 6.9 years respectively. GAG was enhanced in early adulthood (**Fig. 5D**) before diminishing in middle-aged adults, reaching the halfway point between the minimum and maximum values at ages 17 and 29 years.

H_{A0} was correlated (**Fig. 6A-D**) with water, COL and GAG. Univariate regression (**Table 3**) showed a correlation between H_{A0} and water (**Fig. 6A**, %, r^2=0.49, SE=0.004, p<0.001), GAG (**Fig. 6B**, mg/g WW, r^2=0.80, SE=0.001, p<0.001), and COL (**Fig. 6C**, mg/g WW, r^2=0.27, SE=0.001, p=0.01). Multiple linear regression (**Table 4**) considering GAG, COL, RES, and CELL contents generally agreed, indicating that H_{A0} is related (r^2=0.89) to COL (p<0.001, SE=0.0003) and GAG (p<0.0001, SE=0.0008) content according to H_{A0} = 0.001*COL + 0.009*GAG - 0.151.

k_p was correlated with COL and RES. Univariate regression (**Table 3**) indicated a correlation between k_p and water (**Fig. 6E**, r^2=0.33, SE=0.006, p<0.0001), GAG (**Fig. 6F**, r^2=0.13, SE=0.004, p<0.001), COL (**Fig. 6G**, r^2=0.22,SE=0.001, p<0.0001), and RES (**Fig. 6H**, mg/g WW, r^2=0.27, 0.001, p<0.0001). Multiple linear regression (**Table 4**) considering GAG, COL, RES, and CELL contents generally agreed, indicating that k_p is related (r^2=0.41) to COL (p<0.001, SE=0.001), CELL (mg/g WW, p<0.001, SE=0.020), and RES (p<0.001, SE=0.002) according to k_p = -0.004*COL - 0.070*CELL - 0.007*RES - 13.74.

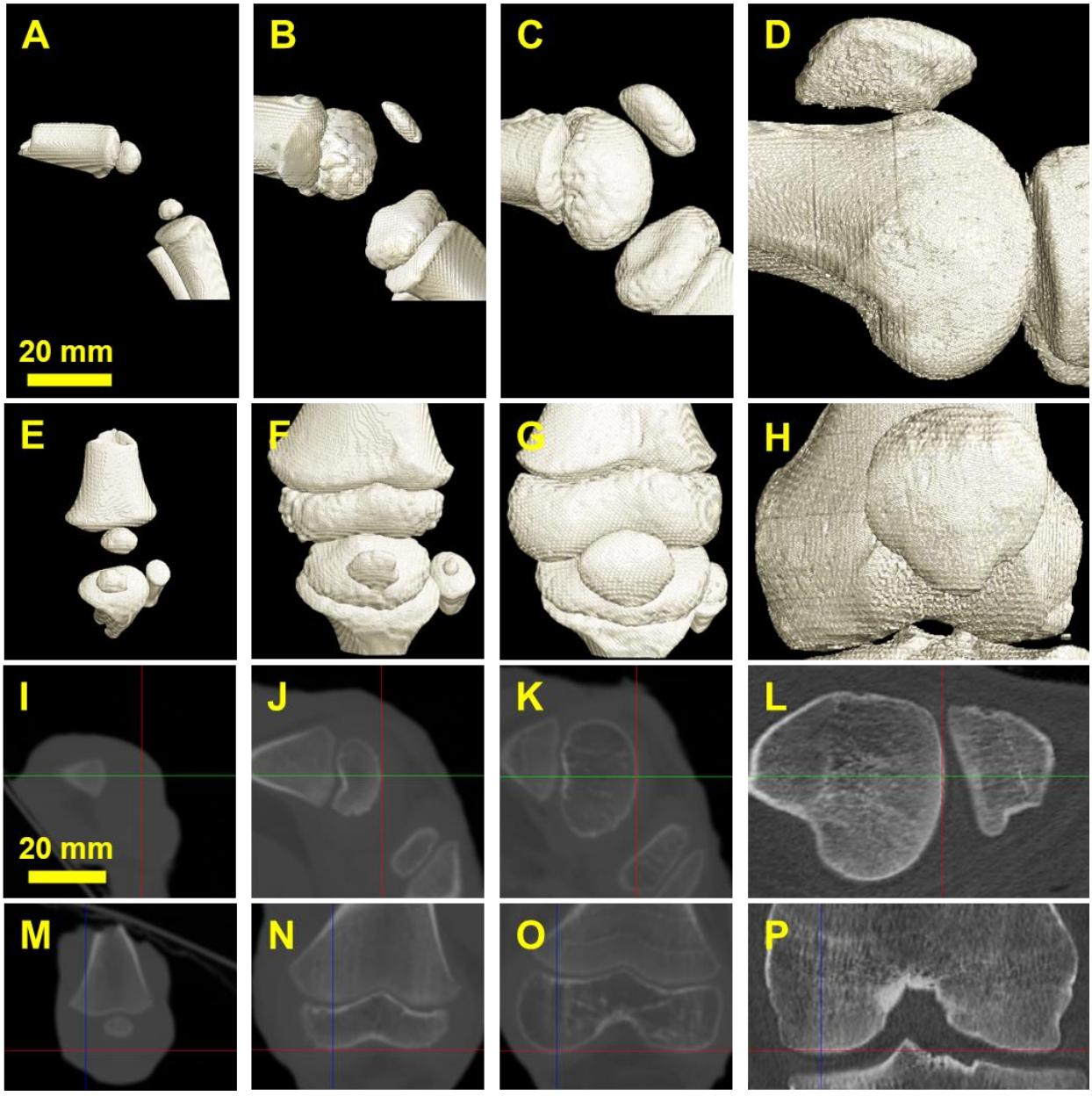


Figure 3.1. 3D renders of the mineralized components of the distal femur. (A-H) 3D renders and **(I-P)** 2D CT images of distal femurs in the **(A-D, I-L)** sagittal and **(E-H, M-P)** coronal perspectives of **(A,E,I,M)** 1 month, **(B,F,J,N)** 4 year, **(C,G,K,O)** 10 year, and **(D,H,L,P)** 31 year old donors, generated from clinical CT image datasets. Images are of left knees except for the 31 year old, which is a mirrored right knee.

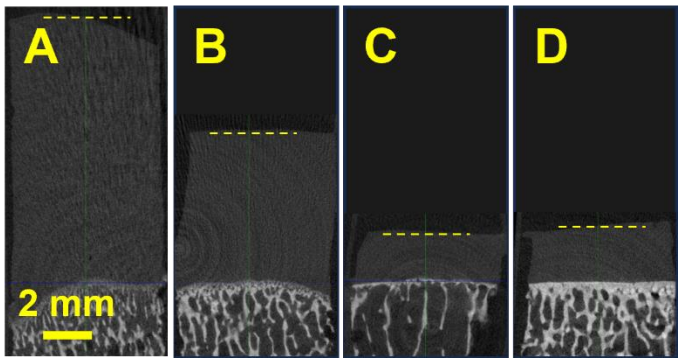


Figure 3.2. uCT scans of articular cartilage and cartilage-bone interface.2D images of osteochondral cores from the distal femur of **(A)** 1 year, **(B)** 4 year, **(C)** 8 year, and **(D)** 19 year old donors. Dashed line indicates articular surface boundary.

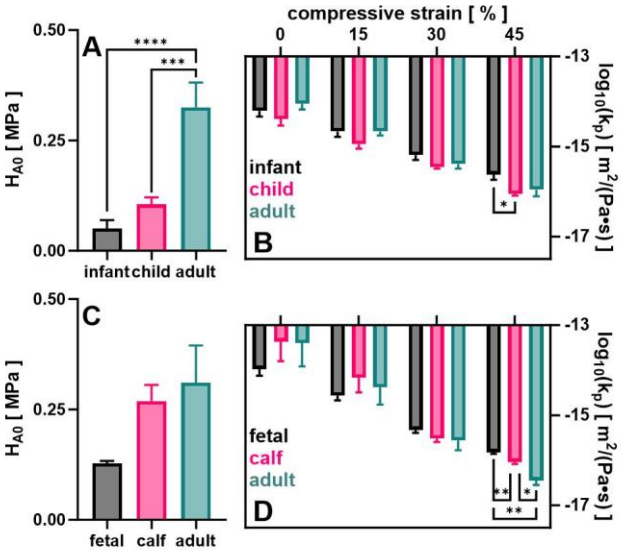


Figure 3.3. Effect of developmental stage on biomechanical properties.(A,B) Human (infant, child, adult) and (**C,D**) bovine (fetal, calf, adult). (**A,C**) Equilibrium confined compression modulus at free swelling thickness, H_{A0}, and **(B,D)** hydraulic permeability, k_p, at 0%, 15%, 30%, and 45% offset compression. *p<0.05, **p<0.01, ***p<0.001, ****p<0.0001. Bovine data from literature.[9]

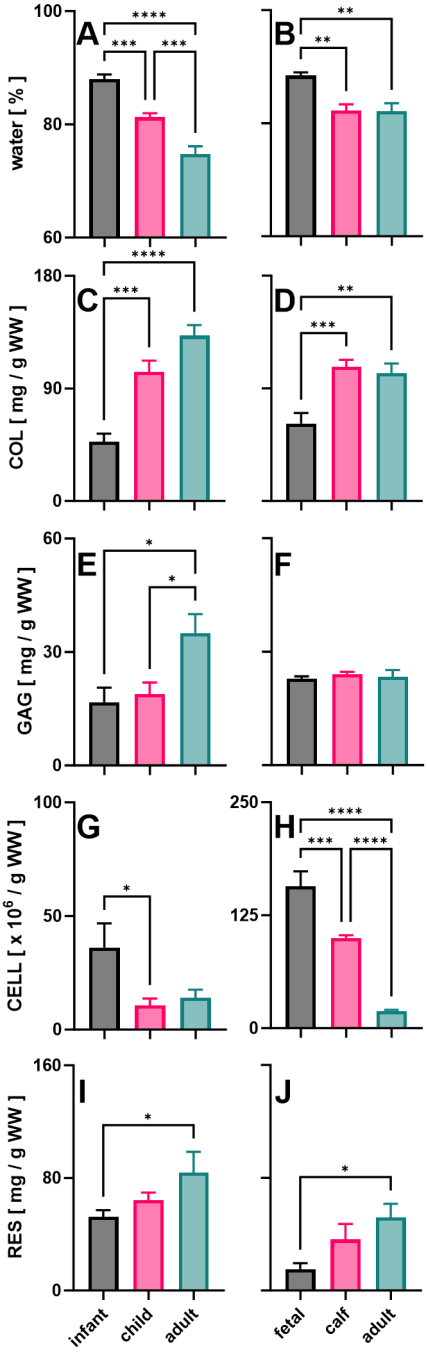


Figure 3.4. Effect of developmental stage on cartilage composition. (**A,B**) Water, (**C,D**) collagen (COL), (**E,F**) glycosaminoglycan (GAG), (**G,H**) cell number (CELL), and (**I,J**) residual (RES) contents normalized to tissue wet weight from (**A,C,E,G,I**) human (infant, child, adult) and (**B,D,F,H,J**) bovines (fetal, calf, adult) donors according developmental stage. *p<0.05, **p<0.01, ***p<0.001, ****p<0.0001. Bovine data from literature.[9].

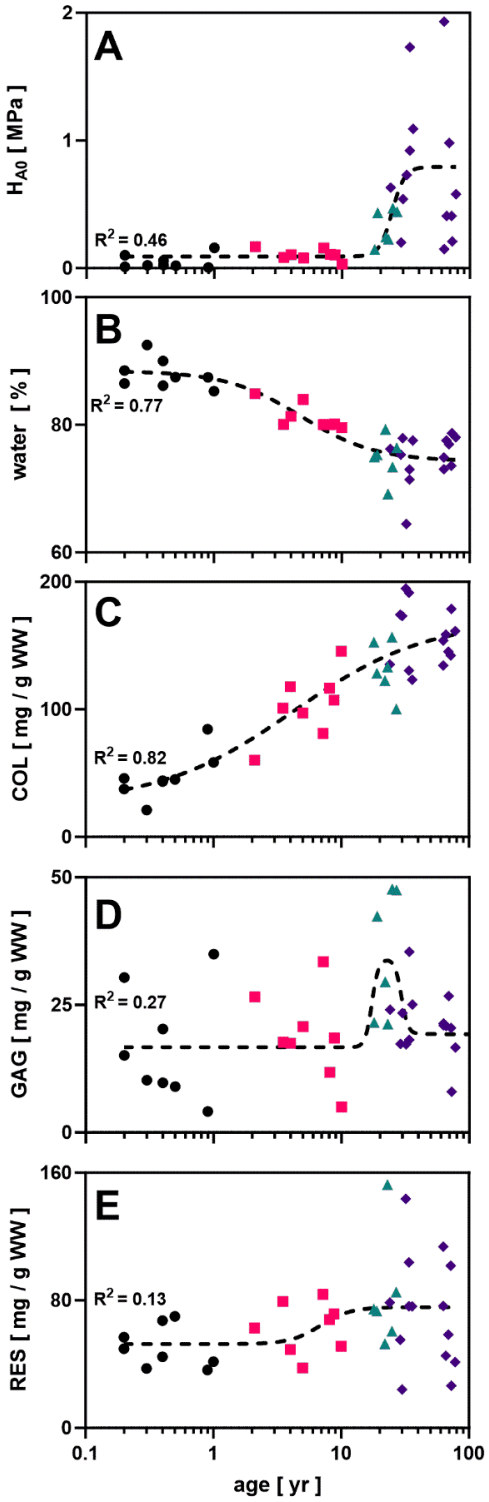


Figure 3.5. Effect of maturation and ageing on cartilage compressive modulus and composition. (A) equilibrium confined compressive modulus (H_{A0}), **(B)** water (%), **(C)** collagen (COL), **(D)** glycosaminoglycan (GAG), and **(E)** residual (RES) contents according to age.

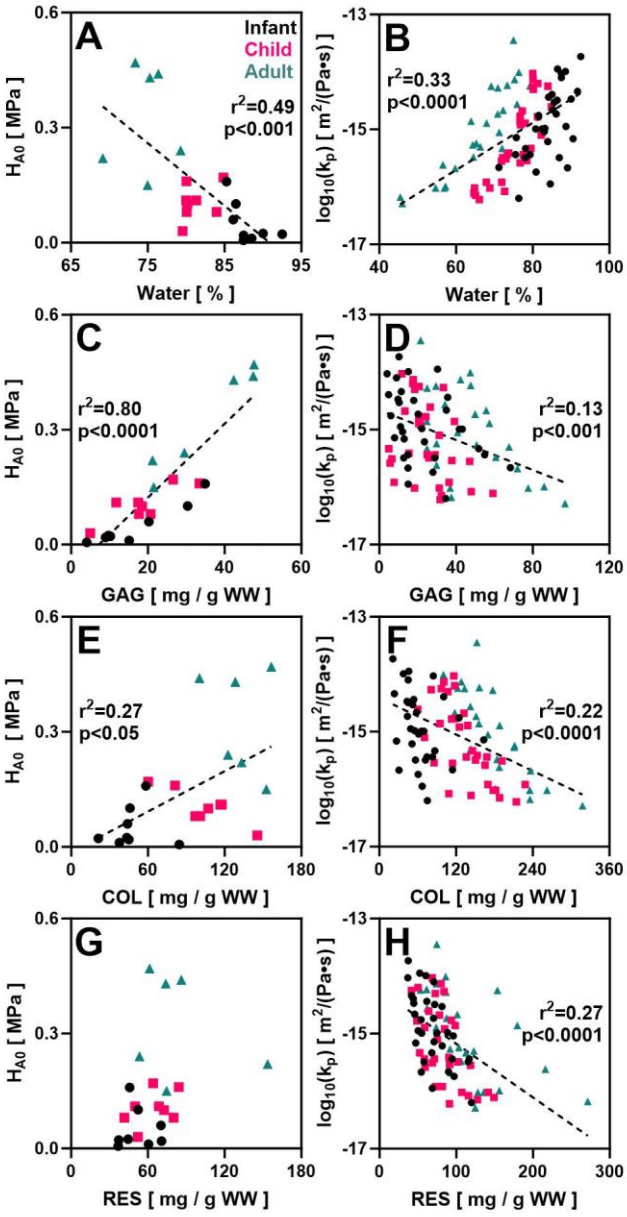


Figure 3.6. Relationship between biomechanical properties and cartilage composition.. Relationship between (**A,B**) water, (**C,D**) GAG, (**E,F**) COL, and (**G,H**) RES contents with (**A,C,E,G**) equilibrium confined compression modulus, H_{A0}, and (**B,D,F,H**) hydraulic permeability, k_p, for infant (●), child (■), and adult (▲) donors. Significant univariate regression lines are shown (dashed line).

Table 3.1. Relative change in biomechanical and biochemical properties between human donors and bovine animals, relative to the human. Background color indicates p-value where red is highly significant ($p<0.01$), yellow indicates a moderate trend ($0.1 < p < 0.2$) and green indicates no difference ($p>0.5$). Positive values indicate that the bovine value is greater than the human value.

p-value
0.01 0.5 1.0

			HUMAN		
			Infant	Child	Adult
BOVINE	H_{A0} [MPa]	Fetal	155%	22%	-61%
		Calf	435%	156%	-17%
		Adult	518%	196%	-4%
	water [%]	Fetal	1%	9%	18%
		Calf	-7%	1%	10%
		Adult	-7%	1%	10%
	COL [mg / g WW]	Fetal	30%	-40%	-53%
		Calf	126%	4%	-19%
		Adult	115%	-1%	-23%
	GAG [mg / g WW]	Fetal	37%	21%	-35%
		Calf	44%	27%	-31%
		Adult	40%	24%	-33%
	CELL [x 10^6 / g WW]	Fetal	335%	1380%	1015%
		Calf	176%	840%	608%
		Adult	-47%	81%	36%
	RES [mg / g WW]	Fetal	-71%	-76%	-82%
		Calf	-31%	-43%	-57%
		Adult	-1%	-19%	-38%

Table 3.2. Parameters of logistic fits of effect of maturation and ageing on cartilage compressive modulus and composition.

		Sum of four-parameter logistics $Y(t) = \left(B_1 + \frac{A_1 - B_1}{1 + \left(\frac{t}{C_1}\right)^{D_1}} \right) + \left(B_2 + \frac{A_2 - B_2}{1 + \left(\frac{t}{C_2}\right)^{D_2}} \right)$							
	R^2	**A_1**	**B_1**	**C_1**	**D_1**	**A_2**	**B_2**	**C_2**	**D_2**
H_{A0} [MPa]	0.46	0.09	0.79	25	8.9				
Water [%]	0.77	74	89	4.8	-1.5				
COL [mg / g WW]	0.82	26	170	4.2	0.8				
GAG [mg / g WW]	0.27	-1.5	16	17	17	18	3.4	29	17
RES [mg / g WW]	0.13	53	76	6.9	3.7				

Table 3.3. Parameters of simple linear regression between compressive biomechanical properties and biochemical content.

		H_{A0} [MPa]				$\log_{10}(k_p)$ [$m^2/(Pa*s)$]			
		best-fit slope	**std. error**	**r^2**	**P value**	**best-fit slope**	**std. error**	**r^2**	**P value**
water [%]	**Infant**	-0.014	0.007	0.39	0.10	0.075	0.018	0.38	0.00
	Child	0.009	0.008	0.16	0.32	0.101	0.012	0.71	0.00
	Adult	0.004	0.020	0.01	0.86	0.075	0.008	0.78	0.00
	ICA	-0.016	0.004	0.49	0.00	0.041	0.006	0.33	0.00
GAG [mg / g WW]	**Infant**	0.005	0.001	0.90	0.00	-0.015	0.007	0.15	0.03
	Child	0.004	0.001	0.71	0.01	-0.019	0.009	0.12	0.05
	Adult	0.011	0.001	0.95	0.00	-0.021	0.006	0.31	0.00
	ICA	0.010	0.001	0.80	0.00	-0.013	0.004	0.13	0.00
COL [mg / g WW]	**Infant**	0.000	0.001	0.01	0.80	-0.006	0.004	0.09	0.09
	Child	-0.001	0.000	0.72	0.01	-0.011	0.002	0.46	0.00
	Adult	-0.002	0.003	0.06	0.65	-0.012	0.002	0.61	0.00
	ICA	0.002	0.001	0.27	0.01	-0.005	0.001	0.22	0.00
RES [mg / g WW]	**Infant**	0.000	0.002	0.00	0.96	-0.017	0.004	0.40	0.00
	Child	0.001	0.001	0.19	0.28	-0.015	0.004	0.34	0.00
	Adult	-0.001	0.002	0.08	0.58	-0.009	0.003	0.33	0.00
	ICA	0.002	0.001	0.12	0.12	-0.009	0.002	0.27	0.00
CELL [mg / g WW]	**Infant**	0.015	0.004	0.67	0.01	-0.051	0.026	0.11	0.06
	Child	-0.016	0.020	0.09	0.47	-0.155	0.115	0.06	0.19
	Adult	0.031	0.079	0.04	0.71	-0.121	0.134	0.03	0.37
	ICA	-0.005	0.014	0.01	0.70	-0.027	0.024	0.01	0.28

Table 3.4. Parameters of multiple linear regression between compressive biomechanical properties and biochemical content.

	Confined Compression Modulus $H_{A0}\,[\,MPa\,] = \beta_0 + \beta_1(COL) + \beta_2(GAG) + \beta_3(CELL) + \beta_4(RES)$ r^2=0.89				
Variable	β_0	β_1	β_2	β_3	β_4
Estimate	-0.151	0.001	0.009		
Standard error	0.028	0.0002	0.001		
P value	<0.0001	0.001	<0.0001		
	Hydraulic Permeability $log_{10}(k_p)\left[\frac{m^2}{Pa * s}\right] = \beta_0 + \beta_1(COL) + \beta_2(GAG) + \beta_3(CELL) + \beta_4(RES)$ r^2=0.41				
Variable	β_0	β_1	β_2	β_3	β_4
Estimate	-13.74	-0.004		-0.070	-0.007
Standard error	0.182	0.001		0.020	0.002
P value	<0.0001	0.0003		0.001	0.0001

3.5. Discussion

This study indicates substantial mechanical and biochemical adaptations during maturation of human AC. Between infant, child, and adult stages, there was a marked increase in compressive modulus that paralleled an increase in GAG and COL that may be indicative of variations in mechanical demand during this period.

The focus of this study on AC from infants and children had advantages and limitations. Despite the variability in joint size, consistent geometries for AC compression testing were used and allowed a standardized protocol to be implemented for all ages. Although donors were skewed towards male in children (75%) and adults (83%), female and male infants and children undergo similar height gains up to ~10 yrs, and only begin to diverge at puberty.[33] In healthy young adults, cartilage MRI T2 mapping, indicative of cartilage structure and composition, does not differ with gender.[34] Thus, AC properties in these age groups are predicted to be similar. However, future studies should be designed to elucidate sex-related differences that may arise during puberty, as well as the regional variation across the joint surface, and the effect of demographic and clinical variables such as race/ethnicity, BMI, and level of activity.

The time course of variation in cartilage compressive properties during maturation is distinctive between humans and bovines. In humans, H_{A0} is similar between infants and children and increases ~3 fold between the child and adult state (~0.33 MPa; **Fig. 3A**) and tends to be less permeable in children compared to infants and adults (**Fig. 3B**). The measured values for adult human compressive mechanical properties are generally consistent with previous studies of AC, with intact surface, in the patella,[35] femoral head,[36] and knee.[37] Conversely, bovine AC H_{A0} increased ~2 fold between fetal bovines and calves (~0.27 MPa) but was not different between calves and adult bovines (**Fig. 3C**) and was generally less permeable in the adults compared to fetal bovines and calves (**Fig. 3D**).

The distinctive time course of matrix changes in human AC appear different than the timing of matrix changes in common animal models. In humans, there is an early ~2-fold increase in COL (**Fig. 4CD**) between infants and children and later ~2-fold increase in GAG (**Fig. 4EF**). These values for adult human biochemical properties are generally consistent with previous studies of healthy adult AC from the medial femoral condyle.[14] Comparatively, in bovines, COL (**Fig. 4D**) increases ~1.5 fold between fetal and calf, while GAG (**Fig. 4F**) is maintained at ~25 mg/g WW between throughout perinatal and postnatal maturation.

This study supports the concept that the milieu of tissue constituents, which vary in content throughout maturation, are the basis of mechanical function. By univariate analysis, GAG and COL independently predict ~80% and ~30% of the variation in H_{A0}, and, when correlated together by multivariate regression, ~90% of the variation. For k_p, COL and RES independently predict ~20% and ~30%, respectively, of variation by univariate analysis, and when correlated together by multivariate regression with the dry cellular content, predict ~40% of the variation. These results are similar to previous studies which correlate compressive properties with matrix content.[9,35]

The maturation-related differences between COL and GAG contents in animals and humans (**Table 1**), and thus attainment of mature compressive functionality, may be related to differences in mechanical demands. In the bovine,[9,38] equine,[15] porcine,[39] and lapine animals,[40] collagen undergoes substantial increases during maturation compared to GAG, contributing to tissue stiffening. Since human infants begin to walk at ~1 yr of age,[41] while quadruped animals can stand and walk hours after birth,[42] the progression of early COL and later GAG deposition may be a response to age-varying mechanical demands as an individual begins to locomote and gain mass. The ~1 yr age of increased loading demands is similar to the characteristics ages of

constituent change, ~4-5 yrs for water reduction (**Fig. 5B**) and COL deposition (**Fig. 5C**), which approaches the mature value by ~10 yrs. Thus, the ages where matrix, particularly COL, begins to rapidly accumulate and approach the mature content may reflect the roles of mechanotransduction as well as hormonal control associated with the onset of puberty as a mechanism of AC maturation.[43,44]

Tissue engineered cartilage and some cartilage regeneration products recapitulate the properties of immature AC.[45,46] Cartilage repair strategies may seek to replicate the time course of increasing COL, then GAG, or reproduce maturation-associated loading regimes, as a strategy for biomimetic cartilage regeneration. The mechanical and biochemical properties reported may serve as benchmarks for postnatal maturation of normal human femoral condyle AC.

3.6. Acknowledgements

This chapter, in full, will be submitted to *Journal of Bone and Joint Surgery*. The dissertation author was the primary author. Thanks to co-authors Yehudit H. Gerassi, Albert C. Chen, Christine L. Farnsworth, William D. Bugbee, Kevin G. Shea, Eric W. Edmonds, and Robert L. Sah. We are grateful to Allosource and the donors, and their families. We also thank Brendon Mitchell, MD and Liane Chun, MD for their help collecting donor tissues. This work was supported by NSF GRFP (EGG) and the Wu Tsai Human Performance Alliance.

3.7. References

1. Tanner JM, Whitehouse RH, Takaishi M. Standards from birth to maturity for height, weight, height velocity, and weight velocity: British children, 1965. II. *Arch Dis Child*. 1966;41:613-35.

2. Tanner JM, Whitehouse RH, Takaishi M. Standards from birth to maturity for height, weight, height velocity, and weight velocity: British children, 1965. I. *Arch Dis Child*. 1966;41:454-71.

3. Sidharthan S, Yau A, Almeida BA, Shea KG, Greditzer HGt, Jones KJ, et al. Patterns of articular cartilage thickness in pediatric and adolescent knees: A magnetic resonance imaging-based study. *Arthrosc Sports Med Rehabil*. 2021;3:e381-e90.

4. Ellermann JM, Ludwig KD, Nissi MJ, Johnson CP, Strupp JP, Wang L, et al. Three-dimensional quantitative magnetic resonance imaging of epiphyseal cartilage vascularity using vessel image features: New insights into juvenile osteochondritis dissecans. *JB&JS Open Access*. 2019;4:e0031.

5. Mow VC, Kuei SC, Lai WM, Armstrong CG. Biphasic creep and stress relaxation of articular cartilage in compression: theory and experiment. *J Biomech Eng*. 1980;102(1):73-84.

6. Frank EH, Grodzinsky AJ. Cartilage electromechanics--II. A continuum model of cartilage electrokinetics and correlation with experiments. *J Biomech*. 1987;20(6):629-39.

7. Lee RC, Frank EH, Grodzinsky AJ, Roylance DK. Oscillatory compressional behavior of articular cartilage and its associated electromechanical properties. *J Biomech Eng*. 1981;103:280-92.

8. Kwan MK, Lai WM, Mow VC. A finite deformation theory for cartilage and other soft hydrated connective tissues--I. equilibrium results. *J Biomech*. 1990;23:145-55.

9. Williamson AK, Chen AC, Sah RL. Compressive properties and function-composition relationships of developing bovine articular cartilage. *J Orthop Res*. 2001;19:1113-21.

10. Brommer H, Brama PA, Laasanen MS, Helminen HJ, van Weeren PR, Jurvelin JS. Functional adaptation of articular cartilage from birth to maturity under the influence of loading: a biomechanical analysis. *Equine Vet J*. 2005;37:148-54.

11. Heinegard D, Oldberg A. Structure and biology of cartilage and bone matrix noncollageneous macromolecules. *FASEB J*. 1989;3:2042-51.

12. Buckwalter JA, Mankin HJ. Articular cartilage. Part I: tissue design and chondrocyte-matrix interactions. *J Bone Joint Surg Am*. 1997;79-A:600-11.

13. Buckwalter JA, Mankin HJ, Grodzinsky AJ. Articular cartilage and osteoarthritis. *Instr Course Lect*. 2005;54:465-80.

14. Temple MM, Bae WC, Chen MQ, Lotz M, Amiel D, Coutts RD, et al. Age- and site-associated biomechanical weakening of human articular cartilage of the femoral condyle. *Osteoarthritis Cartilage*. 2007;15:1042-52.

15. Oinas J, Ronkainen AP, Rieppo L, Finnilä MAJ, Iivarinen JT, van Weeren PR, et al. Composition, structure and tensile biomechanical properties of equine articular cartilage during growth and maturation. *Sci Rep*. 2018:11357.

16. Han E, Chen SS, Klisch SM, Sah RL. Contribution of proteoglycan osmotic swelling pressure to the compressive properties of articular cartilage. *Biophys J*. 2011;101:916-24.

17. Eisenberg SR, Grodzinsky AJ. Electrokinetic micromodel of extracellular matrix and other polyelectrolyte networks. *Physicochemical Hydrodynamics*. 1988;10:517-39.

18. Buschmann MD, Grodzinsky AJ. A molecular model of proteoglycan-associated electrostatic forces in cartilage mechanics. *J Biomech Eng*. 1995;117:179-92.

19. Maroudas A, Ziv I, Weisman N, Venn M. Studies of hydration and swelling pressure in normal and osteoarthritic cartilage. *Biorheology*. 1985;22:159-69.

20. Maroudas AI. Balance between swelling pressure and collagen tension in normal and degenerate cartilage. *Nature*. 1976;260:808-9.

21. Chen AC, Bae WC, Schinagl RM, Sah RL. Depth- and strain-dependent mechanical and electromechanical properties of full-thickness bovine articular cartilage in confined compression. *J Biomech*. 2001;34:1-12.

22. Lai WM, Mow VC, Roth V. Effects of nonlinear strain-dependent permeability and rate of compression on the stress behavior of articular cartilage. *J Biomech Eng*. 1981;103:61-6.

23. Schinagl RM, Gurskis D, Chen AC, Sah RL. Depth-dependent confined compression modulus of full-thickness bovine articular cartilage. *J Orthop Res*. 1997;15:499-506.

24. Farndale RW, Buttle DJ, Barrett AJ. Improved quantitation and discrimination of sulphated glycosaminoglycans by use of dimethylmethylene blue. *Biochim Biophys Acta*. 1986;883:173-7.

25. Woessner JF. The determination of hydroxyproline in tissue and protein samples containing small proportions of this imino acid. *Arch Biochem Biophys*. 1961;93:440-7.

26. McGowan KB, Kurtis MS, Lottman LM, Watson D, Sah RL. Biochemical quantification of DNA in human articular and septal cartilage using PicoGreen and Hoechst 33258. *Osteoarthritis Cartilage*. 2002;10(7):580-7.

27. Jackson DS, Cleary EG. The determination of collagen and elastin. *Methods Biochem Anal*. 1967;15:25-76.

28. Stockwell RA. The cell density of human articular and costal cartilage. *J Anat*. 1967;101:753-63.

29. Freed LE, Marquis JC, Langer R, Vunjak-Novakovic G, Emmanual J. Composition of cell-polymer cartilage implants. *Biotechnol Bioeng*. 1994 Mar 25;43(7):605-14.

30. Sokal RR, Rohlf FJ. Biometry. 3rd ed. New York: WH Freeman and Co.; 1995. 887 p.

31. Tanner JM. Normal growth and techniques of growth assessment. *Clin Endocrinol Metab*. 1986;15:411-51.

32. Mosher TJ, Collins CM, Smith HE, Moser LE, Sivarajah RT, Dardzinski BJ, et al. Effect of gender on in vivo cartilage magnetic resonance imaging T2 mapping. *J Magn Reson Imaging*. 2004;19:323-8.

33. Armstrong CG, Mow VC. Variations in the intrinsic mechanical properties of human articular cartilage with age, degeneration, and water content. *J Bone Joint Surg Am*. 1982;64-A:88-94.

34. Boschetti F, Pennati G, Gervaso F, Peretti GM, Dubini G. Biomechanical properties of human articular cartilage under compressive loads. *Biorheology*. 2004;41(3-4):159-66.

35. Treppo S, Koepp H, Quan EC, Cole AA, Kuettner KE, Grodzinsky AJ. Comparison of biomechanical and biochemical properties of cartilage from human knee and ankle pairs. *J Orthop Res*. 2000;18(5):739-48.

36. Williamson AK, Chen AC, Masuda K, Thonar EJ-MA, Sah RL. Tensile mechanical properties of bovine articular cartilage: variations with growth and relationships to collagen network components. *J Orthop Res*. 2003;21:872-80.

37. Rieppo J, Hyttinen MM, Halmesmaki E, Ruotsalainen H, Vasara A, Kiviranta I, et al. Changes in spatial collagen content and collagen network architecture in porcine articular cartilage during growth and maturation. *Osteoarthritis Cartilage*. 2009 Apr;17(4):448-55.

38. Julkunen P, Harjula T, Iivarinen J, Marjanen J, Seppanen K, Narhi T, et al. Biomechanical, biochemical and structural correlations in immature and mature rabbit articular cartilage. *Osteoarthritis Cartilage*. 2009 Dec;17(12):1628-38.

39. Clark JE, Whitall J, Phillips SJ. Human interlimb coordination: the first 6 months of independent walking. *Dev Psychobiol*. 1988;21:445-56.

40. Whalin L, Weary DM, von Keyserlingk MAG. Understanding behavioural development of calves in natural settings to inform calf management. *Animals*. 2021;11:2446.

41. Hunziker EB, Kapfinger E, Geiss J. The structural architecture of adult mammalian articular cartilage evolves by a synchronized process of tissue resorption and neoformation during postnatal development. *Osteoarthritis Cartilage*. 2007;15:403-13.

42. van Turnhout MC, Schipper H, Engel B, Buist W, Kranenbarg S, van Leeuwen JL. Postnatal development of collagen structure in ovine articular cartilage. *BMC Dev Biol*. 2010;10:62.

43. Makris EA, Gomoll AH, Malizos KN, Hu JC, Athanasiou KA. Repair and tissue engineering techniques for articular cartilage. *Nat Rev Rheumatol*. 2015;11:21-34.

44. Hunziker EB. The elusive path to cartilage regeneration. *Adv Mater*. 2009;21:3419-24.

CHAPTER 4

NORMAL HUMAN ARTICULAR CARTILAGE EXHIBITS IMPORVED TENSILE MECHANICAL PROPERTIES WITH PREPUBESCENT MATURATION, DEPTH, AND COLLAGEN CONTENT

4.1. Abstract

Adult articular cartilage (AC) biomechanical function is a manifestation of the extracellular matrix content and structure. The biomechanical properties of articular cartilage allow the tissue to function as a tough and resilient load-bearing surface throughout postnatal growth and maturation. However, immature AC tensile properties, and the basis for age-related variations in humans are unknown. The objective of this study was to assess the tensile properties and biochemical composition in the superficial and deep zones of normal articular cartilage during prepubescent maturation and determine if tensile properties are depth- and age-dependent and correlated with matrix constituents. Cadaveric knee specimens from the distal femurs of infants (0-2 yrs), and medial femoral condyles of children (2-10 yrs) and adults (+18 yrs) were analyzed for tensile biomechanical and biochemical properties in the superficial and deep zones. Tensile equilibrium modulus, ramp modulus, failure strength, and failure strain were determined. Tissue water, collagen, sulfated glycosaminoglycan, cell, and residual matrix content were assessed. The variation of biomechanical and biochemical properties during prepubescent maturation was analyzed and correlated by nonlinear, univariate and multivariate regression. Tensile mechanical properties are enhanced during prepubescent maturation in infants and children. In children, tensile properties were elevated in the DZ, compared to the SZ, and there was a marked loss of tensile

integrity between AC from children and adults. Ramp modulus and failure strain are positively correlated with collagen and residual matrix content and negatively correlated with water. In general, tensile biomechanical properties increased with age in infants and children and, in children, and were correlated with matrix content. In children, tensile properties were depth-varying, and were greater in the DZ, compared to the SZ. Age variation in tensile and biochemical properties implicates loading-associated mechanotransduction and puberty as mechanisms involved in AC maturation. These findings extend previous studies on the tensile properties of normal human AC by characterizing the variation of tensile and biochemical properties during prepubescent maturation which may be useful in informing the design and development of cartilage repair strategies.

4.2. Introduction

During growth and development, humans undergo increases in size and mass in four distinct phases.[1,2] Alterations in growth velocity with age indicate periods of rapid initial growth during infancy (0-2 yrs), growth deceleration during childhood (2-10 yrs), a period of growth rate acceleration ("growth spurt") with initiation coinciding with onset of puberty (~10 yrs), followed by height maintenance as the individual proceeds into adulthood (~18 yrs).[1-3]. During prepubescent maturation (<10 yrs), the distal femur and constituent articular cartilage (AC) undergo rapid alterations in structure.[4-6]

The evolution of tensile load bearing properties with maturation is complex and depth-varying. Generally, tensile properties of AC are thought to increase during postnatal growth, plateau in the mature state, then undergo tensile weakening with ageing.[7-10] However, several studies indicate that tensile properties peak in the juvenile stage before skeletal maturity.[11-14] The depth-varying properties of AC are also maturation dependent. In mature AC, cartilage is stiffest near the articular surface.[9] Conversely, immature AC is more compliant near the articular surface and increases in tensile stiffness towards the deeper tissue.[11,15] Analogous maturation- and depth-related variations in tensile properties of human AC are unknown.

The biomechanical behavior of AC is a manifestation of the extracellular matrix content and structure. In mature AC, the ECM structure and content vary with depth such that collagen fibrils exhibit an arcade-like structure orientation, GAG increases, and cellularity decreases with depth from the surface.[16] In quadrupeds, there is a ~2-3 fold elevation in COL content between fetal and juvenile animals, and maintenance of GAG throughout postnatal growth.[8,12,13,17] Similar maturation-related variations in biochemical properties of human AC during prepubescent maturation are unknown.

During human development there is little known about AC tensile properties, and the basis

for age-related variations. The hypothesis of this study was that AC tensile properties improve between infants, children, and adults, and that functional AC changes are related to increases in matrix content, particularly COL. The specific aims of this study are to assess AC tensile properties and biochemical composition in the superficial and deep zones and determine if enhanced biomechanics is correlated with matrix constituents.

4.3. Methods

4.3.1. Study Design

Cadaveric knee specimens from anonymized donors (n=22), including from the distal femurs of infants (0-2 yr, 4M+4F, 0.5±0.1 yr), and the medial femoral condyles of children (2-10 yr, 6M+2F, 6.1±1.0 yr), and adults (18+ yr, 5M+1F, 22.3±1.4 yr) were analyzed for tensile biomechanical and biochemical properties. Infant and child donors who were 1 mo to 10 yrs of age, provided by AlloSource, were presumed to be normal and without evidence of joint disease. Specimens were received and kept frozen prior to sample preparation. Adult cadaveric knee specimens from 6 donors were obtained from tissue banks with donation areas in the Western and Southern areas of the United States.

4.3.2.Sample Preparation

AC discs, including the articular surface, were obtained using a 6 mm punch. AC from superficial and deep layers were created. From the articular surface, the cartilage was sliced into three successive ~0.5 mm thick layers. The first layer (‘SZ’), including the articular surface, and the third layer (‘DZ’), were reserved and assessed as superficial and deep cartilage, respectively. The slices were cut into tapered specimens, with a 0.8 mm wide and 2.0 mm long gage region. For child and adult tissues, specimens were collected from the medial femoral condyle and oriented parallel to the typical split line pattern.[18] Tissue from infant donors was collected from areas across the joint including both femoral condyles and the patellofemoral groove. Tapered tensile specimens and tissues directly adjacent to tensile samples were maintained in phosphate buffered saline without magnesium and calcium and supplemented with proteinase inhibitors (PBS+PIs; 2 mM Na2-EDTA, 1 mM phenylmethylsulfonyl fluoride, 5 mM benzamidine-HCl, 10 mM N-Ethylmaleimide).

4.3.3. Mechanical Testing

Tensile mechanical properties were assessed using a combined equilibrium and constant strain-rate test protocols.[8,9,11,19,20] Briefly, each tapered specimen was elongated to 10 and 20% strains at 0.25%/s and allowed to relax to equilibrium at each strain. This was followed by elongation of the specimen at a continuous strain rate of 5 mm/min until failure. The equilibrium test results were analyzed to determine tensile equilibrium modulus, and the dynamic test results were used to assess tensile ramp modulus, failure strength, and failure strain.

4.3.4. Biochemical Analysis

Water, sulfated GAG, collagen, and DNA content of tissue adjacent to the tensile specimens were assessed from tissue digests after conclusion of the compression test. Each tissue portion was weighted wet, lyophilized, weighed dry, and solubilized with Proteinase K. Each sample was digested with 100 μl Proteinase K (0.5 mg/ml in 100 mM phosphate and 10 mM EDTA, pH 7.1) at 60°C for 18 hours and diluted to 500 μl with water before storage at -20°C. Portions of solubilized tissues were used to determine total sulfated GAG,[21] hydroxyproline,[22] and DNA content.[23] The hydroxyproline content was converted to collagen (COL) content assuming a mass ratio of collagen to hydroxyproline of 7.1.[24] The DNA content was converted to cell content assuming a conversion constant of 7.3 pg DNA/chondrocyte (CELL).[25] The total dry mass attributed to the cells was then calculated using a conversion of 0.1 ng dry weight/cell.[26] The residual dry weight (RES) was computed as the remaining dry weight not accounted for by GAG, collagen, or the mass of the cells. The mass of various constituents was expressed normalized to the tissue wet weight.

4.3.5.Statistical Analysis

The effect of developmental stage (infant, child, adult) and zone (SZ, DZ) on biomechanical (equilibrium modulus, ramp modulus, failure strength, failure strain) and biochemical (water, COL, GAG, CELL, RES) were analyzed by multiway analysis of variance (ANOVA) with GraphPad Prism 10.0.2. Where significant ($p < 0.05$) effects were detected, comparisons between groups were performed using the Tukey post-hoc test.

To assess dependence of mechanical function and biochemical content on age, measures were fit by least-squares regression to either a single logistic function, or a sum of two logistic functions, of the form $\boldsymbol{Y(t)} = \left(\boldsymbol{B_1} + \frac{\boldsymbol{A_1 - B_1}}{\boldsymbol{1 + \left(\frac{t}{C_1}\right)^{D_1}}}\right) + \left(\boldsymbol{B_2} + \frac{\boldsymbol{A_2 - B_2}}{\boldsymbol{1 + \left(\frac{t}{C_2}\right)^{D_2}}}\right)$ where $Y(t)$ is the property value with respect to age, $t\,[yr]$ is the age of the donor, A is the left (immature) horizontal asymptote, B is the right (mature) horizontal asymptote, C is the age at which the property value is halfway between the minimum and maximum value, and D is a measure of the slope of the curve. The sum of two logistic functions form was utilized if the data featured a peak or trough during intermediate age groups.

The dependencies of mechanical properties on biochemical constituents were analyzed by univariate regression and multivariate regression utilizing the backward elimination procedure.[27] All data are expressed as mean ± SEM.

4.4. Results

4.4.1. Biomechanical Properties

Variation in tensile biomechanical properties, especially tensile equilibrium modulus (**Fig. 1A-C**), ramp modulus (**Fig. D-F**), and failure strength (**Fig. 1G-I**) with developmental stage and zone followed similar patterns. In general, tensile biomechanical properties varied significantly with developmental stage, zone, and interactive effect. In both the SZ and DZ, the biomechanical properties tended to increase between infants and children before decreasing in adults. In children, the equilibrium modulus, ramp modulus, and failure strength were ~1.3-2 times greater in the DZ, compared to the SZ. In the DZ, tensile properties of AC from children were ~3 times greater than adults. In the SZ, differences between developmental stages were not as evident as in the DZ.

Conversely, strain at failure (**Fig. 1J-L**) did not vary significantly with developmental stage ($p=0.09$), but varied with zone (**Fig. 1J**, $p<0.001$), and with interactive effects ($p<0.05$). Strain in the SZ was low (~0.7 mm/mm) and did not vary with age. In contrast, strain in the DZ, relative to adult (~1.3 mm/mm), was low in infants and children (~0.8 mm/mm). In the SZ, lower strains, relative to adults, were not evident in infants and children.

During maturation and ageing the relationship between tensile biomechanical properties and age were stable during the first year and at maturity (**Fig. 1**). Including previously published data,[9] biomechanical properties were fitted using a function that is the sum of two logistics. The ages at which tensile properties were enhanced and diminished were ~1-2 years and ~16 years, respectively (**Table 1**).

4.4.2. Biochemical Properties

Biochemical properties of distal femoral AC generally varied with age and zone (**Fig. 2**). Decreases in water content with age occurred in parallel with increases in collagen content, and a

decrease in cellularity.

In general, AC biochemical properties varied with developmental stage, zone, and with interactive effects. In both zones, water content (**Fig. 2A-C**) was greater in infants (+12%) and children (+4%) compared to adults (78%). Conversely, COL content (**Fig. 2D-F**) was less in infants (-60%) and children (-16%) compared to adults (130 mg/g WW). At all developmental stages, GAG content (**Fig. 2G-I**) was enhanced in the DZ (~29 mg/g WW) compared to the SZ (~17 mg/g WW). Cellularity (**Fig. 2J-L**) decreased with age and was reduced in the DZ compared to the SZ. Residual AC content (**Fig. 2M-O**), dry mass not attributed to collagen, GAG, or cells, did not vary with developmental stage or zone.

During maturation and ageing, the relationship between AC biochemical properties were similar between the SZ and DZ (**Table 2**). Considering previously published data,[9] water (**Fig. 2BC**) and collagen content (**Fig. 2EF**) were logistically related to age, with similar time constants in the SZ and DZ, of ~20-30 yrs. Cellularity (**Fig. 2KL**) was also logistically related to age, with time constants of ~1 yrs and 10 yrs in the SZ and DZ, respectively.

4.4.3. Correlative Analysis

Several AC tensile mechanical properties were univariately correlated with tissue matrix constituents (**Fig. 3**) during prepubescent maturation of the superficial and deep zones. Correlations between mechanical and biochemical properties in the SZ and DZ were grouped according to significance of zone in the biomechanical property (**Fig 2**, **Table 3**). Tensile ramp modulus (**Fig. 3D-F**) and failure strength (**Fig. 3G-I**) showed negative correlations with water content and positive correlations with COL and RES. Correlation coefficients were highest for failure strength in the DZ, reaching R^2 values of 0.70 (**Fig. 3G**, $p<0.0001$), and 0.76 (**Fig. 3H**, $p<0.0001$) with water and COL content, respectively. Correlation coefficients were also high for

ramp modulus in the SZ and DZ, reaching R^2 values of 0.60 ($p<0.01$) with both water (**Fig. 3D**) and COL content (**Fig. 3E**). Equilibrium and ramp modulus also trended positively with RES, with R^2 values of 0.28 in the SZ (**Fig. 3C**, $p=0.05$) and 0.21 for the SZ and DZ (**Fig. 3F**, $p<0.01$), respectively.

Analysis of correlation between mechanical properties and tissue matrix constituents by multivariate regression generally supported the univariate analysis and indicated additive effects of matrix in some properties (**Table 4, 5**). Specifically, the tensile ramp modulus (**Fig. 3D-F**) varied positively with COL ($p<0.0001$, S.E.=0.04) and RES content ($p<0.005$, S.E.=0.06), with an R^2 value of 0.59. In the deep zone, failure strength (**Fig. 3G-I**) varied positively with COL ($p<0.001$, S.E.=0.02), and CELL ($p<0.05$, S.E.=0.84), and negatively with GAG ($p<0.05$, S.E.=0.11) for an R^2 value of 0.96.

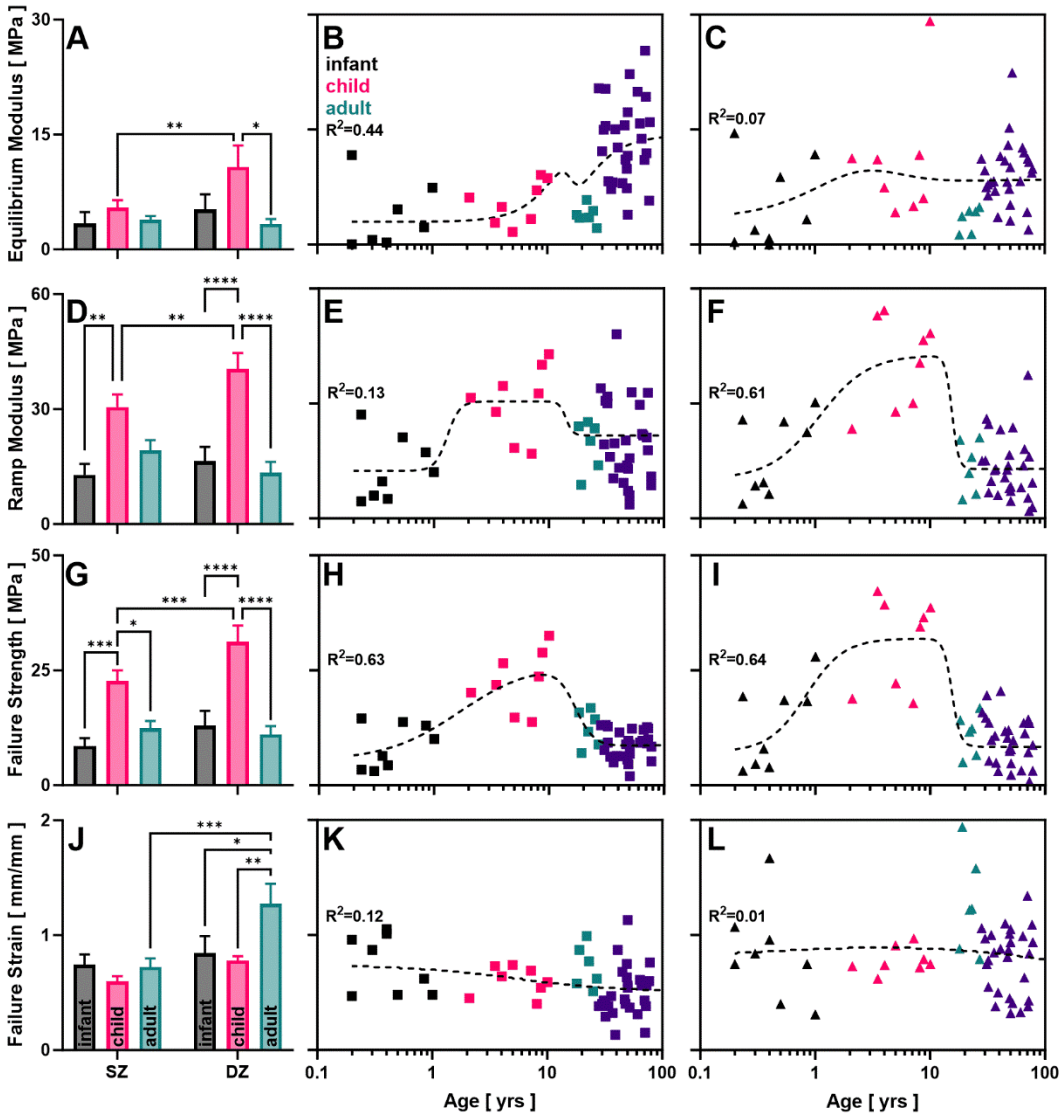


Figure 4.1. Effect of developmental stage on tensile biomechanical properties. (**A-C**) Equilibrium modulus, (**D-F**) ramp modulus, (**G-I**) failure strength, and (**J-L**) failure strain according to (**A,D,G,J**) developmental stage (**infant**, **child**, **adult**) and age in the (■; **B,E,H,K**) SZ and (▲; **C,F,I,L**). p<0.05, **p<0.01, ***p<0.001, ****p<0.0001. Additional data from older adults (**purple**, ~30+ yrs) incorporated from previously published data.[9]

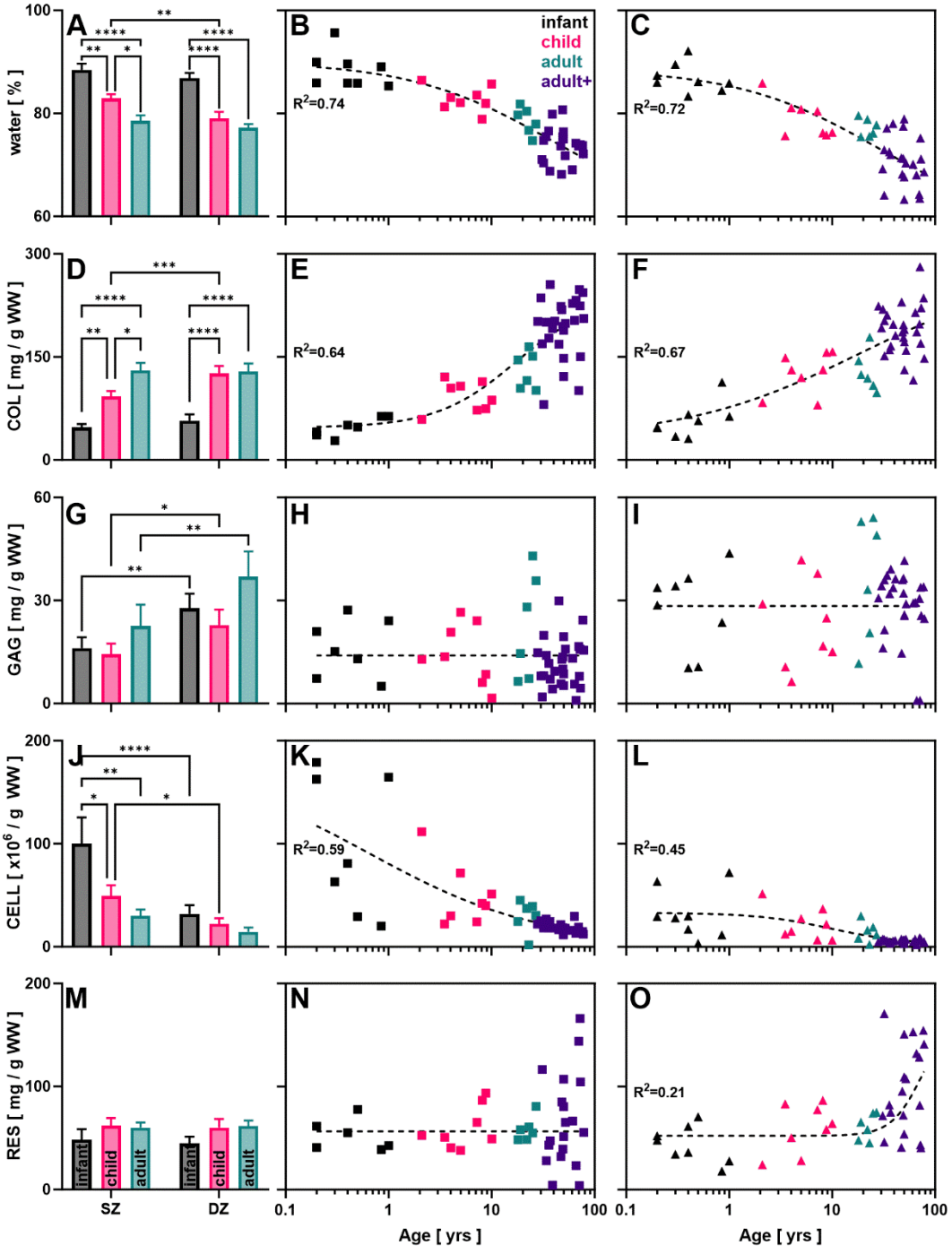


Figure 4.2. Effect of developmental stage on tensile biochemical properties. (**A-C**) Water, (**D-F**) COL, (**G-I**) GAG, (**J-L**) CELL, and (**M-O**) RES content, according to (**A,D,G,J,M**) developmental stage (**infant**, **child**, **adult**) and age in the (■; **B,E,H,K,N**) SZ and (▲; **C,F,I,L,O**) DZ. p<0.05, **p<0.01, ***p<0.001, ****p<0.0001. Additional data from older adults (**purple**, ~30+ yrs) incorporated from previously published data.[9]

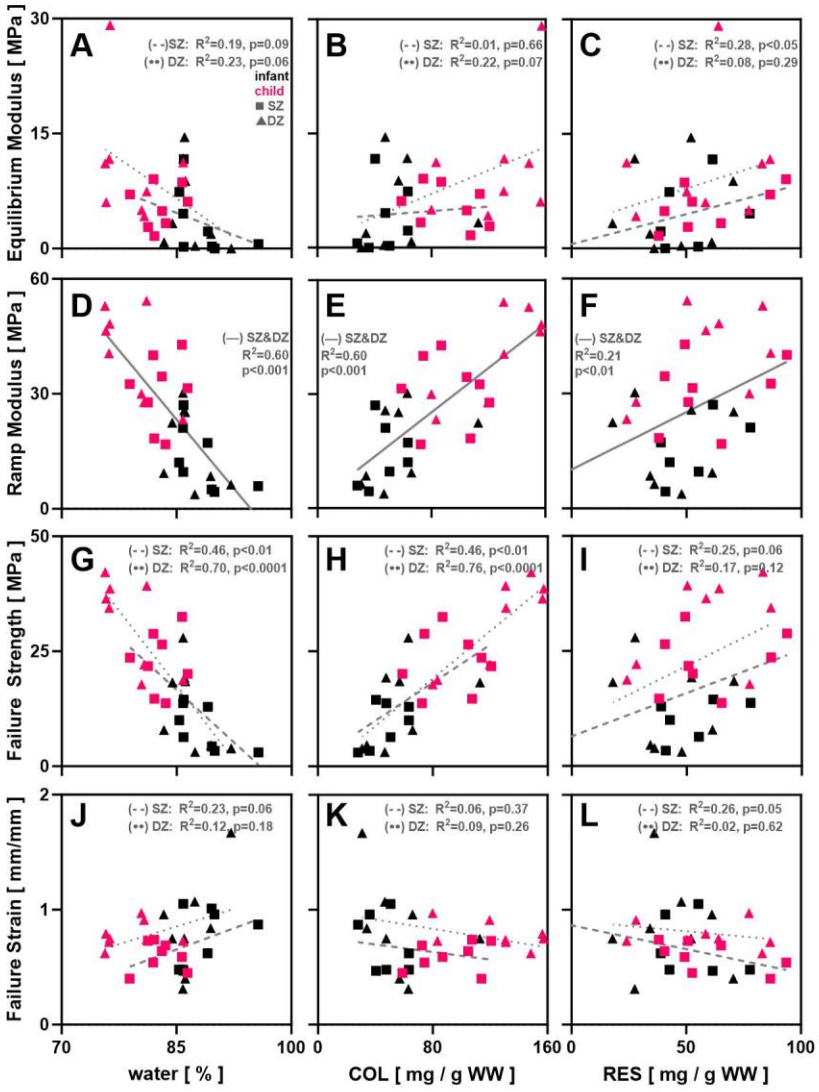


Figure 4.3. Relationship between cartilage tensile properties and cartilage composition. Dependence of (**A-C**) equilibrium tensile modulus, (**D-F**) ramp modulus, (**G-I**) failure strength, and (**J-L**) failure strain, on (A,D,G,J) water, (B,E,H,K) COL, and (C,F,I,L) RES contents for infants (**black**) and children (**pink**) in the SZ (■, square) an DZ (▲, triangle)

Table 4.1. Coefficients for logistic fits of variation of tensile biomechanical properties during maturation and ageing. Fits for biochemical properties consider donors from infant , child, and adults, as well as additional adult donors incorporated from previously published data.[9]

				Logistic $Y(t) = Y_1(t) + Y_2(t) = \left(B_1 + \frac{A_1 - B_1}{1 + \left(\frac{t}{C_1}\right)^{D_1}} \right) + \left(B_2 + \frac{A_2 - B_2}{1 + \left(\frac{t}{C_2}\right)^{D_2}} \right)$							
Y	**Zone**	**fit type**	**R^2**	A_1 $C(t \to 0)$	B_1 $C(t \to \infty)$	C_1 [yrs]	D_1 slope factor	A_2 $C(t \to 0)$	B_2 $C(t \to \infty)$	C_2 [yrs]	D_2 slope actor
Equilibrium Modulus [MPa]	SZ	logistic	0.44	-5.12	14	16	2.3	8.1	0.75	16	10
	DZ	logistic	0.07	-4.6	11	1.9	1.4	7.9	-2.4	4.0	1.9
Ramp Modulus [MPa]	SZ	logistic	0.13	-0.78	17	1.3	8.0	13	4.4	14	15
	DZ	logistic	0.61	-10	22	1.1	2.0	21	-9.0	16	15
Failure Strength [MPa]	SZ	logistic	0.63	-7.1	14	1.7	1.4	12	-5.4	17	5.3
	DZ	logistic	0.64	-8.2	16	0.84	2.7	16	-8.0	16	12
Failure Strain [mm / mm]	SZ	logistic	0.12	0.74	0.5	5.5	0.88				
	DZ	logistic	0.01	-0.06	0.73	4.8	0.40	0.82	-0.35	100	0.4

Table 4.2. Coefficients for offset and logistic fits of variation of biochemical properties during maturation and ageing. Fits for biochemical properties consider donors from infant , child, and adults, as well as additional adult donors incorporated from previously published data.[9]

				Offset	**Logistic**			
				$Y(t) = B$	$Y(t) = B_1 + \frac{A_1 - B_1}{1 + \left(\frac{t}{C_1}\right)^{D_1}}$			
Y	**Zone**	**fit type**	**R^2**	**B**	A_1 $C(t \to 0)$	B_1 $C(t \to \infty)$	C_1 [yrs]	D_1 slope factor
Water	SZ	logistic	0.74		90	59	39	0.63
[%]	DZ	logistic	0.72		89	58	29	0.63
COL	SZ	logistic	0.64		47	240	17	1.1
[mg / g WW]	DZ	logistic	0.67		31	280	19	0.51
GAG	SZ	offset		14				
[mg / g WW]	DZ	offset		28				
CELL	SZ	logistic	0.59		180	2.1	0.66	0.53
[mg / g WW]	DZ	logistic	0.45		33	2.3	9.9	1.2
RES	SZ	offset		57				
[mg / g WW]	DZ	logistic	0.21		42	170	75	2.9

Table 4.3. Coefficients for univariate regression of tensile biomechanical properties with biochemical content in infants and children.

		Water [%]				COL [mg / g WW]				RES [mg / g WW]				GAG [mg / g WW]				CELL [mg / g WW]			
	zone	**slope**	**S.E**	**R^2**	**p**	**slope**	**S.E**	**R^2**	**p**	**slope**	**S.E**	**R^2**	**p**	**slope**	**S.E**	**R^2**	**p**	**slope**	**S.E**	**R^2**	**p**
Equilibrium Modulus [MPa]	SZ	-0.39	0.21	0.19	0.09	0.01	0.03	0.01	0.66	0.08	0.04	0.28	**<0.05**	-0.08	0.12	0.03	0.51	0.14	0.17	0.05	0.42
	DZ	-0.69	0.33	0.23	0.06	0.08	0.04	0.22	0.07	0.10	0.09	0.08	0.29	-0.13	0.16	0.05	0.42	0.33	0.96	0.01	0.73
Ramp Modulus [MPa]	SZ, DZ	-2.40	0.36	0.60	**<0.0001**	0.29	0.04	0.60	**<0.0001**	0.30	0.11	0.21	**<0.01**	-0.34	0.22	0.07	0.14	-0.94	0.55	0.09	0.10
Failure Strength [MPa]	SZ	-1.52	0.45	0.46	**<0.01**	0.21	0.06	0.46	**<0.01**	0.19	0.09	0.25	0.06	-0.42	0.27	0.15	0.15	-0.70	0.40	0.19	0.11
	DZ	-2.16	0.38	0.70	**<0.0001**	0.26	0.04	0.76	**<0.0001**	0.25	0.15	0.17	0.12	-0.41	0.27	0.15	0.15	-0.66	1.74	0.01	0.71
Failure Strain [mm/ mm]	SZ	0.02	0.01	0.23	0.06	0.00	0.00	0.06	0.37	0.00	0.00	0.26	0.05	0.01	0.01	0.07	0.35	0.00	0.01	0.00	0.96
	DZ	0.02	0.01	0.12	0.18	0.00	0.00	0.09	0.26	0.00	0.00	0.02	0.62	0.00	0.01	0.01	0.75	-0.04	0.04	0.06	0.35

Table 4.4. Parameters of multiple linear regression between compressive biomechanical properties and biochemical content in infants and children. est. = estimate, S.E. = standard error. ****p<0.0001

			$Y = \beta_0 + \beta_1(COL) + \beta_2(GAG) + \beta_3(CELL) + \beta_4(RES)$														
			intercept			**COL [mg / g WW]**			**GAG [mg / g WW]**			**CELL [mg / g WW]**			**RES [mg / g WW]**		
Y	**Zone**	**R^2**	**p**	**β_0**	**S.E.**	**p**	**β_1**	**S.E.**	**p**	**β_2**	**S.E.**	**p**	**β_3**	**S.E.**	**p**	**β_4**	**S.E.**
Equilibrium Modulus [MPa]	**SZ**	0.74													<0.0001	0.09	0.01
	DZ	0.66				<0.0001	0.09	0.02									
Ramp Modulus [MPa]	**SZ, DZ**	0.92				<0.0001	0.24	0.04							<0.05	0.12	0.06
Failure Strength [MPa]	**SZ**	0.88				<0.0001	0.23	0.02									
	DZ	0.96				<0.0001	0.26	0.02	<0.05	-0.32	0.12	<0.05	2.33	0.84			
Failure Strain [mm / mm]	**SZ**	0.00	<0.0001	0.67	0.05												
	DZ	0.00	<0.0001	0.81	0.08												

Table 4.5. P-values for multivariate regression with the backward elimination procedure. Tensile biomechanical properties correlated against biochemical content normalized to wet weight [mg / g WW] in infants and children

		SUPERFICIAL LAYER					DEEP LAYER					SUPERFICIAL + DEEP LAYER			
		R1	**R2**	**R3**	**R4**	**R5**	**R1**	**R2**	**R3**	**R4**	**R5**	**R1**	**R2**	**R3**	**R4**
Equilibrium Modulus [MPa]	**Intercept**	0.62	0.94	0.58			0.66								
	COL	0.49					0.10	0.08	0.00	0.00	<0.0001				
	GAG	0.44	0.48				0.44	0.22	0.25	0.98					
	CELL	0.14	0.17	0.19	0.21		0.15	0.15	0.14						
	RES	0.07	0.04	0.03	0.00	<0.0001	0.46	0.52							
Ramp Modulus [MPa]	**Intercept**											0.86			
	COL											<0.0001	<0.0001	<0.0001	<0.0001
	GAG											0.24	0.11	0.11	
	CELL											0.71	0.73		
	RES											0.06	0.03	0.02	<0.05
Failure Strength [MPa]	**Intercept**	0.65	0.59				0.31								
	COL	0.02	0.01	0.00	0.00	<0.0001	<0.0001	<0.0001	<0.0001						
	GAG	0.13	0.10	0.08	0.11		0.09	0.01	<0.05						
	CELL	0.95	0.15	0.05			0.01	0.02	<0.05						
	RES	0.17					0.17	0.32							
Failure Strain [mm / mm]	**Intercept**	0.00	0.00	0.00	<0.0001	<0.0001	0.00	0.00	0.00	<0.0001	<0.0001				
	COL	0.46	0.66				0.19	0.17	0.12	0.26					
	GAG	0.41	0.50	0.48			0.88								
	CELL	0.47					0.23	0.14	0.15						
	RES	0.13	0.12	0.08	0.05		0.56	0.56							

4.5. Discussion

This data shows marked changes in tensile biomechanical properties (**Fig. 1**) and biochemical composition (**Fig. 2**) of normal human AC during prepubescent maturation, and adulthood. Throughout prepubescent maturation, during infancy and childhood, tensile properties are enhanced, indicated by increased ramp modulus (**Fig. 1D-F**) and failure strength (**Fig. 1G-I**). Strikingly, in AC from children, tensile properties were elevated in the DZ, compared to the SZ, and there was a marked loss of tensile integrity between AC from children and adults. During prepubescent maturation improvement of tensile properties occurred in tandem with loss of water content (**Fig. 2A-C**), increased COL (**Fig. 2D-F**), and decreased CELL (**Fig. 2J-L**) with maturation. Correlation analysis (**Fig. 3**) indicated that variation in ramp modulus and failure strain during prepubescent maturation are associated with water, collagen, and residual content. The delineation of variation in normal human AC tensile and biochemical properties provides insight into the mechanisms of cartilage growth during prepubescent maturation.

The focus of this study on AC from infants and children had advantages and limitations. Specimens from similar depths from the articular surface to a previous study were chosen,[9]and allowed for analysis of biochemical properties throughout human maturation and ageing from infancy (< 2 yrs) to late adulthood (~80 yrs). Despite the variability in joint size, consistent geometries for tensile testing were used and allowed a standardized tensile specimen to be utilized for all ages. The sample thickness chosen was similar to those used in our previous studies,[8,9] although with a smaller (2 mm) gage length to accommodate specimens from smaller immature joints. Thus, we chose not to directly compare the biomechanical properties assessed herein, with those studies.[8,9] Although use of a constant sample thickness minimizes confounding effects when comparing between samples, in AC of varying maturity constant-thickness layers may represent different proportions of the superficial, middle, and deep cartilage layers.[28,29] While tensile strip

specimens from infant donors were not all prepared from the media femoral condyle nor in an orientation parallel to the expected split line direction,[18] collagen fibrils in immature AC is less organized and are not expected to have significant variation or anisotropy along the joint surface during the early postnatal period.[15,30] Importantly, all tensile test specimens from children and adult donors were acquired in similar regions and orientations on the medial femoral condyle where the split-line orientation is expected to become increasingly oriented along the articular surface in the medial-lateral direction during maturation. Tensile strengthening during prepubescent maturation is indicative of increasing collagen-fibril alignment in this region.

The biomechanical results extend previous studies on the tensile properties of normal human AC by characterizing the variation of these properties during prepubescent maturation. The marked increase in tensile properties between AC from infant and child donors, is consistent with maturation-related increases found in bovine,[8] and porcine animals.[12] The ramp modulus, failure strength, and failure strain of adult donors are consistent with previous studies.[9]

The biochemical results extend previous studies on the composition of normal human AC, by assessing depth- and maturation- associated changes in tissue composition. In animals, COL undergoes similar substantial increases during maturation compared to GAG in the bovine,[8,17] equine,[13] porcine,[12,31] and lapine animals.[32]

The univariate and multivariate function-composition analysis supports the notion that AC tensile integrity is largely driven by overall matrix and collagen content, which increases during maturation, as well as other factors including GAG and other matrix components. Additional analyses are required to determine the effects of collagen crosslinks, which positively correlate with tensile strength, [8] and collagen orientation on variation in tensile function during maturation.

The evolution of tensile and biochemical properties appear to have different dynamics

which may reflect the influence of different mechanisms influencing AC maturation. Ramp modulus and failure strength increase logistically with age in the DZ, increasing rapidly at ~1-2 years of age. Similarly, water and COL content vary logistically with age, reaching ~50% of their mature value by 35 and 18 years, respectively. The rapid enhancement in tensile properties during late infancy align with the age at which human infants typically begin to walk (~1 yr)[33] and implicates mechanotransduction as a possible mechanism modulating cartilage maturation. In addition, the slowed accumulation of COL at ~18 yrs suggests regulation by hormones associated with puberty.

The elevation in tensile equilibrium modulus, ramp modulus, and failure strength in the DZ of AC from child donors, compared to SZ supports the presence of age-dependent depth-wise variation in collagen content and structure in immature tissues. In PLM analyses of immature bovine,[34] equine,[34] and lapine AC,[32] collagen fibrils run tangential to the surface at the articular surface, as well as in a deeper layer of AC, separated by a transitional layer. At the same depth from the surface in mature AC, the subjacent layer of formerly tangentially oriented collagen fibrils is largely oriented perpendicular to the surface, indicative of classically defined cartilage zones. The elevated tensile properties of deeper cartilage in immature humans and bovines,[11] may be indicative of the depth-variation of collagen architecture in immature cartilage. Additional studies are required to ascertain possible functional roles or causes that lead to the development and disappearance of this subjacent layer.

Apparent weakening between AC from child and adult donors may be indicative of early degradation within the MFC. In macroscopically normal human cartilage, ageing-associated reductions in cellularity, matrix content, and increased surface wear occurred at an earlier age in the MFC than in the LFC.[9] Accordingly, even in young adults (~30 yrs), tensile properties were

reduced ~50% in the MFC, compared to the LFC.[9] Further study is needed of joints in the adolescent age range (10-20 yrs), and of comparative LFCs during the prepubescent period to establish the sequence of events leading to tensile weakening of the MFC by early adulthood.

The characterization of changes in tensile properties during normal AC development, concurrent alterations in biochemical content, and the relationship between these properties may be useful in informing the design and development of cartilage repair strategies. These properties may serve as benchmarks for postnatal maturation of normal human femoral condyle and as design criteria for engineered tissues. Design of tissues with enhanced child-like tensile properties, rather than adult, may help to produce tissue that is better able to adapt to withstand years of repetitive loading.[35]

4.6. Acknowledgements

This chapter, in full, will be submitted to *Cartilage*. The dissertation author was the primary author. Thanks to co-authors Albert C. Chen, Christine L. Farnsworth, William D. Bugbee, Kevin G. Shea, Eric W. Edmonds, and Robert L. Sah. We are grateful to Allosource and the donors, and their families. We also thank Brendon Mitchell, MD and Liane Chun, MD for their help collecting donor tissues . This work was supported by NSF GRFP (EGG) and the Wu Tsai Human Performance Alliance.

4.7. References

1. Tanner JM, Whitehouse RH, Takaishi M. Standards from birth to maturity for height, weight, height velocity, and weight velocity: British children, 1965. II. *Arch Dis Child*. 1966;41:613-35.

2. Tanner JM, Whitehouse RH, Takaishi M. Standards from birth to maturity for height, weight, height velocity, and weight velocity: British children, 1965. I. *Arch Dis Child*. 1966;41:454-71.

3. Tanner JM. Normal growth and techniques of growth assessment. *Clin Endocrinol Metab*. 1986;15:411-51.

4. Sidharthan S, Yau A, Almeida BA, Shea KG, Greditzer HGt, Jones KJ, et al. Patterns of articular cartilage thickness in pediatric and adolescent knees: A magnetic resonance imaging-based study. *Arthrosc Sports Med Rehabil*. 2021;3:e381-e90.

5. Ellermann JM, Ludwig KD, Nissi MJ, Johnson CP, Strupp JP, Wang L, et al. Three-dimensional quantitative magnetic resonance imaging of epiphyseal cartilage vascularity using vessel image features: New insights into juvenile osteochondritis dissecans. *JB&JS Open Access*. 2019;4:e0031.

6. Mundy A, Ravindra A, Yang J, Adler BH, Klingele KE. Standardization of patellofemoral morphology in the pediatric knee. *Pediatr Radiol*. 2016;46:255-62.

7. Charlebois M, McKee MD, Buschmann MD. Nonlinear tensile properties of bovine articular cartilage and their variation with age and depth. *J Biomech Eng.* 2004;126:129-37.

8. Williamson AK, Chen AC, Masuda K, Thonar EJ-MA, Sah RL. Tensile mechanical properties of bovine articular cartilage: variations with growth and relationships to collagen network components. *J Orthop Res.* 2003;21:872-80.

9. Temple MM, Bae WC, Chen MQ, Lotz M, Amiel D, Coutts RD, et al. Age- and site-associated biomechanical weakening of human articular cartilage of the femoral condyle. *Osteoarthritis Cartilage*. 2007;15:1042-52.

10. Kempson GE. Relationship between the tensile properties of articular cartilage from the human knee and age. *Ann Rheum Dis*. 1982;41:508-11.

11. Roth V, Mow VC. The intrinsic tensile behavior of the matrix of bovine articular cartilage and its variation with age. *J Bone Joint Surg Am*. 1980;62-A:1102-17.

12. Bielajew BJ, Donahue RP, Lamkin EK, Hu JC, Hascall VC, Athanasiou KA. Proteomic, mechanical, and biochemical development of tissue-engineered neocartilage. *Biomater Res*. 2022;26:34.

13. Oinas J, Ronkainen AP, Rieppo L, Finnilä MAJ, Iivarinen JT, van Weeren PR, et al. Composition, structure and tensile biomechanical properties of equine articular cartilage during growth and maturation. *Sci Rep*. 2018:11357.

14. Kempson GE. Age-related changes in the tensile properties of human articular cartilage: a comparative study between the femoral head of the hip joint and the talus of the ankle joint. *Biochim Biophys Acta*. 1991;1075:223-30.

15. Silverberg JL, Dillavou S, Bonassar L, Cohen I. Anatomic variation of depth-dependent mechanical properties in neonatal bovine articular cartilage. *J Orthop Res*. 2013;31:686-91.

16. Buckwalter JA, Mankin HJ, Grodzinsky AJ. Articular cartilage and osteoarthritis. *Instr Course Lect*. 2005;54:465-80.

17. Williamson AK, Chen AC, Sah RL. Compressive properties and function-composition relationships of developing bovine articular cartilage. *J Orthop Res*. 2001;19:1113-21.

18. Below S, Arnoczky SP, Dodds J, Kooima C, Walter N. The split-line pattern of the distal femur: A consideration in the orientation of autologous cartilage grafts. *Arthroscopy*. 2002;18:613-7.

19. Akizuki S, Mow VC, Muller F, Pita JC, Howell DS, Manicourt DH. Tensile properties of human knee joint cartilage: I. influence of ionic conditions, weight bearing, and fibrillation on the tensile modulus. *J Orthop Res*. 1986;4:379-92.

20. Kempson GE, Muir H, Pollard C, Tuke M. The tensile properties of the cartilage of human femoral condyles related to the content of collagen and glycosaminoglycans. *Biochim Biophys Acta*. 1973;297:456-72.

21. Farndale RW, Buttle DJ, Barrett AJ. Improved quantitation and discrimination of sulphated glycosaminoglycans by use of dimethylmethylene blue. *Biochim Biophys Acta*. 1986;883:173-7.

22. Woessner JF. The determination of hydroxyproline in tissue and protein samples containing small proportions of this imino acid. Arch Biochem Biophys. 1961;93:440-7.

23. McGowan KB, Kurtis MS, Lottman LM, Watson D, Sah RL. Biochemical quantification of DNA in human articular and septal cartilage using PicoGreen and Hoechst 33258. *Osteoarthritis Cartilage*. 2002;10:580-7.

24. Jackson DS, Cleary EG. The determination of collagen and elastin. *Methods Biochem Anal.* 1967;15:25-76.

25. Stockwell RA. The cell density of human articular and costal cartilage. *J Anat*. 1967;101:753-63.

26. Freed LE, Marquis JC, Langer R, Vunjak-Novakovic G, Emmanual J. Composition of cell-polymer cartilage implants. *Biotechnol Bioeng.* 1994 Mar 25;43(7):605-14.

27. Sokal RR, Rohlf FJ. Biometry. 3rd ed. New York: WH Freeman and Co.; 1995. 887 p.

28. Hunziker EB, Kapfinger E, Geiss J. The structural architecture of adult mammalian articular cartilage evolves by a synchronized process of tissue resorption and neoformation during postnatal development. *Osteoarthritis Cartilage*. 2007;15:403-13.

29. Hunziker EB, Quinn TM, Hauselmann HJ. Quantitative structural organization of normal adult human articular cartilage. *Osteoarthritis Cartilage*. 2002;10:564-72

30. Erickson IE, van Veen SC, Sengupta S, Kestle SR, Mauck RL. Cartilage matrix formation by bovine mesenchymal stem cells in three-dimensional culture is age-dependent. *Clin Orthop Relat Res*. 2011;469:2744-53.

31. Rieppo J, Hyttinen MM, Halmesmaki E, Ruotsalainen H, Vasara A, Kiviranta I, et al. Changes in spatial collagen content and collagen network architecture in porcine articular cartilage during growth and maturation. *Osteoarthritis Cartilage*. 2009;17:448-55.

32. Julkunen P, Harjula T, Iivarinen J, Marjanen J, Seppanen K, Narhi T, et al. Biomechanical, biochemical and structural correlations in immature and mature rabbit articular cartilage. *Osteoarthritis Cartilage*. 2009;17:1628-38.

33. Clark JE, Whitall J, Phillips SJ. Human interlimb coordination: the first 6 months of independent walking. *Dev Psychobiol*. 1988;21:445-56.

34. Camosso M, Marotti G. The mechanical behavior of articular cartilage under compressive stress. *J Bone Joint Surg Am.* 1962;44-A:699-709.

35. Butler DL, Goldstein SA, Guilak F. Functional tissue engineering: the role of biomechanics. *J Biomech Eng.* 2000;122:570-5.

CHAPTER 5

KINEMATIC MODEL OF COLLAGEN NETWORK REORIENTATION DURING MURINE FEMORAL CONDYLE GROWTH AND MATURATION

5.1. Abstract

Immature articular cartilage (AC) undergoes substantial growth and functional maturation between birth and skeletal maturity. The medial femoral condyle (MFC) increases in size, as cartilage thins, surface area increases, and collagen network orientation (CNO) changes throughout the depth to become tangential at the articular surface and transition to vertical at the interface with bone. Axial and lateral expansion may drive formation of such CNO. The aim of this study was to determine the extent to which the kinematics of axial and lateral expansion, individually and in combination, in accordance with the growth of the mouse MFC, may explain observed changes in CNO. A theoretical model was developed to relate immature AC growth to kinematic reorientation of the collagen network. Joint-scale growth strains during postnatal maturation were determined, based on the growth of the murine MFC as determined from measurements of microcomputed tomography datasets of mice from P0 to P42, fitting dimensions to logistic equations, and computing growth strain rate and strain. For the cases of (1) axial growth strain, (2) lateral growth strain, and (3) combined axial and lateral growth strain, and either (A) uniform or (B) depth-varying axial and lateral strain, the resulting CNO from the immature to mature stages were computed. In a simplified two-dimensional model, an initial undeformed reference configuration, describing the immature state, undergoes a deformation according to a specified deformation gradient. Based on the initial CNO and applied deformation, the CNO between the immature and

deformed mature state is altered. In the mouse MFC, the perimeter and radii along the articular surface and cartilage-bone interface at the secondary ossification center increased logistically with time constants of ~3-6 days as radii and perimeter along the articular surface increased ~250% between birth and maturity. Applying a uniform axial deformation of 250%, CNO increases from 10° to ~65° at the surface and from 45° to 70° in the deeper cartilage. Applying a uniform lateral deformation of 250% reorients the CN to ~5° at the surface and ~20° in the deeper cartilage. However, with axial deformation increasing exponentially with depth, and lateral deformation decreasing linearly with depth, CNO attained mature-like depth-variation with a 187% increase in AC area and CN of ~1° at the surface and ~70° in the deeper cartilage. Depth-associated variation in axial and lateral articular cartilage growth may be responsible for the kinematic reorganization of cartilage to attain the CNO characteristic of mature adult articular cartilage.

5.2. Introduction

In skeletally immature individuals, the covering of bone ends includes a layer of epiphyseal growth cartilage (EC) and articular cartilage (AC) which are collectively known as the articular–epiphyseal cartilage complex (AECC).[1] Specifically, the cartilage at the outermost boundary of the epiphysis adjacent to the joint space is the AC, the cartilage adjacent to the metaphysis forms the physis, and the cartilage between the articular cartilage and physeal cartilage is the EC. During maturation of the distal femur, overall AECC thinning occurs in tandem with AC thickening, and results from robust and rapid mineralization of the EC layer during formation and growth of the secondary ossification center (SOC).[2,3] The immature AC layer also undergoes extensive lateral growth during maturation to cover various joint surfaces, ranging from convex, to flat, to concave.

Collagen network orientation (CNO) also changes during growth and maturation. In immature tissues, the AC is comprised of two layers of tangential orientation, one at the articular surface and another at a subjacent deeper layer.[4-6] The deeper layer of tangentially oriented tissue makes up the EC.[6] By maturity, the CN has remodeled to the classical Benninghoff architecture, where fibrils at the surface zone remain parallel to the surface, the deep zone fibrils are roughly perpendicular to the articular surface, with a transitional zone in between, near the surface.[4,5,7]

Immature AC undergoes substantial growth and functional maturation between birth and skeletal maturity. However, the way in which immature AC attains its adult form, (1) increasing in thickness, (2) covering an increasing surface area, and (3) achieving the adult CNO is unclear. The hypothesis of this study is that immature AC undergoes depth-varying deformations which allow for increased surface area and thickness, and kinematically reorients the CN. Thus, the aims of this study are to (1) develop a model coupling immature AC growth to kinematic reorientation of the CN, and identify (2) growth constraints based on maturation of the murine distal femur , and (3) hypothetical deformations which convert the CN from the immature to mature orientation.

5.3. Methods

5.3.1. Study Design

The effect of kinematic growth on reorientation of the CN of immature AC was analyzed in the context of growth of the murine medial femoral condyle (MFC). First, a theoretical model was developed to relate growth kinematics to evolution of CNO. Second, joint-scale growth strains during postnatal maturation were determined, based on the growth of the murine MFC. Left hindlimbs of strain CD-1 mice at postnatal days P0 (4M+2F), P7 (3M+3F), P14 (4M+5F), P21 (3M+3F), P28 (2M+4F), P35 (3M+3F), and P42 (3M+3F) were sacrificed and imaged by microcomputed tomography (μCT) before and after staining with phosphotungstic acid (PTA). To assess age-related variation in the MFC, μCT datasets were analyzed for anterior-posterior and proximal-distal radii, and cartilage thickness of medial femoral condyle in the mid-sagittal plane. Finally, CNO resulting from kinematic growth from immature to mature stages were computed for the cases of (1) axial growth strain, (2) lateral growth strain, and (3) combined axial and lateral growth strain, with strains being either (A) uniform or (B) depth-varying for both axial and lateral strain.

5.3.2. Model of 2D deformation induced collagen fibril reorientation

In a simplified two-dimensional model, the vector fields $\boldsymbol{X} = X_r\hat{\imath} + X_z\hat{k}$ defines the initial undeformed reference configuration, and $\boldsymbol{x} = x_r\hat{\imath} + x_z\hat{k}$ defines the deformed configuration (**Fig. 1**).[8] Between t_0 and maturity, t_m, the tissue area undergoes a deformation according to a specified deformation gradient $\boldsymbol{F}$.

$$F_{ij} = \begin{bmatrix} \frac{\partial x_r}{\partial X_r} & \frac{\partial x_r}{\partial X_z} \\ \frac{\partial x_z}{\partial X_r} & \frac{\partial x_z}{\partial X_z} \end{bmatrix} \qquad \textbf{(Equation 1)}$$

From the deformation gradient, $\boldsymbol{F}$, and initial configuration, $\boldsymbol{X}$, the displacement, $\boldsymbol{u}$, and

deformed configuration, $\boldsymbol{x}$, are calculated.

$$\boldsymbol{F} = \frac{\partial}{\partial X}(\boldsymbol{X} + \boldsymbol{u}) \quad \textbf{(Equation 2)}$$

$$\boldsymbol{u}(z, t_m) = \boldsymbol{x}(z, t_m) - \boldsymbol{X}(z, t_m) \quad \textbf{(Equation 3)}$$

The stretch ratio in the lateral and axial directions are given by the ratio of the vector components in the initial reference and mature deformed states.

$$\lambda_r(\boldsymbol{X}, \boldsymbol{F}) = \frac{x_r(\boldsymbol{X},\boldsymbol{F})}{X_r} \quad \textbf{(Equation 4)}$$

$$\lambda_z(\boldsymbol{X}, \boldsymbol{F}) = \frac{x_z(\boldsymbol{X},\boldsymbol{F})}{X_z} \quad \textbf{(Equation 5)}$$

Within the initial area, collagen has a predominant orientation which varies with depth and age. Assume that at an initial time, $t_0 = 0\ days$, there is a CNO of $\theta_0(\boldsymbol{X})$. As the continuum is growing, according to $\boldsymbol{F}$, the CNO, $\theta(\boldsymbol{X}, \boldsymbol{F})$, changes accordingly relative to the orientation at the reference state $\big(\theta_0(\boldsymbol{X})\big)$ (**Eqn. 6**).

$$\tan\big(\theta(\boldsymbol{X}, \boldsymbol{F})\big) = \frac{\lambda_z(\boldsymbol{X},\boldsymbol{F})}{\lambda_r(\boldsymbol{X},\boldsymbol{F})}\tan(\theta_0(\boldsymbol{X})) \quad \textbf{(Equation 6)}$$

For numerical analysis of mouse MFC growth, we assume the following. (1) The initial AC area is 100 μm wide in the lateral direction ($\hat{\imath}$) tangential to the articular surface and extends 50 μm deep from the articular surface towards the bone-cartilage interface in the axial direction ($\hat{k}$). (2) The initial CNO varies with depth, becoming increasingly perpendicular relative to the surface, from a predominant orientation angle of 10° at the articular surface, and 45° at a depth of 50 μm.

To determine the extent to which the kinematics of axial and lateral expansion, individually and in combination, in accordance with the growth of the mouse MFC, may explain observed changes in CNO several deformation cases were studied. First, the effect of uniform deformations consisting of (1) only axial, (2) only lateral, and (3) axial and lateral deformation in combination

on CNO were assessed.

Depth-varying axial and deformations were also assessed. The superficial zone, which makes up the initial ~10% of the cartilage thickness near the surface, [9] and the deep zones have varying biosynthetic capacities reflecting their differing functional roles. The biosynthetic capacity of the deep zone is particularly enhanced and is necessary to form and maintain the dense cartilaginous matrix.[10,11] There is also evidence that collagen fibrils in the superficial zone are interwoven with perichondral structures.[12] Tensioning of these fibrils during growth may lead to increasing CN alignment near the surface as the joint grow and contribute to cartilage split line behavior.[13,14] Thus, the effect of (4) depth-varying axial deformation, where zero axial stretch occurs at the surface and increases exponentially, in the form of a bounded exponential, toward the deeper tissue was assessed. The effect of (5) depth-varying lateral deformation, where maximal lateral stretch occurs at the surface and decreases linearly with depth was assessed. These depth-varying deformations were also assessed (6) in combination.

5.3.3.Sample Preparation

All animal care and use protocols were approved by the Institutional Animal Care and Use Committee (IACUC) of the University of California San Diego. All animals received an intraperitoneal injection of a fatal dose of Ketamine/Xylazine cocktail. Following complete anesthesia, animals received a transcardial perfusion of PBS followed by 4% PFA. Following perfusion, specimens were skinned, eviscerated, immersed in graded ethanol (EtOH) / PBS solutions up to 70% EtOH, and the hindlimbs dissected at the hip-joint and stored in 70% EtOH at 4˚C.

5.3.4. Microcomputed tomography (μCT) and phosphotungstic acid staining

Each hindlimb was scanned by μCT at $(9\ \mu m)^3$ isotropic voxel resolution (SkyScan 1076;

SkyScan. Kontich, Belgium; 50 kVp, 200 μA, 0.5 mm aluminum filter, 180° scan, Δ=0.8°) before and after staining with phosphotungstic acid (PTA). Hindlimbs were stained with PTA (0.7% w/v in 70%EtOH) at room temperature with gentle agitation for up to 2 weeks, then equilibrated with graded EtOH/PBS solutions to PBS before imaging. Images were reconstructed using NRecon (Bruker, Belgium). Non-contrast (NC) images were reconstructed with a smoothing factor of 1, ring artifact reduction factor of 6, beam hardening correction factor of 40%, and with a dynamic range from 0 to 0.11 attenuation units. PTA image datasets were reconstructed similarly, with a dynamic range from 0 to 0.20 attenuation units.

5.3.5. Measurement of tissue structure and geometry from μCT

To assess MFC geometry, 2D images of PTA-stained MFCs in the mid-condylar sagittal plane were imported into MATLAB (MathWorks, Inc., Natick, MA). From each image, the contour of the articular surface and bone-cartilage interface were manually traced and fitted to an ellipse (**Fig. 2**). Geometrical parameters of the ellipse were determined (**Table 1**) as the elliptical radii along the anterior-posterior axis (semi-major) and proximal-distal axis (semi-minor). From the trace of the articular surface, the perimeter of the MFC was calculated (P^{MFC}). The average cartilage thickness (H^{AC}) was estimated from the average of the differences between the radii of the articular surface and bone-cartilage interface in the anterior-posterior direction and proximal-distal direction. For modeling, maximal stretches were limited in the circumferential direction (**Eqn. 7**) and axial direction (**Eqn. 8**).

$$\max(\lambda_r) = \frac{\lim_{t \to t_m} P_{MFC}(t)}{\lim_{t \to t_o} P_{MFC}(t)} \qquad \textbf{(Equation 7)}$$

$$\max(\lambda_z) = \frac{\lim_{t \to t_m} R_{MFC}^{ProDis}(t)}{\lim_{t \to t_o} R_{MFC}^{ProDis}(t)} \qquad \textbf{(Equation 8)}$$

5.3.6.Statistics

The effect of age on MFC geometry was analyzed by non-linear regression with GraphPad Prism 10.0.2. Measures were fit by least-squares regression to a linear or logistic function of the forms $Y(t) = mt + b$, or $Y(t) = \frac{Y_M Y_0}{(Y_M - Y_0)e^{-kt} + Y_0}$. $Y(t)[\mu m]$ is the property value with respect to age and t $[days]$ is the animal age, $m\left[\frac{\mu m}{day}\right]$ is the slope, b $[\mu m]$ is the intercept, $Y_M[\mu m]$ is the property value at maturity, $Y_0[\mu m]$ is the property value at birth, and k $\left[\frac{1}{day}\right]$ is the growth rate constant. Logistic and linear fits were compared with the Extra Sum-of-Squares F test to select the simpler model unless $p<0.05$ in which case both models were considered.

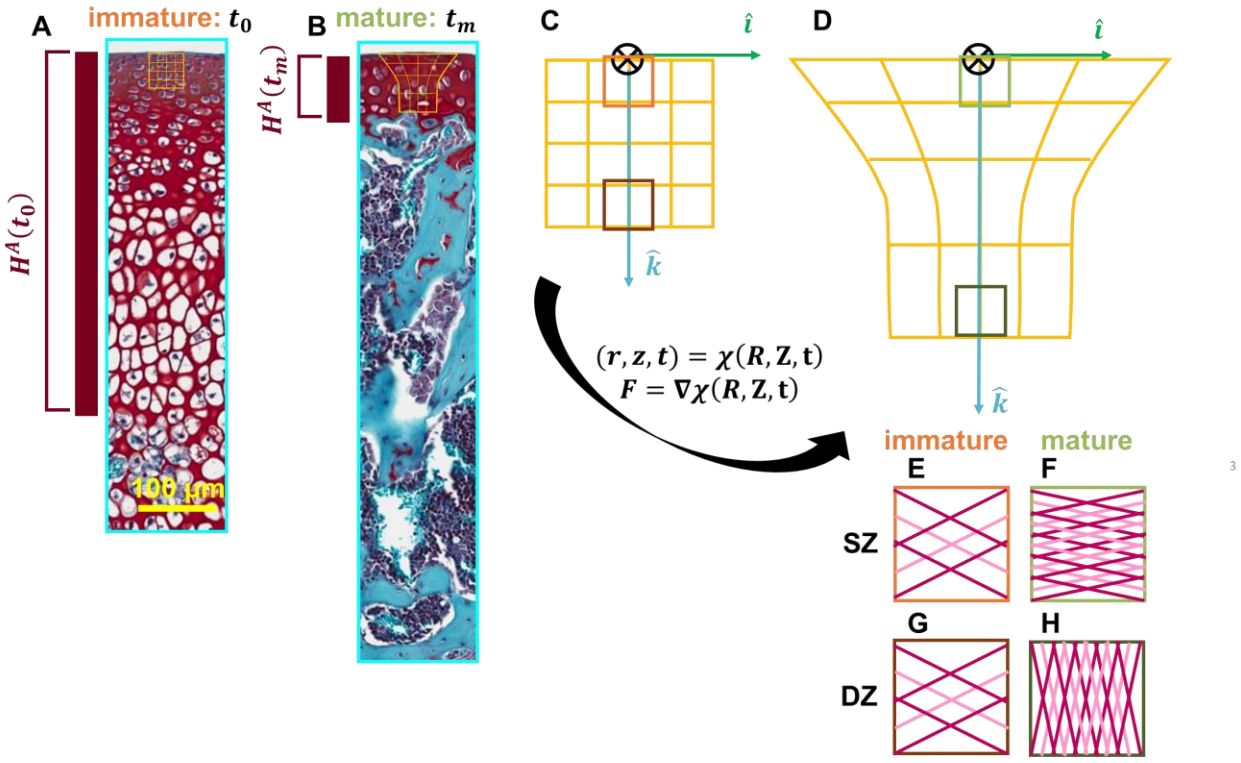


Figure 5.1. Schematic model of collagen reorientation during growth. Safranin O/Fast Green histology of murine femoral condyle in the (**A**) immature and (**B**) mature state. The (**C**) initial and (**D**) mature configurations and effect on superficial (**E,F**) and deep (**G,H**) collagen orientations in the (**E,G**) immature and (**G,H**) mature states.

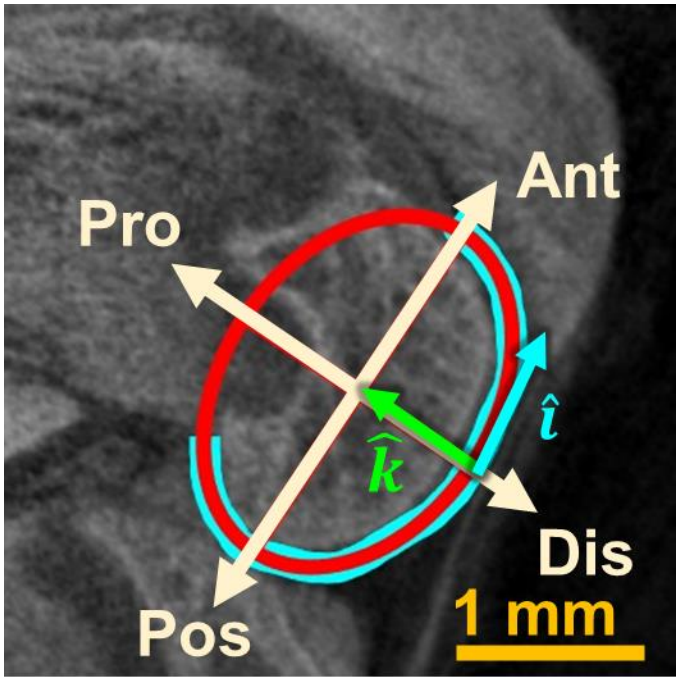


Figure 5.2. The elliptic fit of the murine medial femoral condyle. The proximal-distal direction defines the axial coordinate (k) that is orthogonal to the anterior-posterior direction. The lateral coordinate (i) is tangential to the articular surface.

Table 5.1. MFC shape parameters from ellipse fit.

Parameter	Unit	Description
$R_{MFC}^{AntPost}$	[μm]	Radius of the MFC, at the articular surface, in the anterior-posterior direction
R_{MFC}^{ProDis}	[μm]	Radius of the MFC, at the articular surface, in the proximal-distal direction
P_{MFC}	[μm]	Perimeter of the MFC, at the articular surface
$R_{SOC}^{AntPost}$	[μm]	Radius of the SOC, at the bone-cartilage interface, in the anterior-posterior direction
R_{SOC}^{ProDis}	[μm]	Radius of the SOC, at the bone-cartilage interface, in the proximal-distal direction
P_{SOC}	[μm]	Perimeter of the SOC, at the bone-cartilage interface
H_{AC}	[μm]	Cartilage thickness

5.4. Results

5.4.1. Quantification of murine femoral condyle growth

PTA staining enabled visualization of AECC at all time points. Initially, at d0, the distal femoral epiphysis was radiolucent (**Fig. 3**), and visible only in PTA-stained μCT images (**Fig. 4**). The SOC became radiolucent at P7, and the epiphysis increased rapidly in size during postnatal growth.

The perimeter and radii of the medial femoral condyle at the articular surface (**Fig. 5A-C**) increased logistically, with time constants of ~5-6 days. The MFC increased ~250% between immature and immature values for the perimeter and both the anterior-posterior and proximal-distal directions. The perimeter and radii of the medial femoral condyle along the cartilage-bone interface at the secondary ossification center (**Fig. 5D-F**) also increased logistically, with time constants of ~3 days. The cartilage thickness (**Fig. 6**) decreased logistically, from an initial thickness of ~450 μm to a mature thickness of ~50 μm. In general, gross measures of the MFC during postnatal maturation were similar between males and females.

5.4.2.Depth-varying axial and lateral deformation yield mature-like collagen network orientations

Relative to the initial immature cartilage area (**Fig. 7A**), application of homogeneous axial or lateral deformation caused changes in CNO but did not achieve that of the adult state. Application of homogeneous axial deformation to 250% resulted in a corresponding increase in thickness, and thus area, by 250% (**Fig. 7B**) and CNOs which are more perpendicular, relative to the articular surface with CNO increasing from 10° to ~65° at the surface and from 45° to 70° in the deeper cartilage.

Application of homogeneous lateral deformation of 250% resulted in corresponding increases in width and area of the initial cartilage area by 250%, but results in CNOs which are

more tangential to the articular surface, reorienting the CN to ~5° at the surface and ~20° in the deeper cartilage (**Fig. 7C**).

Simultaneous application of homogeneous axial and lateral deformations, each by 250%, resulted in similar increases in thickness and width, and an increase in area of 625% (**Fig. 7D**). However, in contrast to effects on CNO of isolated axial and lateral deformations, application of homogeneous and equal axial and lateral deformations did not change CNO, relative to those of the immature state.

In contrast, inhomogeneous depth-varying axial and lateral deformations yielded CNO resembling that of the classical adult state. Application of an axially-directed deformation gradient, in which stretch increased exponentially with depth, reaching an overall 250% stretch resulted in a corresponding increase in thickness, and thus area, by 250% (**Fig. 7E**). The CNO at the surface was largely unchanged, and became more perpendicular, relative to the articular surface, with depth. Application of a laterally-directed deformation gradient in which stretch decreased linearly with depth from 250% lateral stretch at the surface and 0% lateral stretch in the deeper tissue, resulted in deformation of the initial rectangular cartilage area into a trapezoidal shape that was 175% larger in area relative to the initial immature state, without a change in thickness (**Fig. 7F**). Here, the CNO became more tangential to the articular surface at the surface, but was relatively unchanged in the deeper tissue. In contrast, simultaneous application of these strain gradients resulted in a trapezoidal shape that was 187% larger in area due to an increase in width and thickness (**Fig. 7G**). Here, relative to the immature state, the CNO achieved a mature-like architecture, more tangentially oriented near the surface, ~1°, and increasingly perpendicular, ~70°, in the deeper tissue.

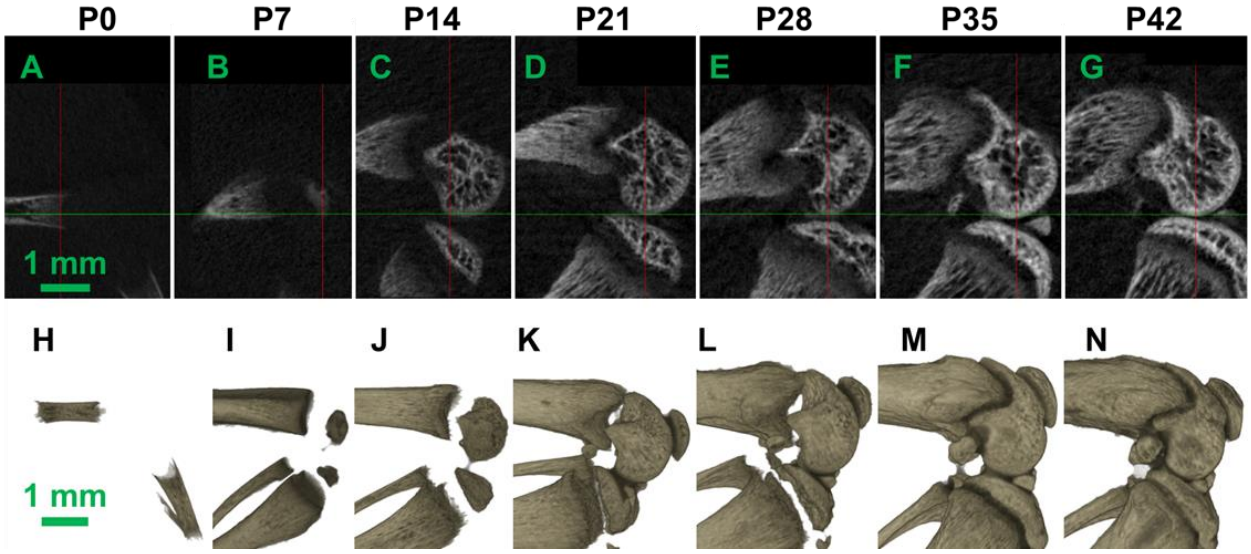


Figure 5.3. Maturation of the murine MFC. (**A-G**) Sagittal images and (**H-N**) 3D renders of the MFC at (**A,H**) P0, (**B,I**) P7, (**C,J**) P14, (**D,K**) P21, (**E,L**) P28, (**F,M**) P35, and (**G,N**) P42.



Figure 5.4. PTA-stained murine MFC during postnatal maturation

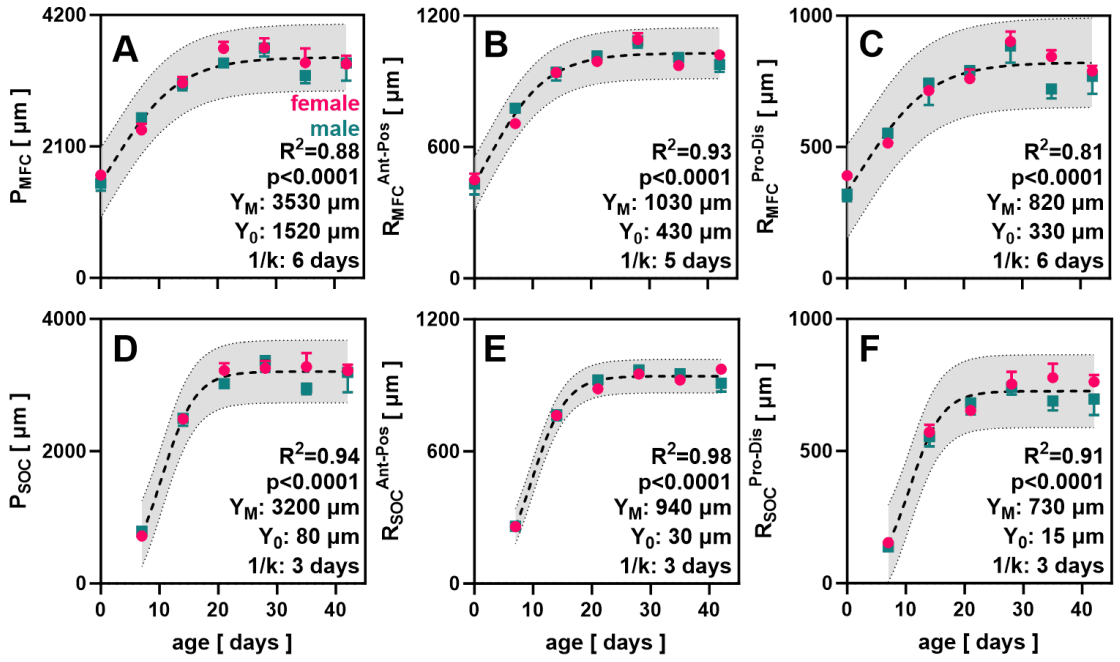


Figure 5.5. Effect of maturation on gross measures of the MFC. Gross measures of the MFC at the (**A-C**) articular surface and at the (**D-F**) bone-cartilage interface. (**A,D**) Perimeter. (**B,F**) Radius in the anterior-posterior direction, (**C,F**) Radius in the proximal-distal direction. Dashed line indicates logistic fit with 95% confidence interval shaded.

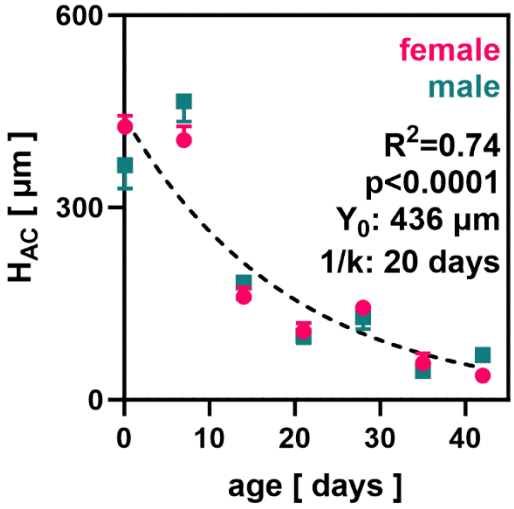


Figure 5.6. Effect of maturation on cartilage thickness. Dashed line indicates logistic fit

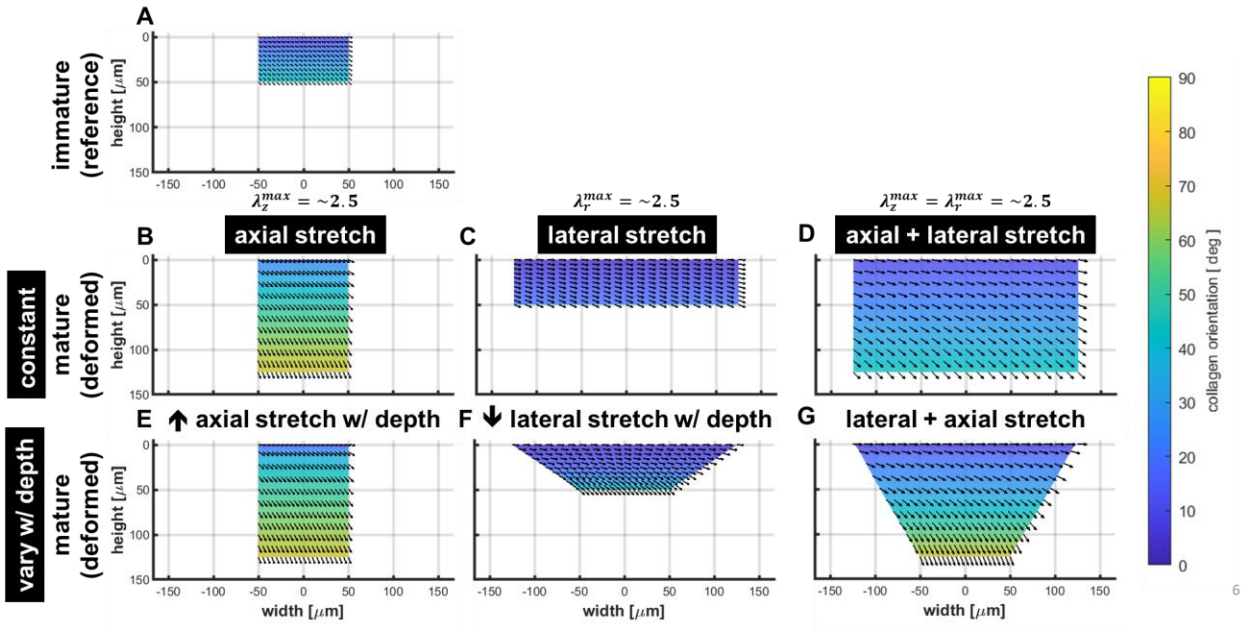


Figure 5.7. Effect of deformation on collagen network. (**A**) Initial immature state. Mature state after constant (**B**) axial stretch, (**C**) lateral stretch, and (**D**) combined axial and lateral stretch. Mature state after depth-varying (**E**) axial stretch, (**F**) lateral stretch, and (**G**) combined axial and lateral stretch.

5.5. Discussion

This combined theoretical and experimental study evaluated whether the change in CNO associated with maturation of articular cartilage could be attributed to kinematic reorientation with mouse MFC as a model system. The MFC is only one of many articulating joint surfaces, but it is one that is frequently afflicted with osteoarthritis,[15] and thus of translational importance. The approach of constraining the kinematic input to the theoretical model evaluated the final grown state, but it could be expanded to evaluate the time-variation in CNO, based on the time-course of mouse MFC growth, the model assumed that CNO was only affected by kinematics, and not other mechanical or biological processes. Overall, a similar combination of theoretical and experimental analysis could be applied to other joint surfaces and other animal models.

Our experimental analyses extend and support the observation that the murine femoral condyles attain their mature state within ~30 days of birth. Coincident with maturation-related variations in CNO, gross measures of the MFC at the articular surface and at the bone-cartilage interface of the developing SOC increase rapidly within the first week after birth and reach the stable mature value by P21 (**Fig. 5**). The formation of the SOC and zonal collagen architecture, within 5-10 days postnatal,[6] coincides with the age at which mice begin to transition from crawling to walking.[16] After P21, the continued thinning of cartilage (**Fig. 6**) is associated with formation and consolidation of the calcified cartilage layer and skeletal maturation.[7,9,17]

The kinematic model, predicting change in CNO, depends on both the initial state of the tissue as well as the imposed kinematics. In mice, incipient articular cartilage at birth, P0, is ~50 μm thick, and is composed of 6-7 highly cellular cell layers.[2] During the perinatal period, the collagen fibrils are generally tangential with the articular surface, and this alignment extends to ~150 μm at P5.[6] During early postnatal maturation, the articular cartilage increases in thickness and achieves a zonal architecture by P12.[6] Accordingly, by P14, gross measures of the MFC at the

articular surface and at the bone-cartilage interface have reached ~90% of their mature value (**Fig. 5**). Thus, exact model predictions would depend on assumptions about the immature AC that evolves into the adult AC.

Analysis with this kinematic model identified hypothetical two-dimensional deformation gradients which transform CNO from the immature to mature state. Maximal axial and lateral deformations were constrained by observations of the MFC growth at the articular surface and bone-cartilage interface. The results suggest that AC undergoes depth-varying axial and lateral deformation during postnatal growth and maturation. Such axial growth may be driven by depth-varying deposition of proteoglycan,[18] while such lateral growth may be governed by appositional circumferential addition of cartilage emanating from the Node of Ranvier.[19]

The growth model could be refined to include a combination of elastic and residual stress and strain.[20-24] Reorientation of the CN due to increases in MFC size, implies nonuniform growth and remodeling which influences the residual stresses within the tissue.[8,25,26] Additional studies are required to elucidate the effects of alterations in tissue biophysical state during maturation, due to variations in CNO, as well as content of collagen and proteoglycan. For example, *in vitro* curling behavior of articular cartilage may change due to maturation-related variation in the balance of proteoglycan swelling and the collagen restraining during growth.[27] Conversely, mechanical loading may induce changes in cartilage shape.[28]

Depth-varying axial and lateral deformations also can directly impact tissue cellularity with a growth-associated expansion of tissue associated with a reduction in cellularity. In mice, the incidence of proliferating cells in the articular cartilage is greatly diminished within two weeks postnatal.[2] Accordingly, between P7 and 1 month, cell density decreases from ~1.25 to ~60 million cells/mm^3,[29] which in the absence of proliferation, may be attributed to an increase in tissue volume

of ~200%. In addition, axial growth that is enhanced in the deeper cartilage, compared to near the articular surface, may contribute to the relative scarcity of cells in that region. Further analysis could relate kinematic growth to variations in cellularity.

Overall, this study quantified murine femoral condyle growth and its implications for cartilage maturation. Depth-variation in axial and lateral articular cartilage growth may contribute to kinematic reorientation of the CN from the immature to mature configuration. Concentrated lateral growth near the articular surface may contribute to the overall increase in cartilage surface area during maturation. In addition, growth of the articular cartilage, particularly depth-variation in the axial direction, may also contribute to depth-variation in cellular organization.

5.6. Acknowledgements

Thanks to Ceri J. Weber and Kimbler L. Cooper of the Cooper Lab in the Department of Cell and Developmental Biology at the University of California, San Diego who provided murine specimens for analysis. This work was supported by NSF GRFP and the Wu Tsai Human Performance Alliance.

5.7. References

1. Carlson CS, Hilley HD, Henrikson CK: Ultrastructure of normal epiphyseal cartilage of the articular-epiphyseal cartilage complex in growing swine. *Am J Vet Res.* 1985;46:306-13.

2. Decker RS, Um HB, Dyment NA, Cottingham N, Usami Y, Enomoto-Iwamoto M, Kronenberg MS, Maye P, Rowe DW, Koyama E, Pacifici M: Cell origin, volume and arrangement are drivers of articular cartilage formation, morphogenesis and response to injury in mouse limbs. *Dev Biol.* 2017;426:56-68.

3. Decker RS, Koyama E, Pacifici M: Genesis and morphogenesis of limb synovial joints and articular cartilage. *Matrix Biol.* 2014;39:5-10.

4. Rieppo J, Hyttinen MM, Halmesmaki E, Ruotsalainen H, Vasara A, Kiviranta I, Jurvelin JS, Helminen HJ: Changes in spatial collagen content and collagen network architecture in porcine articular cartilage during growth and maturation. *Osteoarthritis Cartilage.* 2009;17:448-55.

5. Julkunen P, Iivarinen J, Brama PA, Arokoski J, Jurvelin JS, Helminen HJ: Maturation of collagen fibril network structure in tibial and femoral cartilage of rabbits. *Osteoarthritis Cartilage.* 2010;18:406-15.

6. Hughes LC, Archer CW, ap Gwynn I: The ultrastructure of mouse articular cartilage: collagen orientation and implications for tissue functionality. A polarised light and scanning electron microscope study and review. *Eur Cell Mater.* 2005;9:68-84.

7. van Turnhout MC, Schipper H, Engel B, Buist W, Kranenbarg S, van Leeuwen JL: Postnatal development of collagen structure in ovine articular cartilage. *BMC Dev Biol.* 2010;10:62.

8. Skalak R: Growth as a finite displacement field. In *Proceedings of the IUTAM Symposium on Finite Elasticity, 1981*. Martinus Nijhoff, The Hague.

9. Hunziker EB, Kapfinger E, Geiss J: The structural architecture of adult mammalian articular cartilage evolves by a synchronized process of tissue resorption and neoformation during postnatal development. *Osteoarthritis Cartilage.* 2007;15:403-13.

10. Eger W, Schumacher BL, Mollenhauer J, Kuettner KE, Cole AA: Human knee and ankle cartilage explants: catabolic differences. *J Orthop Res.* 2002;20:526-34.

11. Poole AR, Rosenberg LC, Reiner A, Ionescu M, Bogoch E, Roughley PJ: Contents and distributions of the proteoglycans decorin and biglycan in normal and osteoarthritic human articular cartilage. *J Orthop Res.* 1996;14:681-89.

12. Clark JM: The organisation of collagen fibrils in the superficial zones of articular cartilage. *J Anat.* 1990;171:117-30.

13. Bae WC, Wong VW, Hwang J, Antonacci JM, Nugent-Derfus GE, Blewis ME, Temple-Wong MM, Sah RL: Wear-lines and split-lines of human patellar cartilage: relation to tensile biomechanical properties. *Osteoarthritis Cartilage.* 2008;16:841-5.

14. Below S, Arnoczky SP, Dodds J, Kooima C, Walter N: The split-line pattern of the distal femur: A consideration in the orientation of autologous cartilage grafts. *Arthroscopy.* 2002;18:613-7.

15. Bae WC, Payanal MM, Chen AC, Hsieh-Bonassera ND, Ballard BL, Lotz MK, Coutts RD, Bugbee WD, Sah RL: Topographic patterns of cartilage lesions in knee osteoarthritis. *Cartilage.* 2010;1:10-19.

16. Williams E, Scott JP: The development of social behavior patterns in the mouse, in relation to natural periods. *Behaviour.* 1953;6:35-65.

17. Chan EF, Harjanto R, Asahara H, Inoue N, Masuda K, Bugbee WD, Firestein GS, Hosalkar HS, Lotz MK, Sah RL: Structural and functional maturation of distal femoral cartilage and bone during postnatal development and growth in humans and mice. *Orthop Clin North Am.* 2012;43:173-85.

18. DiMicco MA, Sah RL: Dependence of cartilage matrix composition on biosynthesis, diffusion, and reaction. *Transport Porous Media.* 2003;50:57-73.

19. Karlsson C, Thornemo M, Henriksson HB, Lindahl A: Identification of a stem cell niche in the zone of Ranvier within the knee joint. *J Anat.* 2009;215:355-63.

20. Klisch SM, Chen SS, Sah RL, Hoger A: A growth mixture theory for cartilage with applications to growth-related experiments on cartilage explants. *J Biomech Eng.* 2003;125:169-79.

21. Rodriguez EK, Hoger A, McCulloch AD: Stress-dependent finite growth in soft elastic tissues. *J Biomech.* 1994;27:455-67.

22. Taber LA: Biomechanics of growth, remodeling, and morphogenesis. *Appl Mech Rev.* 1995;48:487-545.

23. Menzel A, Kuhl E: Frontiers in growth and remodeling. *Mech Res Commun.* 2012;42:1-14.

24. Humphrey JD: Constrained mixture models of soft tissue growth and remodeling - Twenty years after. *J Elast.* 2021;145:49-75.

25. Fung YC, *Biomechanics: Motion, Flow, Stress, and Growth*. 1981, New York: Springer-Verlag. pp. 499-546 pp.

26. Skalak R, Gasgupta G, Moss M, Otten E, Dullemeijer P, Vilmann H: Analytical description of growth. *J Theor Biol.* 1982;94:555-77.

27. Wan LQ, Guo XE, Mow VC: A triphasic orthotropic laminate model for cartilage curling behavior: fixed charge density versus mechanical properties inhomogeneity. *J Biomech Eng.* 2010;132:024504.

28. Williams GM, Lin JW, Sah RL: Cartilage reshaping via in vitro mechanical loading. *Tissue Eng.* 2007;13:2903-11.

29. Li L, Newton PT, Bouderlique T, Sejnohova M, Zikmund T, Kozhemyakina E, Xie M, Krivanek J, Kaiser J, Qian H, Dyachuk V, Lassar A, Warman ML, Barenius B, Adameyko I, Chagin A: Superficial cells are self-renewing chondrocyte progenitors, which form the articular cartilage in juvenile mice. *FASEB J.* 2016;31:1067-84.

CHAPTER 6

ARTICULAR CARTILAGE EXPLANT GROWTH IS DEPTH-VARYING, REGULATED, AND MEDIATED BY EXTRACELLULAR MATRIX

6.1. Abstract

The objectives of this study were to assess the depth-varying growth kinematics of immature calf cartilage explants and quantify effect of enhanced matrix catabolism and modulation of tissue swelling pressure. Immature cartilage half-discs were cultured up to 2 weeks and tissue displacement and strain during growth were calculated by relative motion of cell nuclei at the vertical cut surface. Chondrocyte phenotype was regulated during culture by stimulation with TNF-α. The effect of matrix structure and content was investigated removal of cartilage proteoglycans by C-ABC and inhibition of the formation of lysyl oxidase mediated collagen crosslinks with BAPN. Explant growth was time- and space- varying, stimulated by treatment with BAPN, and inhibited by treatment with TNF-α and C-ABC. Overall explant growth is primarily attributed to an increase in explant height during culture occurring mostly within the superficial ~300 μm. Manipulation of tissue swelling pressure had depth-varying effects on cartilage explant growth. Depth-varying growth during maturation may allow for concurrent expansion of the tissue near the articular surface and maturation of the deeper regions. The intrinsic depth-varying properties of AC may predispose the tissue to anisotropic and heterogenous growth in vitro.

6.2. Introduction

Articular cartilage (AC) growth and maturation is associated with age- and depth-dependent variation in tissue composition, structure, and function. During in vivo growth, the extracellular matrix, including collagen and proteoglycan, are synthesized and remodeled by indwelling chondrocytes to increase the overall tissue density and volume, and to achieve functional maturation.[1,2]

The cell and matrix properties of mature AC vary as a function of depth from the articular surface. Mature AC has three characteristic zones: the superficial (tangential) zone (~10%), the middle (transitional) zone (~10%), and the deep (radial) zone (~80%), which comprises most of the tissue thickness.[3] In particular, cell organization varies with depth, is particularly dense near the surface and organized into horizontal clusters, and becomes sparse deeper into the tissue with vertical columns of cells present.[4,5]

It is unclear how immature tissue progresses to the mature state. In general, immature AC is characterized as a highly cellular and relatively homogenous tissue compared to the mature state.[4,5] Depth- and maturation- related AC compositional and structural properties may arise due to growth-associated tissue strain imparted as the joint increases in size as well as directed (i.e. depth-varying) cell fate and metabolic processes which affect cell and matrix content and distribution. [6,7]

Growth of tissues have been analyzed by tracking motion of intrinsic or extrinsic surface markers. Cartilage growth occurs in vitro,[8] with cell death at the cut surfaces,[9] and these cells have been utilized as intrinsic markers for bulk deformation during growth.[10] Within AC, tissue biophysical properties are governed by the balance between the restraining ability of the collagen network, facilitated by collagen crosslink formation, and the swelling pressure imbued by the negatively charged proteoglycan aggregates.[11,12] Disrupting the balance between these forces in

favor of the swelling pressure is allows tissue growth,[13,14] although the nature of this growth throughout the tissue is unknown.

The specific depth-dependent properties of AC that exist in immature tissue may predispose it to characteristic depth-varying growth deformations during in vitro culture. The hypothesis of this study is that (1) in vitro growth deformation varies from the articular surface to the deep regions and (2) this growth deformation is affected by selective alteration of the content or assembly of ECM components. The objectives of this study were (1) to assess the depth-varying growth kinematics of AC explants in vitro by tracking chondrocyte nuclei and quantify effect of (2) enhanced matrix catabolism and (3) modulation of tissue swelling pressure by (a) inhibition of collagen crosslink formation and (b) depletion of GAGs on depth-dependent in vitro growth deformation.

6.3. Methods

6.3.1. Study Design

Cartilage was prepared, AC discs harvested, cultured up to 15 days in media with additives, and imaged on days 2, 8, and 15 to determine the effect of treatment on growth (**Fig. 1**). Specifically, AC half-discs (2.5 mm diameter, 1 mm thick), with intact articular surface, from immature (N=3 animals, 1-3 weeks old) were harvested from the medial femoral condyle. AC half-discs were pre-treated for 2 days with media (n=24), media supplemented with CABC (n=6), to remove GAGs, or BAPN (n=6), to inhibit collagen crosslinking, and then labeled with Ethidium Homodimer and cultured up to 16 days in media with and without BAPN. A subset of discs (n=12) were terminated and assessed for tissue biochemical content after pre-treatment in media. Cultured half-discs were imaged to assess overall explant growth and cellular displacement on days 2, 8, and 15. After culturing, the remaining half-discs (n=24) were assessed for tissue biochemical content.

6.3.2. Sample Preparation and Culture

Half-discs were incubated for 2 days in media (n=36, DMEM supplemented with 10% FBS, 50 ug/ml ascorbate, 10 mM HEPES, 0.1 mM NEM, 0.4 mM L-proline, 2 mM L-glutamine, 100 U/ml penicillin, 100 ug/ml streptomycin, 0.25 ug/ml amphotericin B), media with 0.1 mM β-aminopropionitrile (Sigma, St. Louis, MO.) to inhibit lysyl oxidase mediated collagen crosslinking (‘BAPN’, n=6), or media with 0.5 U/ml protease-free chondroitinase-ABC (C-ABC) (Associates of Cape Cod, East Falmouth, MA) to deplete glycosaminoglycans (‘C-ABC’, n=6). A subset of discs was terminated and assessed for tissue biochemical content after pre-treatment in media (‘initial’, n=12).

After 2 days, each half-disc was rinsed with media and labeled with pre-warmed PBS

containing 0.5 mM Ethidium Homodimer (EtH; 60 ul/sample), a fluorescent nuclear label that penetrates the cell membranes of dead cells. Half-discs were incubated for an additional 14 days (up to 16 days after harvest) in media ('media', n=12; 'C-ABC', n=6) as well as media supplemented with 0.01% BSA, ('basal', n=6) and 25 ng/ml TNF-α ('TNF-α', n=6). Samples originally cultured with BAPN, continued to be supplemented with BAPN throughout the culture duration ('BAPN', n=6).

6.3.3.Imaging and Image Analysis

Fluorescence images were analyzed to determine macroscopic growth and inter-tissue growth strains. Upon imaging, AC half-discs were oriented such that the imaging plane was the cut surface that is perpendicular to the articular surface, such that the full thickness (superficial to deep) of the explant is visualized. Images were imported into MATLAB (MathWorks, Inc., Natick, MA), and rotated to a standard orientation, with the articular surface parallel to the horizontal image axis. The midpoint of the two superficial corners at the articular surface were used as a reference to establish an orthogonal coordinate system (r, z) such that the r-axis is the horizontal line defined by the superficial corners (-1250 μm < r < 1250 μm), and the z-axis extends from the articular surface towards the deep tissue (0 μm < z < ~1000 μm).

Macroscopic tissue growth was assessed by measuring tissue thickness (superficial to deep) and tissue width, each at three locations across the explant cut surface. The area of the imaged tissue face was also calculated.

To assess spatial variations in cartilage growth, images from day 2 and day 8 of culture were analyzed. Cell displacements were assessed based on visibility of EtH-labeled cell nuclei at Day 2 and Day 8. Images were processed to determine displacement of fluorescently tagged cells as an indicator of local strain due to growth over the culture duration. Images were further

processed to enhance contrast of cells relative to background using a 17x17 pixel Mexican Hat filter with σ equal to 2.8 and thresholding to binarize at 0.1 standard deviation from the highest pixel intensity based on the image histogram. In this way, objects of comparable size and shape to cell nuclei with a high intensity were enhanced. A set of ~60-100 stained cell nuclei were identified and marked in each image pair. Nuclei were chosen based on visibility at both time points, spanning the entire sample face, and included points at or near the tissue surfaces. The lateral and axial displacements, $u_r(r,z)$ and $u_z(r,z)$, of each nucleus was determined for each image relative to the day 2 image.

Growth strains were calculated from displacement data by interpolation and calculation of the displacement gradient. The raw displacement data was interpolated by cubic interpolation to form continuous displacement fields, $u_r(r,z)$ and $u_z(r,z)$, with points spaced at 20 μm increments in the r and z directions. The gradient of each of these fits was found and the strain calculated at 20 μm increments in the lateral (r) direction $\left(\varepsilon_{rr}(r,z) = \frac{\partial u_r}{\partial r}\right)$, in the axial (z) direction $\left(\varepsilon_{zz}(r,z) = \frac{\partial u_z}{\partial z}\right)$ and in shear. $\left(\varepsilon_{rz}(r,z) = \frac{1}{2}\left(\frac{\partial u_r}{\partial z} + \frac{\partial u_z}{\partial r}\right)\right)$ The average strain was calculated in 100 μm bins, (1) as a function of lateral distance (r) from the center of the disk to within ~100 μm mm of the disk edge, and (2) with depth from the articular surface (z) to within ~100 μm of the deep surface.

6.3.4. Biochemical Analysis

Water, sGAG, and DNA content of cartilage samples were assessed from tissue digests. Samples were weighed wet, lyophilized, weighed dry, and solubilized with Proteinase K. Each sample was digested with 20 μl 0.5 mg/ml Proteinase-K in 100mM phosphate and 10 mM EDTA (PBE, pH 7.1) at 60°C for 18 hours, then diluted up to 200 μl with dH2O before freezing. Digests

were stored at -20°C before analysis. Portions of solubilized tissues were used to determine total sulfated GAG,[15] hydroxyproline,[16] and DNA content with Hoechst 33258.[17] The hydroxyproline content was converted to collagen (COL) content assuming a mass ratio of collagen to hydroxyproline of 7.1.[18] The DNA content was converted to cell content assuming a conversion constant of 7.3 pg DNA/chondrocyte (CELL).[19] The total dry mass attributed to the cells was then calculated using a conversion of 0.1 ng dry weight/cell.[20] The residual dry weight (RES) was computed as the remaining dry weight not accounted for by GAG, collagen, or the mass of the cells. The mass of various constituents was expressed normalized to the tissue wet weight.

6.3.5. Statistical Analysis

The effects of matrix perturbation and culture duration on relative changes in tissue explant area, height, and width were assessed by a mixed model analysis with treatment (media, TNF-α, basal, C-ABC, BAPN) as fixed factor, culture duration (2, 8, 15 days) as a fixed repeated factor, and animal as a random factor. The variation of growth strains $(\varepsilon_{rr}, \varepsilon_{zz}, \varepsilon_{rz})$ with depth from the articular surface (z) and lateral position across the explant surface (r) and were similarly assessed with treatment as a fixed factor, depth (10 regions) or lateral position (8 regions) as a fixed repeated factor, and animal as a random factor. The effect of treatment on tissue biochemistry was assessed by univariate general linear model with treatment as a fixed factor (initial, media, TNF-α, basal, C-ABC, BAPN) and animal as a random factor. Post-hoc analysis of treatment as a main effect was assessed by Dunnet's t-test with explants cultured in media alone as the comparison group. Data are presented as the mean±SEM, and significance level was set to 0.05. Statistical analysis was performed using SPSS 28 (IBM), and plotted using GraphPad Prism 10 (GraphPad).

6.4. Results

6.4.1.Effect of Treatment on Overall Explant Growth

During culture, cartilage explants generally increased in size (**Fig. 3**) during culture, and viability was similar between day 2 and day 15 (**Fig 4)**.

The change in area (ΔA, **Fig. 5A**) and height (ΔH, **Fig. 5B**), relative to day 2, varied with treatment ($p<0.001$) and increased with culture duration ($p<0.001$). ΔA and ΔH were reduced in explants treated with C-ABC (ΔA≈ΔH≈0%, $p<0.05$) and TNF-α (ΔA≈ΔH≈0%, $p<0.05$), and enhanced in explants treated with BAPN (ΔA≈ΔH≈15%, $p<0.01$) compared to explants cultured in media alone (ΔA≈ΔH≈7%). Independent of treatment ΔA and ΔH increased by ~8% on day 8, relative to the area and height at day 2. ΔA and ΔH between day 8 and day 15 of culture was not different ($p=1.0$). The change in width (ΔW, **Fig. 5C**) was not affected by treatment ($p=1.0$) nor culture duration ($p=1.0$).

6.4.2.Depth-wise variation in tissue strain

Between day 2 and day 8 of culture, the axial strain ($\varepsilon_{zz}(tmt, z)$, **Fig. 6A**) varied with depth from the articular surface ($p<0.001$) and had slight differences with treatment ($p=0.05$). Independent of location, axial strain tended to be enhanced in explants treated with BAPN ($\varepsilon_{zz}(BAPN) = 14\%$, $p=0.08$), compared to media ($\varepsilon_{zz}(media) = 8\%$). Independent of treatment, axial strain was reduced in the lower two-thirds (300-800 μm) of the explant ($\varepsilon_{zz}(300 - 800\ \mu m) \approx 4\%$, $p<0.05$) compared to the surface layer ($\varepsilon_{zz}(50\mu m) = 18\%$)

Lateral strain ($\varepsilon_{rr}(tmt, z)$, **Fig. 6B**) varied with treatment ($p<0.001$) and depth ($p<0.001$). Independent of location, lateral strain was reduced in explants treated with C-ABC ($\varepsilon_{rr}(CABC) = -0.4\%$, $p=0.003$) and enhanced in explants treated with BAPN ($\varepsilon_{rr}(BAPN) = 1.3\%$, $p=0.001$), compared to media alone ($\varepsilon_{rr}(media) = 0.4\%$). Independent of treatment, lateral strain was

reduced in the lower half (500-800 μm) of the explant ($\varepsilon_{rr}(500-800\,\mu m) \approx -0.4\%$, p<0.001) compared to the surface layer ($\varepsilon_{rr}(50\mu m) = 1\%$).

Shear strain ($\varepsilon_{rz}(tmt, z)$, **Fig. 6C**) did not vary with treatment (p=0.60) nor depth (p=0.08).

6.4.3.Lateral variation in tissue strain

Between day 2 and day 8 of culture, axial strain ($\varepsilon_{zz}(tmt, r)$, **Fig. 7A**) varied with treatment (p<0.001) and lateral position across the explant surface (p<0.001). In dependent of position, axial strain was reduced in explants treated with C-ABC ($\varepsilon_{zz}(CABC) = 0.5\%$, p=0.009), and TNF-α ($\varepsilon_{zz}(TNF) = 1\%$, p=0.015) compared to media ($\varepsilon_{zz}(media) = 9.7\%$). Independent of treatment, axial strain was enhanced in the central part of the explant ($\varepsilon_{zz}(\pm 100\mu m) \approx 8\%$, p<0.05) compared to the edge ($\varepsilon_{zz}(\pm 900\mu m) = 6\%$).

Lateral strain ($\varepsilon_{rr}(tmt, r)$, **Fig. 7B**) varied with treatment (p<0.001), but not lateral position (p=0.29). Independent of location, lateral strain was reduced in explants treated with C-ABC ($\varepsilon_{rr}(CABC) = -0.6\%$, p<0.001) and basal media ($\varepsilon_{rr}(basal) = -0.4\%$, p=0.003), and enhanced in explants treated with BAPN ($\varepsilon_{rr}(BAPN) = -0.6\%$, p=0.006), compared to media ($\varepsilon_{rr}(media) = 0.4\%$)).

Shear strain ($\varepsilon_{rz}(tmt, r)$, **Fig. 7C**) varied with treatment (p=0.04), but not lateral position (p=0.12). However, all treatments had similar shear strains compared to those cultured in media ($\varepsilon_{rz}(media) = -0.5\%$).

6.4.4.Effect of treatment on explant biochemistry

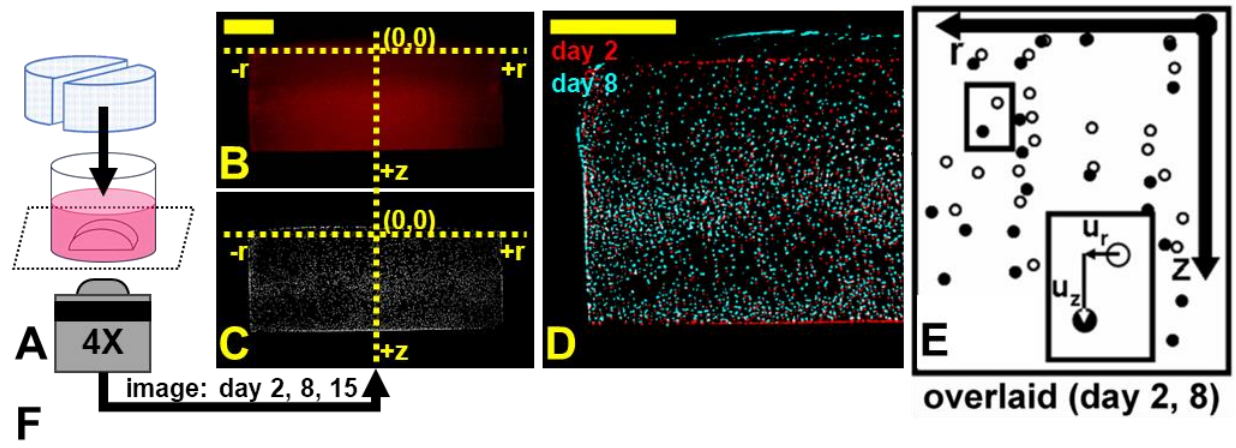
Explant wet weight (**Fig. 8A**), dry weight (**Fig. 8B**), and water content (**Fig. 8C**) varied with treatment (p<0.001). Wet weight (**Fig. 8A**) was reduced in initial control samples (p<0.001), as well as explants cultured and treated with basal conditions (-3%, p=0.03), TNF-α (-34%, p<0.001), and C-ABC (-61%, p<0.001), compared to explants cultured in medial alone (4.7 mg

WW). Similarly, dry weight (**Fig. 8B**) was reduced in initial control samples (-30%, $p<0.001$), as well as in explants cultured and treated with basal media (-19%, $p=0.04$), TNF-α (-22%, $p=0.01$), and C-ABC (-37%, $p<0.001$), compared to those cultured in media alone (0.80 mg DW). Accordingly, water content (**Fig. 8C**) was reduced in explants treated with TNF-α (80% water, $p<0.001$) and enhanced in explants treated with BAPN (86% water, $p<0.001$), compared to those cultured in media alone (83% water)

Treatment affected some measures of absolute mass (**Fig. 8D-G**). Pre-treatment with C-ABC resulted in a ~95% removal of GAG (not shown), compared to initial control samples (~100 μg GAG). After culture, GAG mass (**Fig. 8E**) was reduced in explants treated with TNF (-37%, $p=0.005$) and C-ABC (-63%, $p<0.001$), compared to those cultured in medial alone (110 mg GAG). RES mass (**Fig. 8F**) was reduced in initial control explants (-78%, $p<0.001$) and those cultured under basal conditions basal (-47%, $p<0.001$) and treated with TNF-α (-34%, $p<0.009$), and C-ABC (-57%, $p<0.001$), compared to those cultured in medial alone (360 mg RES). Although the total number of cells (**Fig. 8G**) varied with treatment ($p=0.002$), all groups had similar cell numbers to those cultured in media (~180,000 cells/explant). The total mass of COL (**Fig. 8D**) in each explant was not affected by treatment ($p=0.46$).

Treatment affected all measures of matrix concentration (**Fig. 8H-K**). COL content (**Fig. 8H**) was enhanced in initial control explants (+59%, $p<0.001$) as well as in explants cultured under basal conditions (+39%, $p=0.03$), and treated with TNF-α (+43%, $p=0.02$), and C-ABC (49%, $p=0.01$), compared to those cultured in media alone (68 mg COL/g WW). GAG content (**Fig. 8I**) was enhanced in initial control explants (+31%, $p=0.001$) and reduced those cultured and C-ABC (-41%, $p<0.001$), compared to those cultured in media alone (23 mg GAG/g WW). RES content (**Fig. 8J**) was reduced in initial control samples (-69%, $p<0.001$), as well as in explants cultured

under basal conditions (-33%, p=0.02), and treated with C-ABC (-30%, p=0.04) and BAPN (-35%, p=0.01), compared to those cultured in media alone (78 mg RES/g WW). Cellularity (**Fig. 8K**) was elevated in initial control samples (+67%, p<0.001), and in explants cultured and treated with TNF-α (+29%, p=0.046), and C-ABC (+34%, p=0.02), compared to those cultured in media alone (39 million cells/g WW).



	culture media								
days:	0 - 2				2 - 15				
condition	media	FBS	C-ABC	BAPN	media	FBS	BSA	TNF-α	BAPN
initial	+	+							
media	+	+			+	+			
basal	+	+			+		+		
TNF-α	+	+			+	+		+	
C-ABC	+	+	+		+	+			
BAPN	+	+		+	+	+			+

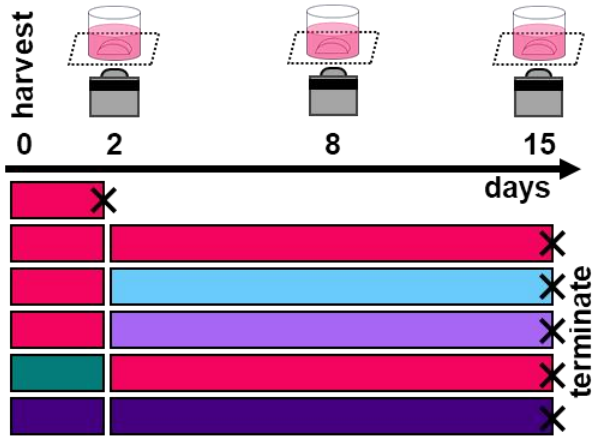


Figure 6.1. Tracking cell displacement in articular cartilage at a cut surface during in vitro growth. (**A**) Schematic of culture and imaging method. Representative (**B**) fluorescent and (**C**) binarized image results at day 2. (**D**) Overlaid binarized images from day 2 (**red**) and day 8 (**cyan**). (**E**) Schematic of marked cells from day 2 (○) and day 8 (●) overlaid, showing relative displacement during *in vitro* growth as a function of distance from center of explant (r) and depth (z). (**F**) Experimental design. Scale bars are 500 μm.

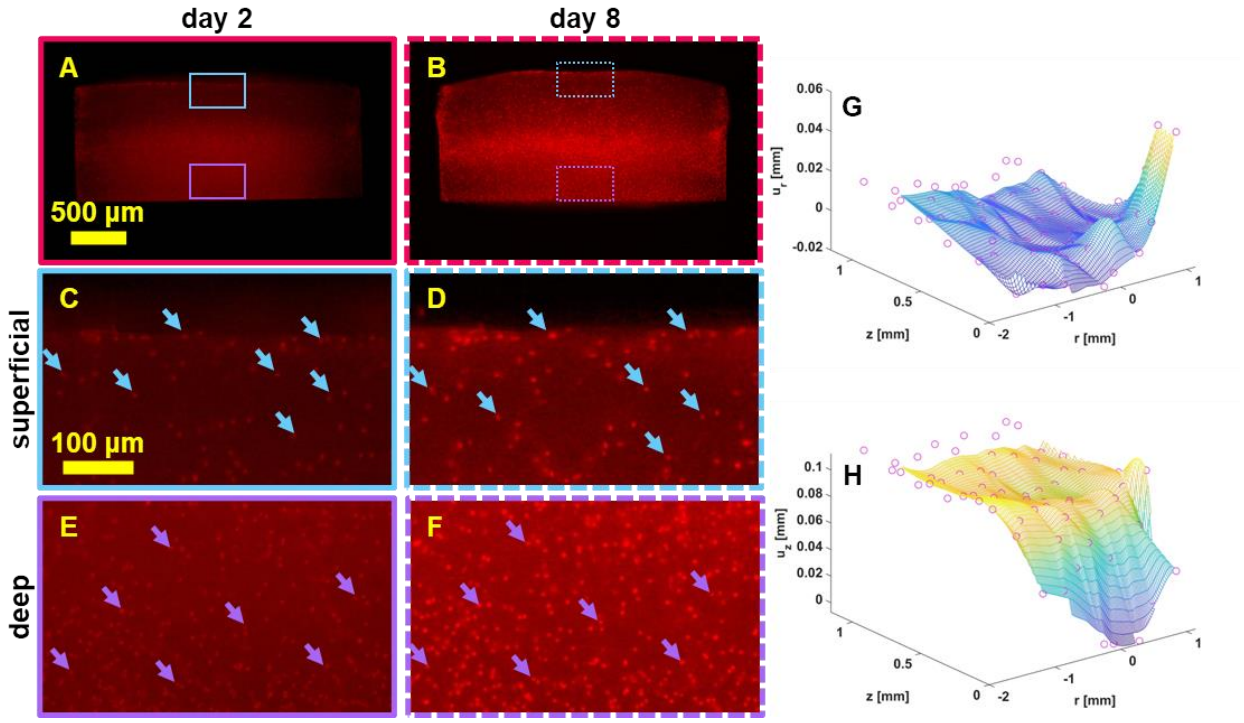


Figure 6.2. Cellular displacements in articular cartilage at a cut surface during in vitro growth. (**A-F**) Images of fluorescently labeled explants at (**A,C,E**) day 2 and (**B,D,F**) day 8. Zoomed images of the (**C,D**) superficial and (**D,F**) deep cartilage. Representative (**G**) lateral (u_r) and (**H**) axial (u_z) displacement maps as a function of distance from the explant center (r) and depth (z).

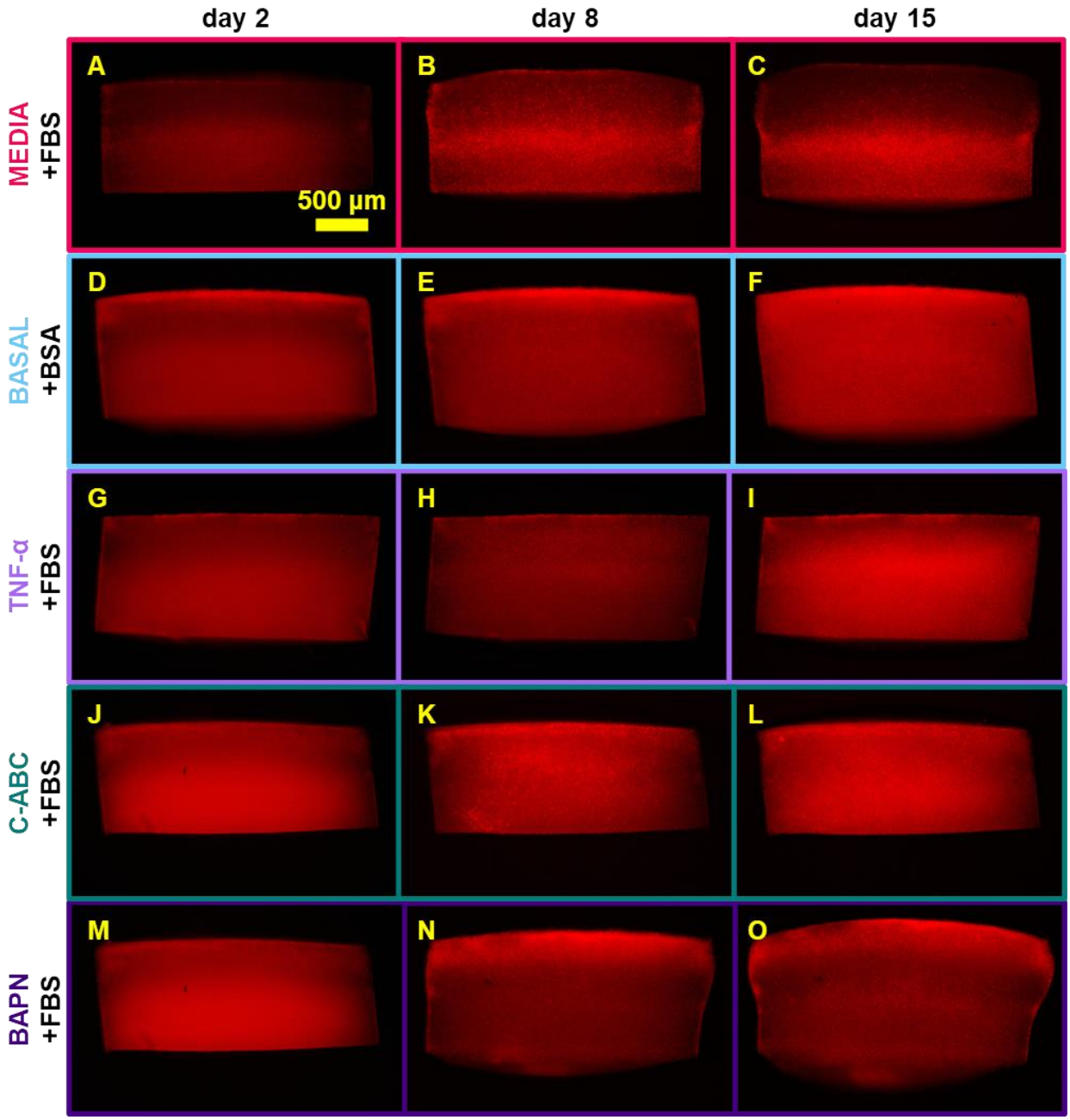


Figure 6.3. Effect of treatment and culture duration on overall explant growth. Representative images of explants treated with (**A-C**) media alone, (**D-F**) basal media, media with (**G-I**) TNF-α, pre-treated with (**J-L**) C-ABC, and media with (**M-O**) BAPN. Images at (**A,D,G,J,M**) day 2, (**B,E,H,K,N**) day 8, and (**C,F,I,L,O**) day 15 of culture.

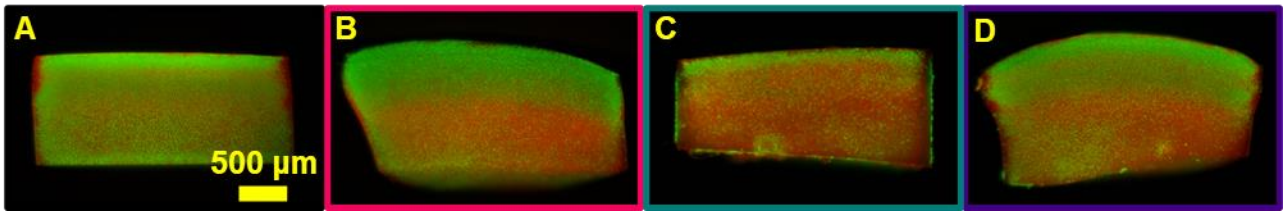


Figure 6.4. Effect of treatment and culture duration on viability after 15 days in culture Images of (**A**) freshly harvested explants, and explants after 15 days in culture and treated with (**B**) media, (**C**) pre-treated with C-ABC, and media with (**D**) BAPN. Live = Green. Dead = Red.

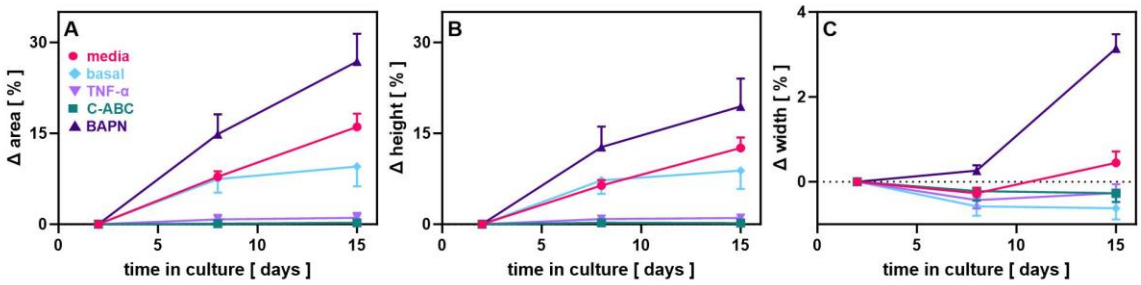


Figure 6.5. Effect of treatment and culture duration on overall explant growth. Overall change in explant (**A**) area, (**B**) height, and (**C**) width. (●) media, (◆) basal, (▼) TNFα, (■) C-ABC, (▲) BAPN. mean ± SEM.

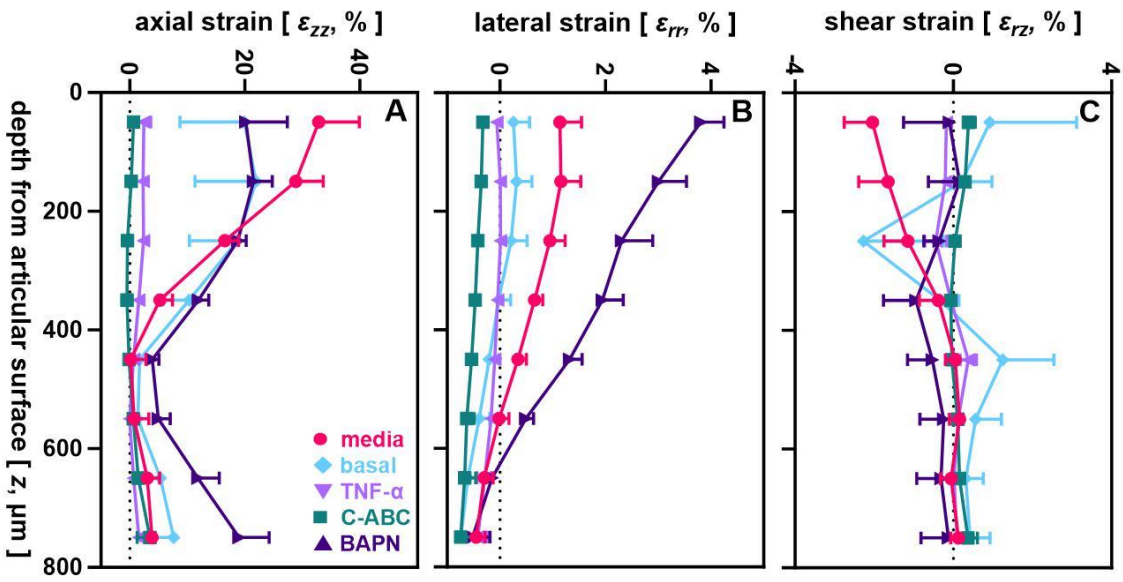


Figure 6.6. Effect of treatment and culture duration on overall variation in strain with depth.(**A**) Axial strain (ε_{zz}), (**B**) lateral strain (ε_{rr}), and (**C**) shear strain (ε_{rz}) as a function of depth from the articular surface (z). (●) media, (◆) basal, (▼) TNFα, (■) C-ABC, (▲) BAPN. mean ± SEM.

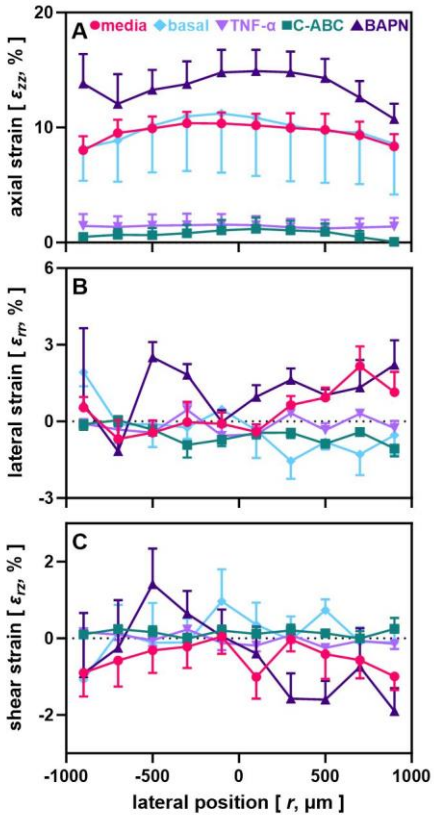


Figure 6.7. Effect of treatment and culture duration on overall variation in strain with lateral position.(**A**) Axial strain (ε_{zz}), (**B**) lateral strain (ε_{rr}), and (**C**) shear strain (ε_{rz}) as a function of distance from center of explant (r). (●) media, (◆) basal, (▼) TNFα, (■) C-ABC, (▲) BAPN. mean ± SEM.

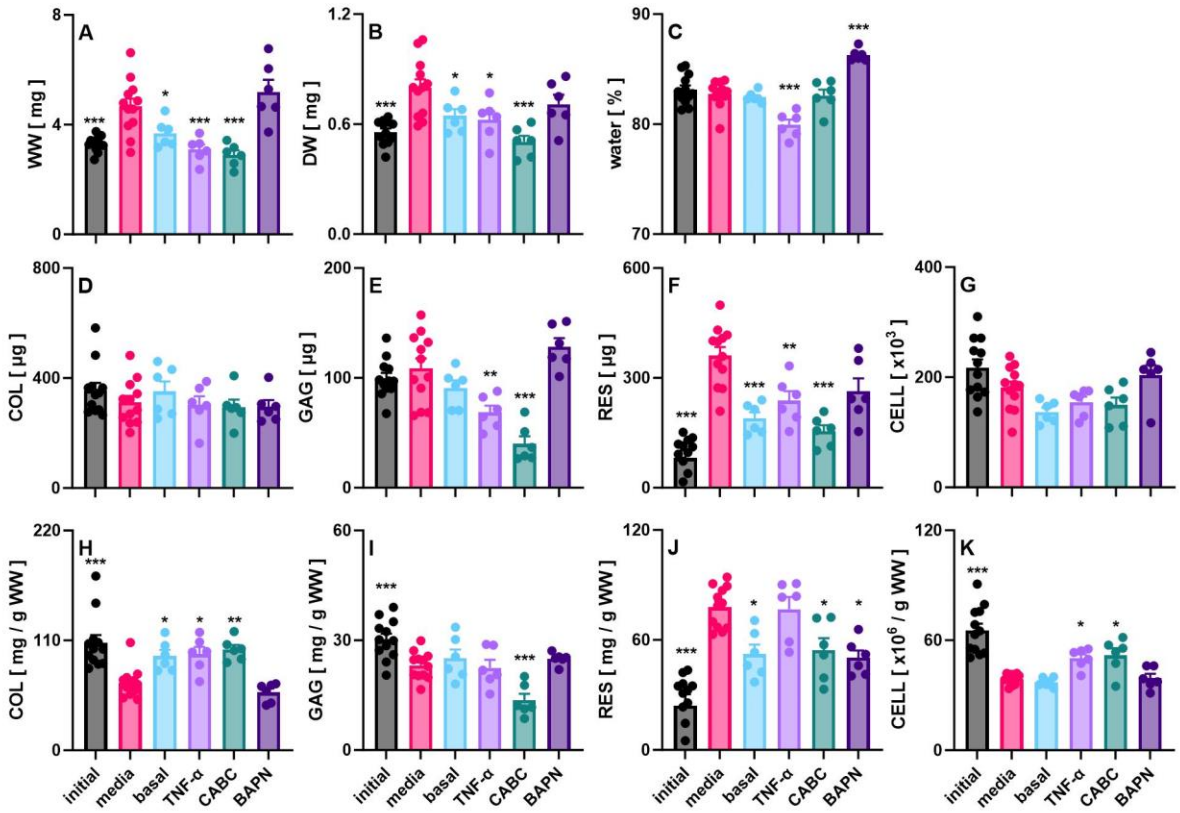


Figure 6.8. Effect of treatment and culture on explant biochemical content. Tissue (**A**) wet weight, (**B**) dry weight, and (**C**) water content. Mass of (**D**) collagen, (**E**) GAG, (**F**) residual matrix, and (**G**) cell number within explant. Content of (**H**) collagen, (**I**) GAG, (**J**) residual, and (**K**) cells within explant. **media**, **basal**, **TNFα**, **C-ABC**, **BAPN**. mean ± SEM. * $p<0.05$, ** $p<0.01$, *** $p<0.001$.

6.5. Discussion

The objective of this study was to assess the spatially varying strain of cartilage explant growth, and determine if such growth-strains are regulated and mediated by extracellular matrix content. Metrics were assessed in comparison to pro-growth conditions, by stimulation with FBS. Chondrocyte phenotype was regulated during culture by stimulation with TNF-α, a pro-inflammatory cytokine which induces a catabolic tissue response.[21] The effect of matrix structure and content was investigated removal of cartilage proteoglycans by C-ABC [22] and inhibition of the formation of lysyl oxidase mediated collagen crosslinks with BAPN.[23] Overall, explant growth was time- and space- varying, stimulated by treatment with BAPN, and inhibited by treatment with TNF-α and C-ABC.

The use of immature calf cartilage explants for this study had advantages and limitations. Small-diameter discs, and immature cartilage with enhanced permeability,[2] were utilized to minimize diffusion non-uniformity throughout the tissue and enable effective diffusion of essential nutrients.[24] Use of ethidium-labeled non-viable cells as fiducial markers at the cut surface enabled measurement of intra-tissue growth strains during culture. Due to the restrained healing ability of AC, dense matrix, and lack of vasculature, clearance of dead cells is limited and labeled cells remained visible throughout the culture duration. Although enhanced deformation limited detection of intra-tissue growth strains after ~1 wk in culture, spatial variation in growth strain were assessed during the period of predominant growth.

In vitro cartilage growth occurred in conjunction with increased explant water and matrix mass. Stimulation of growth with serum or inhibition of crosslinking with BAPN resulted in enhanced water (**Fig. 7A**) and residual matrix content (**Fig. 7F**) compared to explants assessed after 2 days of culture, and those that were growth-inhibited by treatment with C-ABC or stimulation with TNF-α. Thus, deformations measured are attributed to growth and remodeling

mechanisms, rather than bulk tissue swelling (i.e. increases to water content without concomitant increases in mass). Future studies may aim to identify the specific species of macromolecules deposited, and where they localize within the tissue.

In vitro cartilage growth occurred in a spatially varying and time-dependent manner within the 15-day culture period. Growth occurred mostly from day 2 to day 8 of culture (**Fig. 4**). Generally, the overall change in area is attributed to an increase in explant height during culture that occurred primarily within the upper third of the explant, the superficial ~300 μm including the articular surface (**Fig. 5A**). Similarly, increases in explant width similarly occurred near the articular surface (**Fig. 5B**). The delineation of spatial variation in explant growth provides insight into the mechanisms of cartilage maturation.

Treatment with BAPN appeared to have a depth-varying effect on cartilage explant growth. Inhibition of lysyl oxidase mediated collagen crosslinking resulted in enhanced axial growth strains in the deeper cartilage after 8 days in culture (**Fig. 5A**), compared to other conditions. This data supports previous work indicating that pyridinoline crosslinks in immature calf cartilage primarily form within the deeper cartilage layers (~600-800 μm below the articular surface), during serum-stimulated culture.[14] Accordingly, a lack of crosslinks in this layer, by treatment with BAPN, resulted in increased hydration after 13 days in culture.[14] Thus, remodeling of the collagen network may be zonally regulated and modulation of swelling pressure by alterations in crosslinking may be a mechanism of cartilage maturation.

Manipulation of GAG content in AC alters the growth phenotype of cartilage. In normal AC, GAG-rich proteoglycans act to inflate the collagen network and establish a level of pre-stress.[12] Similar to previous studies, minimization of tissue pre-stress by removal of endogenous GAG, by C-ABC, and loss of newly synthesized GAG, by TNF-α, resulted in marginal changes in

tissue size during culture.[13] Thus, under growth-enhancing conditions, the swelling pressure of intrinsic and newly synthesized GAG that remains entrapped within the tissue during culture may be sufficient to expand the endogenous collagen network. Studies to investigate the spatial distribution of newly deposited GAG molecules may provide additional insights into the mechanisms of cartilage maturation.

These studies investigate the depth-varying growth of articular cartilage explants, and the effects of extracellular matrix modulation on growth. Depth-varying growth mechanisms during maturation may allow for concurrent expansion of the tissue near the articular surface and maturation of the deeper regions.

6.6. Acknowledgements

This chapter, in full, will be submitted to *Journal of Orthopaedic Research*. The dissertation author was the primary author. Thanks to co-authors Kyle D. Jadin, Sean S. M. Ewalt, Danielle H. Pham, and Robert L. Sah. This work was supported by NSF GRFP and the Wu Tsai Human Performance Alliance.

6.7. References

1. Williamson AK, Chen AC, Masuda K, Thonar EJ-MA, Sah RL: Tensile mechanical properties of bovine articular cartilage: variations with growth and relationships to collagen network components. *J Orthop Res*.2003;21:872-80.

2. Williamson AK, Chen AC, Sah RL: Compressive properties and function-composition relationships of developing bovine articular cartilage. *J Orthop Res*. 2001;19:1113-21.

3. Hunziker EB, Quinn TM, Hauselmann HJ: Quantitative structural organization of normal adult human articular cartilage. *Osteoarthritis Cartilage*. 2002;10:564-72.

4. Jadin KD, Bae WC, Schumacher BL, Sah RL: Three-dimensional (3-D) imaging of chondrocytes in articular cartilage: growth-associated changes in cell organization. *Biomaterials*. 2007;28:230-9.

5. Jadin KD, Wong BL, Bae WC, Li KW, Williamson AK, Schumacher BL, Price JH, Sah RL: Depth-varying density and organization of chondrocyte in immature and mature bovine articular cartilage assessed by 3-D imaging and analysis. *J Histochem Cytochem*. 2005;53:1109-19.

6. Beaupre GS, Stevens SS, Carter DR: Mechanobiology in the development, maintenance, and degeneration of articular cartilage. *J Rehabil Res Dev.* 2000;37:145-51.

7. Carter DR, Beaupre GS, Wong M, Smith RL, Andriacchi TP, Schurman DJ: The mechanobiology of articular cartilage development and degeneration. *Clin Orthop Relat Res*. 2004;427 Suppl:S69-77.

8. Williamson AK, Masuda K, Thonar EJ-MA, Sah RL: Growth of immature articular cartilage in vitro: correlated variation in tensile biomechanical and collagen network properties. *Tissue Eng*. 2003;9:625-34.

9. Walker EA, Verner A, Flannery CR, Archer CW: Cellular responses of embryonic hyaline cartilage to experimental wounding in vitro. *J Orthop Res*. 2000;18:25-34.

10. Jadin KD, Tcheng SW, Sah RL: Depth-varying growth of articular cartilage explants revealed by biomechanical analysis of displacement of chondrocytes. *Trans Orthop Res Soc*. 2006;31:1495.

11. Han E, Chen SS, Klisch SM, Sah RL: Contribution of proteoglycan osmotic swelling pressure to the compressive properties of articular cartilage. *Biophys J*. 2011;101:916-24.

12. Maroudas AI: Balance between swelling pressure and collagen tension in normal and degenerate cartilage. *Nature*. 1976;260:808-9.

13. Asanbaeva A, Masuda K, Thonar EJ, Klisch SM, Sah RL: Mechanisms of cartilage growth: modulation of balance between proteoglycan and collagen in vitro using chondroitinase ABC. *Arthritis Rheum.* 2007;56:188-98.

14. Asanbaeva A, Masuda K, Thonar EJ-MA, Klisch SM, Sah RL: Cartilage growth and remodeling: modulation of balance between proteoglycan and collagen in vitro with beta-aminopropionitrile. *Osteoarthritis Cartilage.* 2008;16:1-11.

15. Farndale RW, Buttle DJ, Barrett AJ: Improved quantitation and discrimination of sulphated glycosaminoglycans by use of dimethylmethylene blue. *Biochim Biophys Acta.* 1986;883:173-77.

16. Woessner JF: The determination of hydroxyproline in tissue and protein samples containing small proportions of this imino acid. *Arch Biochem Biophys*. 1961;93:440-47.

17. McGowan KB, Kurtis MS, Lottman LM, Watson D, Sah RL: Biochemical quantification of DNA in human articular and septal cartilage using PicoGreen and Hoechst 33258. *Osteoarthritis Cartilage.* 2002;10:580-7.

18. Jackson DS, Cleary EG: The determination of collagen and elastin. *Methods Biochem Anal*. 1967;15:25-76.

19. Stockwell RA: The cell density of human articular and costal cartilage. *J Anat.* 1967;101:753-63.

20. Freed LE, Marquis JC, Langer R, Vunjak-Novakovic G, Emmanual J: Composition of cell-polymer cartilage implants. *Biotechnol Bioeng.* 1994;43:605-14.

21. Goldring MB: Osteoarthritis and cartilage: the role of cytokines. *Curr Rheumatol Rep.* 2000;2:459-65.

22. Yamagata T, Saito H, Habuchi O, Suzuki S: Purification and properties of bacterial chondroitinases and chondrosulfatases. *J Biol Chem.* 1968;243:1523-35.

23. Kagan HM, Sullivan KA: Lysyl oxidase: preparation and role in elastin biosynthesis. *Methods Enzymol.* 1982;82:637-49.

24. Maroudas A, Bullough P, Swanson SA, Freeman MA: The permeability of articular cartilage. *J Bone Joint Surg Br.* 1968;50:166-77.

CHAPTER 7

CONCLUSIONS

7.1. Summary of Findings

The objectives of this works were to (1) describe orthobiologic approaches to cartilage repair, determine maturation-related variation in (2) compressive and (3) tensile mechanical functions, and (4) biochemical content during normal human postnatal development and delineate how (5) depth-varying tissue growth leads to formation of mature collagen network architecture and how (6) regulatory cytokines and growth factors, as well as alterations in tissue content, affect in vitro cartilage growth. The major findings of this dissertation, related to these objectives are:

1. The biomechanical properties of normal human AC vary during postnatal maturation from infant to adult.
    a. The equilibrium confined compression modulus of the ~1 mm thick layer of AC, including the articular surface, increased between children (0.11 MPa) and adults (0.33 MPa), but not between infants and children (**Chapter 3**)
    b. Tensile biomechanical properties varied significantly with developmental stage and zone. In both the SZ and DZ, the biomechanical properties tended to increase between infants and children before decreasing in adults. In children, the equilibrium modulus, ramp modulus, and failure strength were ~1.3-2 times greater in the DZ, compared to the SZ. In the DZ, tensile biomechanical properties of AC from children were ~3 times greater than adults. In the SZ, differences between developmental stages were not as evident as in the DZ. (**Chapter 4**)

2. The biochemical composition of AC also varies during postnatal maturation from infant to adult.
    a. Biochemical properties of the ~1 mm thick layer of AC, including the articular surface varied with developmental stage, and with distinctive timings between collagen and GAG. Water content decreased between infants (88%), children (81%), and adults (75%). COL increased between infants (48 mg/g WW), children (103 mg/g WW), and adults (132 mg/g WW). GAG was similar between infants and children and increased between children and adults (19 to 35 mg/g WW). CELL decreased between infants and children (36 to 11×10^6 cells/g WW). (**Chapter 3**)
    b. Biochemical properties of AC in the SZ and DZ followed similar trends resulting in mature AC that has a denser matrix and reduced cellularity. Biochemical contents were logistically related to age, with time constants of ~30 yrs, ~10 yrs, and ~25 yrs, respectively for water, COL, and cellularity. (**Chapter 4**)
3. There is a correlated variation between AC biomechanical and biochemical properties.
    a. Maturation-associated changes in compressive properties correlated positively with COL and GAG. (**Chapter 3**)
    b. Maturation-associated changes in tensile ramp modulus and failure strength negatively correlated with water content, and positively correlated with COL and RES. (**Chapter 4**)
4. *In vivo*, the murine distal femoral condyle attains its mature state within the first ~30 days (**Chapter 5**). The perimeter and radii of the medial femoral condyle at the articular surface and at the bone-cartilage interface increase logistically, with time constants of ~3-6 days. The MFC increases ~250% between immature and immature values for the perimeter and

both the anterior-posterior and proximal-distal directions, and application of this deformation in a depth-varying manner results in reorientation of the collagen network from an immature to mature-like architecture.

5. *In vitro* cartilage explant growth is primarily axial and is depth varying. Independent of culture media, axial and lateral growth strains occur predominantly near the articular surface. Depth-variation in growth strain is regulated and altered by the content or assembly of COL and GAG which affect tissue swelling pressure. (**Chapter 6**)

7.2. Discussion

This work implicates mechanical loading, hormonal regulation and onset of puberty, and cartilage swelling pressure as mechanisms of cartilage maturation. The distinctive time course of variation in cartilage biomechanical properties and biochemical content during maturation between humans and bovines may be related to differences in mechanical demands. In humans, H_{A0} is similar between infants and children and increases ~3 fold between the child and adult state (**Chapter 3**). Conversely, bovine AC H_{A0} increased ~2 fold between fetal bovines and calves (~0.27 MPa) but was not different between calves and adult bovines.[1] Also, in contrast to humans which undergo significant COL deposition between infants, children, and adults, as well as significant GAG deposition between children and adults, bovine AC reaches the adult mechanical, GAG, and COL levels at early developmental stages.[1] Cartilage tensile function undergoes similar enhancements, with ramp modulus and failure strength beginning to increase rapidly at ~4-9 months (**Chapter 4**). Since human infants begin to walk at ~1 yr of age,[2] while quadruped animals can stand and walk hours after birth,[3] the progression of early COL and later GAG deposition may be a response to age-varying mechanical demands as an individual begins to locomote and gain mass. The evolution in COL content at ~20 yrs suggests regulation by hormones associated with puberty (**Chapter 4**). The above studies establish benchmarks for postnatal maturation of normal human femoral condyle.

Spatial variation in growth deformations *in vivo* (**Chapter 5**) and *in vitro* (**Chapter 6**) may allow for concurrent expansion of the tissue near the articular surface and maturation of the deeper regions. Depth-variation in axial and lateral articular cartilage growth may contribute to kinematic reorientation of the collagen network from the immature to mature configuration. Concentrated lateral growth near the articular surface may contribute to the overall increase in cartilage surface area during maturation. In addition, growth of the articular cartilage, particularly depth-variation

in the axial direction, may also contribute to depth-variation in cellular organization.

In vitro cartilage explant growth is predisposed to depth-varying growth deformation wherein axial and lateral growth strains occur predominantly near the articular surface (**Chapter 6**). Tendency for lateral tissue strain near the surface may enable the cartilage to cover an increasing joint surface area during growth, with surface collagen fibril orientation becoming increasingly tangential. Tendency for axial tissue strain near the surface and in the deeper cartilage may allow for internal restructuring allowing growth of the articular cartilage,[4] and reorientation of collagen fibril orientation in the deep zone that is more perpendicular, relative to the surface. Depth-variation in axial and lateral strain may be due to associated variations in endogenous COL and GAG, as well as cellular metabolic activity throughout the tissue which in turn affects the tissue swelling pressure.

The work presented in this dissertation can be expanded in several ways. Temporal analysis of the age-related variation in AC compressive, tensile, and biochemical properties indicate that mechanical load, perhaps associated with the gained ability to locomote during late infancy and early childhood, affects cartilage maturation. Additional factors which modulate the load experienced by AC include contact forces which vary across the joint surface,[5] as well as body mass,[6] and preference for sport.[7,8] Therefore, future studies should be designed to elucidate the effects of (1) regional variation across the joint surface, as well as (2) BMI, and (3) level of activity on cartilage biomechanical and biochemical properties during maturation.

Another future direction includes determining the age- and depth- related variation in collagen crosslink content during normal human development, and during *in vitro* culture. In bovines, cartilage pyridinoline content increased during maturation and was ~730% greater in adult AC, than in fetal animals, and was strongly correlated with tensile strength.[9] In humans, the

content of mature hydroxypyridinium crosslinks increases during childhood and adolescence, reaching a maximum between ages 15-25.[10] Analysis of post-translational collagen modifications in normal human AC also indicates that maturation of cartilage during adolescence (10-20 yrs) starts in the upper half of the tissue and occurs last in the tissue close to the bone and is zonally regulated.[11] Variation in the time course and mechanisms of collagen maturation between the SZ and DZ is supported by our work indicating that these layer have different characteristic times of change during maturation (**Chapter 4**), and that inhibition of collagen crosslink formation preferentially enhances axial growth strains in the deeper cartilage (**Chapter 6**). However, analyses relating collagen crosslink content and composition and tensile function during development have not yet been reported.

Similarly, the age- and depth- related variation in collagen network architecture during normal human AC development is understudied. PLM analyses of immature bovine,[12] equine,[13]and lapine AC,[14] indicate that collagen fibrils run parallel to the surface at the articular surface, as well as in a deeper layer of AC, separated by a transitional layer. By maturity, the immature trilaminar structure develops into the characteristic Benninghoff arcade.[15] Presence of a subjacent layer of collagen with tangential fiber orientation in humans is supported by our work indicating that the deep cartilage ~1000-1500 μm below the articular surface has enhanced tensile properties compared to the SZ (**Chapter 4**). However, formal analyses of AC collagen network orientation during maturation of the human distal femur and femoral condyle have not yet been reported.

Thus, additional studies are required to determine the role of collagen crosslinks and collagen network architecture on structure-function relationships with age- and depth- in key developmental stages during childhood (<10 yrs) and adolescence (10-20 yrs), as well as how

modulation of collagen assembly, by inhibition or stimulation of collagen crosslink formation with BAPN or lysyloxidase, respectively, during *in vitro* culture affects the collagen architecture.

In summary, the compressive and tensile load bearing function of AC vary with age and depth, between infants, children, and adults, and correlate with matrix content. Spatiotemporal variation may be due to AC growth that is predisposed to different modes (i.e. axial vs lateral strain) throughout the depth. The studies herein establish benchmarks for postnatal maturation of normal human femoral condyle and propose spatiotemporal modulation of *in vitro* growth as a useful tool in recapitulating native-like structural properties in future orthobiologic approaches to cartilage repair (**Chapter 2**). A greater understanding of tissue maturation provides insight for the development of strategies to restore and repair joint function following injury and disease.

7.3. References

1. Williamson AK, Chen AC, Sah RL: Compressive properties and function-composition relationships of developing bovine articular cartilage. *J Orthop Res.* 2001;19:1113-21.

2. Clark JE, Whitall J, Phillips SJ: Human interlimb coordination: the first 6 months of independent walking. *Dev Psychobiol.* 1988;21:445-56.

3. Whalin L, Weary DM, von Keyserlingk MAG: Understanding behavioural development of calves in natural settings to inform calf management. *Animals (Basel).* 2021;11.

4. Decker RS, Um HB, Dyment NA, Cottingham N, Usami Y, Enomoto-Iwamoto M, Kronenberg MS, Maye P, Rowe DW, Koyama E, Pacifici M: Cell origin, volume and arrangement are drivers of articular cartilage formation, morphogenesis and response to injury in mouse limbs. *Dev Biol.* 2017;426:56-68.

5. Brown TD, Shaw DT: In vitro contact stress distribution on the femoral condyles. *J Orthop Res.* 1984;2:190-9.

6. Blazek K, Favre J, Asay J, Erhart-Hledik J, Andriacchi T: Age and obesity alter the relationship between femoral articular cartilage thickness and ambulatory loads in individuals without osteoarthritis. *J Orthop Res.* 2014;32:394-402.

7. Stetter BJ, Ringhof S, Krafft FC, Sell S, Stein T: Estimation of Knee Joint Forces in Sport Movements Using Wearable Sensors and Machine Learning. *Sensors (Basel).* 2019;19:3690.

8. Cassiolas G, Di Paolo S, Marchiori G, Grassi A, Della Villa F, Bragonzoni L, Visani A, Giavaresi G, Fini M, Zaffagnini S, Lopomo NF: Knee Joint Contact Forces during High-Risk Dynamic Tasks: 90° Change of Direction and Deceleration Movements. *Bioengineering (Basel).* 2023;10:179.

9. Williamson AK, Chen AC, Masuda K, Thonar EJ-MA, Sah RL: Tensile mechanical properties of bovine articular cartilage: variations with growth and relationships to collagen network components. *J Orthop Res.* 2003;21:872-80.

10. Eyre DR, Dickson IR, van Ness K: Collagen cross-linking in human bone and articular cartilage: age-related changes in the content of mature hydroxypyridinium residues. *Biochem J.* 1988;252:495-500.

11. Bank RA, Bayliss MT, Lafeber FP, Maroudas A, Tekoppele JM: Ageing and zonal variation in post-translational modification of collagen in normal human articular cartilage. The age-related increase in non-enzymatic glycation affects biomechanical properties of cartilage. *Biochem J.* 1998;330:345-51.

12. Camosso M, Marotti G: The mechanical behavior of articular cartilage under compressive stress. *J Bone Joint Surg Am.* 1962;44-A:699-709.

13. Oinas J, Ronkainen AP, Rieppo L, Finnilä MAJ, Iivarinen JT, van Weeren PR, Helminen HJ, Brama PAJ, Korhonen RK, Saarakkala S: Composition, structure and tensile biomechanical properties of equine articular cartilage during growth and maturation. *Sci Rep.* 2018:11357.

14. Julkunen P, Harjula T, Iivarinen J, Marjanen J, Seppanen K, Narhi T, Arokoski J, Lammi MJ, Brama PA, Jurvelin JS, Helminen HJ: Biomechanical, biochemical and structural correlations in immature and mature rabbit articular cartilage. *Osteoarthritis Cartilage.* 2009*;*17:1628-38.

15. Benninghoff A: Form und bau der gelenkknorpel in ihren beziehungen zur funktion. Zweiter teil: der aufbau des gelenkknorpels in seinen beziehungen zur funktion. *Zeitschrift für Zellforschung.* 1925*;*2:783-862.